

INTERNATIONAL JOURNAL OF MODERN PHYSICS *A*

Volume 4, Number 4
February 1989

Advisors

V Barger (*Wisconsin*)
K C Chou (*Acad. Sinica, Beijing*)
R H Dalitz (*Oxford*)
S Drell (*SLAC*)
T Ericson (*CERN*)
L D Faddeev (*Leningrad*)
E S Fradkin (*Moscow*)
H Feshbach (*MIT*)
F Gilman (*SLAC*)
W Greiner (*Frankfurt*)
J H Hamilton (*Vanderbilt*)
S Hawking (*Cambridge*)
F Iachello (*Yale*)

M Jacob (*CERN*)
L Lederman (*Fermilab*)
T D Lee (*Columbia*)
Y Nambu (*Chicago*)
A M Polyakov (*Moscow*)
T Regge (*Torino*)
A Salam (*ICTP*)
J Steinberger (*CERN*)
Sun Zuxun (*Beijing*)
S C C Ting (*MIT*)
S Weinberg (*Texas*)
B H Wildenthal (*New Mexico*)
C N Yang (*Stony Brook*)



World Scientific

Singapore • New Jersey • London • Hong Kong

CONTENTS

Reviews

THE STANDARD MODEL WITH THREE GENERATIONS: CLOSING IN ON THE TOP QUARK MASS 753

F. Halzen, C. S. Kim and S. Pakvasa

THEORETICAL MODELS FOR ATOMIC CHARGE TRANSFER IN ION-ATOM COLLISIONS 769

D. H. Jakubaša-Amundsen

Research Papers

MEASURING THE CHARGINO MIXING PARAMETERS OF THE MINIMAL SUSY EXTENSION OF THE STANDARD MODEL AT e^+e^- COLLIDERS IN THE TeV REGION 845

A. Leike

COVARIANT BASIC OPERATORS IN BOSONIC STRING THEORY 857

G. Cristofano, F. Nicodemi and R. Pettorino

ASPECTS OF SUPERSTRING QUANTUM COSMOLOGY 873

K. Enqvist, S. Mohanty and D. V. Nanopoulos

$G_N \otimes G_L / G_{N+L}$ CONFORMAL FIELD THEORIES AND THEIR MODULAR INVARIANT PARTITION FUNCTIONS 897

P. Christe and F. Ravanini

TWISTED VERTEX OPERATORS AND REPRESENTATIONS OF FINITE HEISENBERG GROUPS 921

D. Altschüler, P. Béran, J. Lacki and I. Roditi

PROPERTIES OF MESONS IN THE STATISTICAL MODEL 943

S. N. Banerjee, R. K. Das and A. K. Sarker

PERTURBATIVE QED: THE SCHRÖDINGER PICTURE 963

Paul Hoyer

GAUGE-INVARIANT RENORMALIZABILITY OF NON-ABELIAN STOCHASTICALLY QUANTIZED THEORIES 981

V. Ya Fainberg and A. V. Subbotin

THEORETICAL MODELS FOR ATOMIC CHARGE TRANSFER IN ION-ATOM COLLISIONS

D. H. JAKUBAÅA-AMUNDSEN

Physics Section, University of Munich, 8046 Garching, FR Germany

Received 18 June 1988

The current theoretical models for the description of electron transfer in adiabatic, intermediate and high-energy collisions are reviewed. Particular emphasis is laid on the recent development of atomic theories suited for fast or asymmetric ion-atom encounters. The comparison with other theories and with experimental data on total as well as differential capture cross sections is used to determine the applicability of a specific model. The selected examples concern capture to bound states, to continuum states, radiative transfer as well as capture in the presence of an isolated nuclear resonance.

Contents

I. Introduction	770
II. Theoretical Models	772
1. Atomic Three-Body Models	772
1.1. Equivalent Forms of the Transition Amplitude	773
1.2. Discussion of the Potentials	776
1.2.1. Long-Range Atomic Potentials	776
1.2.2. Nuclear Potential	777
1.2.3. Recoil	779
1.3. Approximations to the Transition Amplitude	779
1.3.1. Born Series	780
1.3.2. Continuum Distorted Wave Series (CDW)	783
1.3.3. Strong Potential Born Theory (SPB)	784
1.3.4. Impulse Approximation and its Peaking Versions	788
1.3.5. Distorted-Wave Born Approximation	789
1.3.6. Eikonal Approximation	790
2. Coupled Channel Calculations in a Finite Basis	792
2.1. Atomic Basis	792
2.2. Molecular Basis	794
2.3. Combined Basis	797
3. Variational Methods	797
4. Numerical Solutions of the Schrödinger Equation	801
4.1. Representation in a Very Large Basis	802
4.2. Numerical Integration of the Time-Dependent Schrödinger Equation	804
4.3. Classical Approach and Statistical Theories	805

5. Many-Electron Models	808
5.1. Reduction to a Modified Three-Body Problem	808
5.2. Inclusion of the Static Electron-Electron Coupling	809
5.3. Approaches to the Dynamical N -Body Problem	811
6. Extension to Relativistic Velocities	813
6.1. Atomic Theories	813
6.2. Coupled Channel Calculations	814
6.3. Numerical Integration of the Dirac Equation	815
III. Applications	815
1. Charge Transfer in the Absence of Nuclear Reactions	816
1.1. Capture into Bound States	818
1.2. Capture to the Continuum	822
2. Charge Transfer during Resonant Nucleus-Nucleus Scattering	828
2.1. Capture during Elastic Scattering by Light Projectiles	828
2.2. Comparison with other Clocks for Nuclear Reaction Times	831
IV. Summary and Outlook	837
V. References	838

I. Introduction

There is continued interest being devoted to the study of electron capture from target atoms by ionized projectiles because this is one of the most intricate problems in atomic collision theory. The difficulties in the description of inelastic electronic processes are based on the long-range nature of the Coulomb interaction, which does not even asymptotically permit the scattered particles to leave the interaction zone. Thus a careful treatment of quasi-divergent series is required, and it is crucial to include the correct boundary conditions¹. The additional difficulties occurring for rearrangement processes such as electron capture are connected with the fact that there are different perturbations in the entrance and exit channel. Hence an approximative solution of the three- (or many-) body problem in terms of perturbative approaches is made complicated through the presence of more than one natural expansion parameter². Further problems arise from the non-orthogonality of the initial and final electronic states.

In order to classify the various theories it is useful to divide the collisions into three different regions which are characterized by the collision velocity v . As reference velocity the classical orbiting velocity of the active electron in its initial or final state is taken whichever is more tightly bound, $v_e = \max(Z_T/n_T, Z_P/n_P)$. The projectile and target nuclear charges are denoted by Z_P and Z_T , and the corresponding main quantum numbers by n_P and n_T , respectively. The three regions are chosen to be the adiabatic region ($v \ll v_e$), the intermediate region ($v \approx v_e$) and the high-energy region ($v \gg v_e$).

In the adiabatic region the collision is sufficiently slow for the electron to adjust itself to the instantaneous two-center potential created by the two nuclei, so that an intermediate molecular-like complex is formed³. The excitation or transfer in this case is caused by the variation of the two-center potential with time⁴. In the limit of very small collision velocities there is no difference in the mechanisms for excitation and transfer because both processes occur predominantly at small internuclear distances R where the quasi-

molecular orbitals have not separated into target- or projectile-centered ones. The relevant internuclear distances are determined from the inverse of the momentum q transferred to the active electron, $R \sim q^{-1} \sim v/\Delta E$, ΔE being the energy transfer to the electron, or in special cases also from avoided crossings of the R -dependent energy levels of adjacent electronic states. At somewhat higher (but still adiabatic) velocities larger values of R will often be important, and one has to account for the different reference frames of the electron in the initial and final channel by means of appropriate translational factors^{5,6}. The time-derivative of the molecular orbitals can serve as an expansion parameter in the adiabatic regime as long as the relevant atomic matrix elements vary slowly with time, which is the case for electronic states well separated in energy.

In the intermediate region a description of the transfer process is complicated because in general no appropriate expansion parameter is available which would allow for a perturbative treatment or for a restriction to a small number of intermediate states. The only exception is the case of very asymmetric collision systems (i.e. $Z_P \ll Z_T$ or $Z_T \ll Z_P$) where an expansion in terms of the weaker of the two internuclear potentials can be used⁷. In the general case one has to resort to coupled-channel calculations or to variational procedures. The same is true if more than one electron is transferred and the classification "adiabatic" or "high-energy" does not hold simultaneously for all active electrons.

The high-energy region is again accessible to perturbative approaches. As the target electronic states are only weakly perturbed by the fast projectile (and vice versa), a description in terms of target or projectile eigenstates (atomic description) is possible⁸. It is this region where the difference between excitation and transfer is most prominent: if the velocity v is sufficiently high, excitation is very accurately described by the first-order Born approximation⁹, while for electron transfer at least the second-order Born approximation is required¹⁰, which is in accordance with the classical picture that a double collision is necessary for electron capture to take place¹¹.

In none of the three velocity regions has the ideal theory been found yet, not even in the cases where perturbation theory is applicable. In the adiabatic region, there are ambiguities in the construction of the translational factors, while the most advanced high-energy theories suffer from renormalization problems.

In this article a survey is given of the current theories for charge exchange. The different atomic perturbation approaches are derived from the exact expression of the capture amplitude for a three-body problem. For the lower collision velocities, the electronic wave function is expanded in terms of atomic or molecular basis states, which results in coupled equations for the transfer amplitude. Variational theories are discussed, as are classical and quantum mechanical methods which aim at a direct numerical solution of the Schrödinger equation. For the sake of a transparent presentation of these approaches, the restriction to a single active electron has been made. The extension to multi-electron systems is discussed subsequently, with a special consideration of the problems arising from the electron-electron interaction. Modifications in the case of relativistic impact velocities are also addressed.

The range of applicability of the various theories is estimated by means of comparison with a huge body of experimental data which have become available through the event of

powerful heavy-ion accelerators. There is a rather detailed study of the low-energy region in a recent article by Wille and Hippler⁴ so we shall concentrate on the high-energy region, as well as on the intermediate region in the case of asymmetric collision systems where the atomic perturbation approaches can be tested. An attempt is made to compile the results contained in a great number of original papers as well as to update the review articles^{2,6-8,12} on this rapidly developing field.

The last section deals with an example concerning the interplay between atomic physics and nuclear physics: if the transfer process is influenced by a nuclear reaction, it can serve as an atomic clock to measure nuclear reaction times¹³. As compared to the interference of direct processes such as excitation or ionization, with nuclear reactions^{14,15} the transfer process allows for the study of a larger variety of nuclear resonances. This is mainly due to the fact that the electronic energy transfer which serves as a time scale for the nuclear reaction, depends strongly on the collision velocity. On the other hand, such interference phenomena provide a unique possibility of probing the atomic transfer amplitudes during the collision. Atomic units ($\hbar = m = e = 1$) are used unless otherwise indicated.

II. Theoretical Models

The description of atomic processes is greatly simplified by the fact that the mass m of the electron is much smaller than the mass M of the nucleus. Therefore, the energy transfer ΔE to the electron is in most cases only a negligible fraction of the nuclear collision energy E_i . Restricting ourselves for the moment to the presence of a single electron, we have in the case of charge transfer from the target to the projectile

$$\Delta E = \varepsilon_f - \varepsilon_i + v^2/2 = -Z_P^2/2n_P^2 + Z_T^2/2n_T^2 + v^2/2 \ll E_i ,$$

$$E_i = \frac{1}{2} \mu_i v^2 = \frac{1}{2} \frac{M_P M_T}{M_P + M_T} v^2 , \quad (\text{II.1})$$

where M_P and M_T is the mass of the projectile and target nucleus (in units of m), respectively. It is thus generally possible to neglect the influence of the inelastic electronic processes on the motion of the nuclei and one may define a classical path for the heavy particles¹⁶. This reduces the quantum mechanical problem to a semiclassical one, where the electronic degrees of freedom are governed by a time-dependent electronic Hamiltonian, with the time dependence resulting from a given classical trajectory for the relative internuclear motion. There are only a few exceptions which do not allow for such a semiclassical description. These concern collisions with extremely low impact energy, as well as interference effects between amplitudes which arise from different classical trajectories. In the following, the semiclassical picture is chosen as long as it is equivalent to the quantum mechanical one.

1. Atomic Three-Body Models

In the simplest case of two nuclei and a single electron, the classical treatment of the internuclear motion reduces the three-body problem to the motion of the electron in the

time-dependent fields of the projectile and the target nucleus. Nevertheless, many of the intricacies of the full three-body problem remain because the correct boundary conditions have to be taken into consideration and it is not possible to represent the exact scattering wave function of the electron by means of a tractable closed expression. The wave function can, however, be obtained from the three-body approaches with the nucleus-nucleus interaction put equal to zero. The formal solution can either be defined by the Lippmann-Schwinger integral equation¹⁷, or by the sum of three functions which obey the coupled Faddeev equations¹⁸.

As the scattering wave function enters into the exact transition amplitude, the methods for evaluating this function can immediately be used to calculate the transition amplitude. In the following, the exact transition amplitude is cast into a form suitable as a starting point for approximative treatments. After a discussion of the relevant potentials, the current atomic theories will be derived from it.

1.1. Equivalent Forms of the Transition Amplitude

In the semiclassical approximation the electronic Hamiltonian H_e consists of the kinetic energy T_e plus a time-dependent interaction W . For direct reactions, it is useful to split H_e into an unperturbed part H_0 which defines the asymptotic states, and a small perturbation V . For rearrangement collisions, the splitting of H_e is different for the initial channel i and the final channel f , causing the perturbation to be not necessarily small:

$$\begin{aligned} H_e &= T_e + W(\mathbf{r}, t) = H_{i0} + V_i \\ &= H_{f0} + V_f. \end{aligned} \quad (1.1)$$

It is important to note that the initial and final states, φ_i and φ_f , which are eigenstates to H_{i0} and H_{f0} , respectively, are originally defined in different reference frames. In order to construct a transition amplitude it is necessary to transform to a common reference system. Let us according to Fig. 1 define a reference frame which is centered on the line connecting the two nuclei and displaced from the projectile by a vector \mathbf{x}_f . This frame is

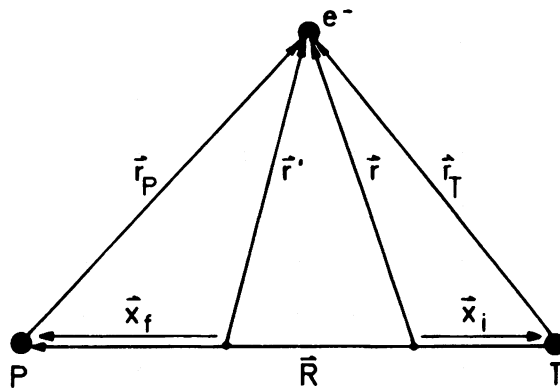


Fig. 1. Coordinates for the three-body system consisting of projectile (P), target (T) and electron (e). \mathbf{r} and \mathbf{r}' denote the location of the electronic initial and final state, respectively, at a given internuclear separation R .

called "projectile correlated" frame and all quantities defined in this system are denoted by a prime. Likewise, the center of the "target correlated" reference system is displaced from the target by a vector \mathbf{x}_i , and all quantities referring to this system are unprimed. Through an appropriate choice of x_i and x_f a selection of special reference frames can easily be made; in particular, a non-zero x_i and x_f allows for the possibility of sliding coordinates for φ_i and φ_f .

The transformation \hat{U} from the target correlated frame to the projectile correlated frame is an extended Galilean transformation

$$\hat{U} = \exp\left(-i \int dt \frac{1}{2}(\dot{\mathbf{R}} + \dot{\mathbf{x}}_i - \dot{\mathbf{x}}_f)^2\right) \times \exp(-i(\dot{\mathbf{R}} + \dot{\mathbf{x}}_i - \dot{\mathbf{x}}_f)\mathbf{r}') \\ \times \exp(i(\mathbf{R} + \mathbf{x}_i - \mathbf{x}_f)\mathbf{p}). \quad (1.2)$$

It consists of a translation in coordinate space (\mathbf{p} is the conjugate momentum to \mathbf{r}), a translation in velocity space plus an energy translation¹⁹. In case of a linear motion ($\ddot{\mathbf{R}} = 0$), \hat{U} reduces to a Galilean transformation.

The transformation of an arbitrary wave function ψ (defined in the target correlated frame) into the projectile correlated frame and vice versa thus reads

$$\psi'(\mathbf{r}', t) = \hat{U}\psi(\mathbf{r}, t), \\ \psi(\mathbf{r}, t) = \hat{U}^+\psi'(\mathbf{r}', t), \quad (1.3)$$

where the second relation follows from the unitarity of \hat{U} .

In the following, the target correlated reference frame (i.e. the frame of φ_i) is chosen for the evaluation of the transition amplitude. Any quantities without primes are understood to be defined in this frame.

Let $\psi_i^{(+)}$ be a state which at early times ($t \rightarrow -\infty$) coincides with the state φ_i , and $\psi_f^{(-)}$ a state which asymptotically ($t \rightarrow +\infty$) develops into the state φ_f . The transition amplitude from $\psi_i^{(+)}$ to $\psi_f^{(-)}$ can be written in the general form²⁰

$$a_{fi}(t) = \langle \psi_f^{(-)}(t) | \psi_i^{(+)}(t) \rangle - i \int_{-\infty}^t dt \langle \psi_f^{(-)}(t) | H_e - i\partial_t | \psi_i^{(+)}(t) \rangle, t \rightarrow \infty. \quad (1.4)$$

This form of the transition amplitude becomes evident by considering two special cases: if $\psi_i^{(+)}$ and $\psi_f^{(-)}$ are exact solutions to H_e the second term vanishes and the transition amplitude reduces to the form well-known from scattering theory²¹. If on the other hand, $\psi_i^{(+)}$ and $\psi_f^{(-)}$ are stationary solutions to H_e which, being defined in the same reference frame ($\mathbf{r} = \mathbf{r}'$, i.e. $\mathbf{R} + \mathbf{x}_i = \mathbf{x}_f$ in Fig. 1) are orthogonal, the first term vanishes and a_{fi} attains the form of molecular perturbation theory²².

In order to cast (1.4) into a form suitable for perturbative treatments we assume at first that $\psi_i^{(+)}$ and $\psi_f^{(-)}$ are exact solutions to H_e , i.e.

$$(i\partial_t - H_e)\psi(t) = 0 \tag{1.5}$$

with $\psi = \psi_i^{(+)}$ or $\psi_f^{(-)}$.

Next we introduce an arbitrary splitting of the Hamiltonian in the entrance and the exit channel

$$H_e = H_i + \hat{V}_i = H_f + \hat{V}_f \tag{1.6}$$

where H_i or H_f need not necessarily be hermitean ($H_i \neq H_i^+$, $\hat{V}_i \neq \hat{V}_i^+$. . .). Correspondingly, distorted waves χ_i and χ_f are defined as eigenstates to H_i and H_f , respectively. In the general case, they do not coincide with φ_i and φ_f , but reduce to them asymptotically

$$\begin{aligned} i\partial_t\chi_i^{(+)}(t) &= H_i\chi_i^{(+)}(t), \chi_i^{(+)}(t \rightarrow -\infty) = \varphi_i \\ i\partial_t\chi_f^{(-)}(t) &= H_f\chi_f^{(-)}(t), \chi_f^{(-)}(t \rightarrow +\infty) = \varphi_f. \end{aligned} \tag{1.7}$$

In order to derive the post form of the transition amplitude, we shall drop the assumption that $\psi_f^{(-)}$ is exact. The prior form is subsequently obtained from an approximation to $\psi_i^{(+)}$.

If in (1.4), $\psi_f^{(-)}$ is replaced by $\chi_f^{(-)}$ and a partial integration is performed in the term containing $i\partial_t$, one obtains with the help of (1.6) and (1.7)

$$a_{fi}(t) = a_{fi}^{D+} - i \int_{-\infty}^t dt \langle \chi_f^{(-)}(t) | \hat{V}_f^+ | \psi_i^{(+)}(t) \rangle, t \rightarrow \infty. \tag{1.8}$$

The term $a_{fi}^{D+} = \langle \chi_f^{(-)}(-\infty) | \psi_i^{(+)}(-\infty) \rangle$ is called surface term. In order to cast it into a more convenient form, the expression

$$-i \int_{-\infty}^t dt [\langle \varphi_i(t) | H_f - i\partial_t | \chi_f^{(-)}(t) \rangle]^* \tag{1.9}$$

which due to (1.7) is zero, is added and a partial integration is carried out. Recalling that $\psi_i^{(+)}(-\infty) = \varphi_i$, one finds for $t \rightarrow \infty$:

$$a_{fi}^{D+} = -i \int_{-\infty}^{\infty} dt \langle \chi_f^{(-)}(t) | V_i - \hat{V}_f^+ | \varphi_i(t) \rangle \tag{1.10}$$

because at $t \rightarrow \infty$, the overlap $\langle \chi_f^{(-)}(t) | \varphi_i(t) \rangle$ vanishes. Equation (1.8) with (1.10) constitutes the post form of the transition amplitude.

In complete analogy, the prior form is obtained from (1.4) by means of replacing $\psi_i^{(+)}$ by $\chi_i^{(+)}$, and by adding $-i \int_{-\infty}^t dt \langle \varphi_f(t) | H_i - i\partial_t | \chi_i^{(+)}(t) \rangle$ to the surface term:

$$\begin{aligned} a_{fi}(t) &= a_{fi}^{D-} - i \int_{-\infty}^t dt \langle \psi_f^{(-)}(t) | \hat{V}_i | \chi_i^{(+)}(t) \rangle, t \rightarrow \infty \\ a_{fi}^{D-} &= -i \int_{-\infty}^{\infty} dt \langle \varphi_f(t) | V_f - \hat{V}_i | \chi_i^{(+)}(t) \rangle. \end{aligned} \tag{1.11}$$

As long as $\psi_i^{(+)}$ in (1.8) and $\psi_f^{(-)}$ in (1.11) are exact solutions to H_e , the prior and the post form are exact and identical. An alternative derivation of (1.8) and (1.11) has been given by Dettmann²³, however, without consideration of the surface terms. These surface terms indeed vanish for the case of $H_i = H_{i0}$ and $H_f = H_{f0}$. Then the distorted waves are identical to the asymptotic states φ_i , φ_f and one has

$$a_{fi}^{D+} = -a_{fi}^{D-} = -i \int_{-\infty}^{\infty} dt \langle \varphi_f(t) | V_i - V_f | \varphi_i(t) \rangle = 0. \quad (1.12)$$

In the general case ($H_i \neq H_{i0}$, $H_f \neq H_{f0}$) however, the surface terms describe the transfer resulting from the perturbation $\hat{V}_i - V_i$ and $\hat{V}_f - V_f$ in the entrance and exit channel, respectively²¹.

1.2. Discussion of the Potentials

The formulas for the transition amplitude as well as the subsequent approximations are, strictly speaking, only valid for short-range potentials. In the following the difficulties related to the Coulomb character of the actual potentials are discussed. Also the influence of the nucleus-nucleus interaction on the transfer cross section is studied, as well as the occurrence of recoil forces.

1.2.1. Long-range atomic potentials

For Coulombic potentials which behave like r^{-1} for large distances, the formal series expansions do not in general converge. In order to avoid such problems one may treat the long-range part separately⁸ such that the remaining potentials decay at least like r^{-2} which is sufficient for the convergence of the series. Let us demonstrate this for the case of the entrance channel where the perturbation V_i contains the Coulomb interaction V_p of the electron with the projectile. We take the splitting $H_e = H_i + \hat{V}_i$ in the following way

$$H_i = H_{i0} + W_i, \quad \hat{V}_i = V_i - W_i, \quad W_i = -Z_p/R. \quad (1.13)$$

For infinite separation of the nuclei $R \rightarrow \infty$, one has $r_p \approx R$ (where r_p is the distance between the projectile and target-bound electron, cf. Fig. 1), and V_p is compensated by $-W_i$. For large but finite separation, $V_p - W_i$ and thus \hat{V}_i behaves like $V_p - W_i \approx -Z_p \mathbf{r} \cdot \mathbf{R} / R^3 \sim R^{-2}$, such that the appearance of logarithmically diverging phases are avoided. On the other hand, it is easily possible to construct eigenfunctions to H_i from (1.13) if the solutions φ_i to H_{i0} are known. Inserting the ansatz

$$\chi_i^{(+)} = e^{iS(t)} \varphi_i \quad (1.14)$$

into the time-dependent Schrödinger equation (1.7), the phase $S(t)$ is, in the case of a straight-line path with impact parameter b , $\mathbf{R} = \mathbf{b} + \mathbf{v}t$, determined from

$$S(t) = - \int dt W_i = - \frac{Z_p}{v} \ln (vR - v^2 t). \quad (1.15)$$

A straight-line path is in most cases a good approximation for high collision velocities v . But even for a Rutherford trajectory, $S(t)$ can be evaluated analytically¹². A similar phase

transformation can be performed for the final channel, such that both \hat{V}_i and \hat{V}_f are made short-range. This procedure has, however, the drawback that these potentials are often not physical in the interaction region and, more severely, that difficulties arise in their use as expansion parameters, because cancellations can occur in the lowest-order expansion terms, which lead to an incorrect behavior of the differential capture cross section.

Other ways out of the Coulomb-tail dilemma consist in using potentials which are ultimately screened; however, this leaves the ambiguity with respect to the determination of the screening parameter. For incomplete screening, the remaining Coulomb tails pose the same problems as in the pure Coulomb case²⁴. Alternatively, the divergence problems may be circumvented by working with wave functions and matrix elements which are off the energy shell¹ and which have the required convergence properties such that series expansions do exist in the mathematical sense. The physical quantities are obtained by eventually performing the on-shell limit²⁵. We shall return to these methods in a subsequent section.

1.2.2. Nuclear potential

In the semiclassical formulation the internuclear potential enters only into the definition of the classical trajectory, and a quantum mechanical theory is necessary to estimate a further influence. Like in the semiclassical case, the nuclear force should not appear in the transition operator, as long as nuclear reactions play no role, and it should not be mixed up with corrections of the type W_i from (1.13) for the Coulomb tail. However, the internuclear interaction is contained in the asymptotic states which are eigenfunctions of both the electronic and the nuclear Hamiltonian. Using the asymptotic form of the nuclear Coulomb waves, this results in an additional phase of the transition amplitude⁸

$$a_{fi}^C = a_{fi}(\mu_i v b)^{2i\eta}, \quad \eta = Z_p Z_T / v. \quad (1.16)$$

For total cross sections this phase is of no consequence. However, the calculation of differential cross sections requires in the quantum mechanical treatment an integration over b which is the component of \mathbf{R} perpendicular to the velocity²⁶

$$\frac{d\sigma}{d\Omega} = \left| i\mu_i v \int_0^\infty db b^{1+2i\eta} J_m(2\mu_i b v \sin \vartheta/2) a_{fi} \right|^2. \quad (1.17)$$

The scattering angle is denoted by ϑ , and $m \geq 0$ is the difference between the magnetic quantum numbers of the electronic states in the initial and final channel. For large arguments, the Bessel function J_m can be approximated by its asymptotic form. Applying the method of stationary phase, (1.17) reduces to the semiclassical formula²⁷

$$\frac{d\sigma}{d\Omega} = |a_{fi}(b)|^2 \frac{d\sigma^{\text{Ruth}}}{d\Omega}, \quad b = \frac{\eta}{\mu_i v} \cot \vartheta/2. \quad (1.18)$$

$d\sigma^{\text{Ruth}}/d\Omega$ is the Rutherford cross section. As quasi-elasticity ($\Delta E \ll E_i$) and small scattering angles are already required for the formulas (1.16) and (1.17) to hold, the

additional condition for the applicability of the stationary phase approximation imposes the following restriction on the validity of the semiclassical theory

$$\frac{1}{\mu_i v} \ll \vartheta \ll 1. \quad (1.19)$$

Strictly speaking, (1.18) assumes the calculation of a_{fi} with a straight-line path for \mathbf{R} . The generalization to Coulomb trajectories is trivial, but then there is no longer such a simple relation to the quantum mechanical results.

A numerical investigation²⁷ shows that the equations (1.17) and (1.18) lead to identical results for small impact parameters (i.e. large scattering angles). The deviations at large impact parameters result from a different decrease of the transfer probability $P(b)$ with b : asymptotically, the quantum mechanical theory postulates a b^{-4} dependence (which is the dependence of the Rutherford cross section) while the semiclassical theory gives a nearly exponential decrease. The two theories are compared in Fig. 2 for electron capture from the Ar K-shell by 6 MeV protons within several atomic models (to be discussed later), and deviations emerge only at rather high b .

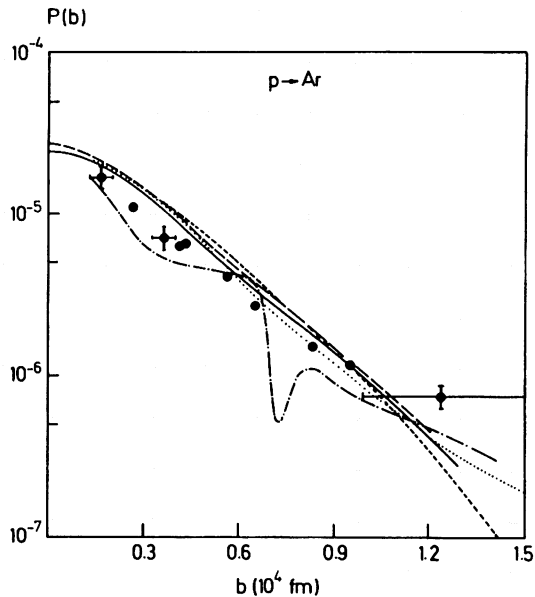


Fig. 2. Capture probability from the Ar K-shell in collisions with 6 MeV protons as a function of impact parameter. The experimental data \bullet (Cocke *et al.*²⁸) are compared with theories for K-K capture. Quantum mechanical calculations: - · - · - CDW (Belkić *et al.*²⁹), · · · · BK (Belkić *et al.*²⁹). Semiclassical theories: — IA (Jakubaša-Amundsen and Amundsen³⁰), — — — SPB (Alston³¹), - - - - BK (Greenland²⁷).

1.2.3. Recoil

If the selected frame of reference does not agree with the center-of-mass system, the electronic Hamiltonian contains a recoil potential. The only exception is the case of a rectilinear nuclear trajectory where an arbitrary translation along \mathbf{R} again leads to an inertial frame. The recoil potential can be obtained by means of a transformation from the center-of-mass system to the selected reference frame, i.e. by means of the operator \hat{U} from (1.2) with the choice $x_i = M_P R / (M_P + M_T)$. An application of \hat{U} to the Schrödinger equation (1.5) yields the transformation formula for H_e

$$H_e \rightarrow H'_e = \hat{U} H_e \hat{U}^+ - i \hat{U} \partial_t \hat{U}^+ . \quad (1.20)$$

The evaluation of H'_e is most easily achieved if \hat{U} is split into its three exponential factors, $\hat{U} = \hat{U}_3 \hat{U}_2 \hat{U}_1$, and if the corresponding transformations are carried out successively¹⁹. With $H_e = T_e + W(\mathbf{r}, t)$ it follows

$$\begin{aligned} H'_e &= \hat{U}_3 \hat{U}_2 [T_e + W(\mathbf{r}' + \alpha \mathbf{R} - \mathbf{x}_f, t) - (\alpha \dot{\mathbf{R}} - \dot{\mathbf{x}}_f) \mathbf{p} - i \partial_t] \hat{U}_2^+ \hat{U}_3^+ \\ &= T_e + W(\mathbf{r}' + \alpha \mathbf{R} - \mathbf{x}_f, t) + V_R; \quad V_R = (\alpha \ddot{\mathbf{R}} - \ddot{\mathbf{x}}_f) \mathbf{r}' \end{aligned} \quad (1.21)$$

with $\alpha = M_T / (M_P + M_T)$. H'_e contains, apart from a coordinate transformation in the potential W , an additional term V_R which is determined by the acceleration. In two special cases,

- (a) the transformation into the target system ($x_f = R$),
- (b) the transformation into the projectile system ($x_f = 0$),

this recoil field is explicitly

$$V_R = \begin{cases} -M_P / (M_P + M_T) \ddot{\mathbf{R}} \mathbf{r}_T, & \text{case (a)} \\ M_T / (M_P + M_T) \ddot{\mathbf{R}} \mathbf{r}_P, & \text{case (b)} \end{cases} \quad (1.22)$$

In many cases, the charge transfer which originates from this potential cannot be neglected. At large scattering angles, the recoil contribution may even be the dominant one ("knock-on" capture³²).

1.3. Approximations to the Transition Amplitude

During the course of time many high-energy approximations have been introduced. They were often closely related to the problem under investigation. A consistent derivation of these approaches from the formal theory, allowing for an estimate of their validity, was given only much later. The connection between some of the methods is presented in recent publications^{7,33,34}. In the following, the derivation and interrelation between all current high-energy theories is carried through, that is to say the Born series, the continuum distorted wave series (CDW), the strong potential Born approximation (SPB), the impulse approximation (IA), the distorted-wave Born approximation (DWB) and the eikonal theory (E). All methods are either based on an expansion in terms of one (or both) of the electron-nucleus potentials, or in terms of gradient terms which relate to the kinetic energy.

Before formulating the theories, some important propagator relations are mentioned. In these relations, surface terms which arise from the partial integrations implemented in the derivation are neglected. Therefore, these relations hold, strictly speaking, only for short-range potentials. For an arbitrary splitting of H_e , $H_e = H_\lambda + V_\lambda$, the retarded ($G_\lambda^{(+)}$) and the advanced ($G_\lambda^{(-)}$) Greens functions to H_λ can be defined by

$$(i\partial_t - H_\lambda(t))G_\lambda^{(\pm)}(t, t') = \delta(t - t') \quad (1.23)$$

with their interrelation $[G_\lambda^{(-)}(t, t')]^+ = G_\lambda^{(+)}(t', t)$. For a time-independent H_λ , their spectral representation reads²³

$$G_\lambda^{(\pm)}(t, t') = \frac{\hbar}{2\pi} \int d\omega \frac{1}{\omega - H_\lambda \pm i\varepsilon} e^{-i\omega(t-t')}, \quad \varepsilon \rightarrow +0. \quad (1.24)$$

An operator related to G_λ is the time-development operator \hat{P}_λ which is defined through $\chi_\lambda(t) = \hat{P}_\lambda(t, t')\chi_\lambda(t')$ where χ_λ is solution to H_λ . With the help of (1.24), the following relation can be derived for time-independent potentials²³

$$G_\lambda^{(+)}(t, t') = -i\Theta(t - t')\hat{P}_\lambda(t, t') \quad (1.25)$$

where Θ is the Heaviside step function. It can be shown that this relation holds also for time-dependent potentials. From G_λ , the Greens function G of the complete H_e can be constructed,

$$\begin{aligned} G(t, t') &= G_\lambda(t, t') + \int d\tau G_\lambda(t, \tau)V_\lambda(\tau)G(\tau, t') \\ &= G_\lambda(t, t') + \int d\tau G(t, \tau)V_\lambda(\tau)G_\lambda(\tau, t'), \end{aligned} \quad (1.26)$$

and correspondingly, the Lippmann-Schwinger equation holds for the exact wave function ψ

$$\psi(t) = \chi_\lambda(t) + \int dt' G(t, t')V_\lambda(t')\chi_\lambda(t'). \quad (1.27)$$

All these relations may be verified through the application of $i\partial_t - H_e$ on both sides of the equations.

1.3.1. Born series

The Born series is an expansion of the transition amplitude in terms of the asymptotic perturbations V_i and V_f . As to each order, V_i and V_f enter in a symmetric way, this method is especially suited for near-symmetric collision systems ($Z_p \approx Z_T$).

With the splitting $H_e = H_{i0} + V_i = H_{f0} + V_f$, the prior form (1.11) of the transition amplitude reads

$$a_{fi} = -i \int_{-\infty}^{\infty} dt \langle \psi_f^{(-)}(t) | V_i(t) | \varphi_i(t) \rangle \quad (1.28)$$

because the surface term vanishes. For the sake of simplicity, we restrict ourselves to a recoil-free motion, such that the total potential W is

$$\begin{aligned} W(t) &= V_i + V_f; & V_i &= V_P \\ & & V_f &= V_T \end{aligned} \quad (1.28a)$$

where V_P denotes the electron-projectile and V_T the electron-target interaction. For the series representation of the exact state $\psi_f^{(-)}$, Eq. (1.27) is used with the choice $V_\lambda = V_f$, and the Greens function G is expressed in terms of the free Greens function G_0 by means of the relation (1.26) with H_λ set equal to T_e . Thus

$$\begin{aligned} \psi_f^{(-)}(t) &= \varphi_f(t) + \int d\tau G_0^{(-)}(t, \tau) V_f(\tau) \varphi_f(\tau) \\ &+ \int d\tau dt' G_0^{(-)}(t, t') [V_i(t') + V_f(t')] G^{(-)}(t', \tau) V_f(\tau) \varphi_f(\tau). \end{aligned} \quad (1.29)$$

Upon expressing G successively in terms of G_0 and inserting this expansion into the transition amplitude (1.28), the Born series is recovered. The second-order Born approximation^{10,35} comprises the first two terms of (1.29)

$$\begin{aligned} a_{fi}^{(1+2)} &= a_{fi}^{\text{BK}} + a_{fi}^{(2)}, & a_{fi}^{\text{BK}} &= -i \int dt \langle \varphi_f(t) | V_i(t) | \varphi_i(t) \rangle \\ a_{fi}^{(2)} &= -i \int d\tau \int dt \langle \varphi_f(\tau) | V_f(\tau) G_0^{(+)}(\tau, t) V_i(t) | \varphi_i(t) \rangle \end{aligned} \quad (1.30)$$

where a_{fi}^{BK} is the Brinkman-Kramers (BK) approximation³⁶. The evaluation of a_{fi}^{BK} is simple and shall not be repeated here. The time integrals in $a_{fi}^{(2)}$ extend formally over the whole region ($-\infty < t, \tau < +\infty$); if, however, G_0 is expressed in terms of \hat{P}_0 by means of (1.25), the restriction $t \leq \tau$ becomes obvious. For further evaluation, one has to insert the projectile final state after its transformation to the target frame of reference (using \hat{U} from (1.2) with $x_i = x_f = 0$)

$$\varphi_f(t) = \hat{U}^+ \varphi_f'(t) = e^{i\dot{\mathbf{R}}\mathbf{r}_T} e^{-i\dot{\mathbf{R}}\mathbf{R}} \exp\left(\frac{i}{2} \int^t \dot{\mathbf{R}}^2 dt\right) \varphi_f'(\mathbf{r}_T - \mathbf{R}, t). \quad (1.31)$$

We introduce the Fourier transform

$$e^{i\dot{\mathbf{R}}\mathbf{r}_T} \varphi_f'(\mathbf{r}_T - \mathbf{R}, t) = e^{i\dot{\mathbf{R}}\mathbf{R}} \int d\mathbf{k} |\mathbf{k}\rangle e^{-i\mathbf{k}\mathbf{R}} \tilde{\varphi}_f'(\mathbf{k} - \dot{\mathbf{R}}, t) \quad (1.32)$$

where $|\mathbf{k}\rangle = (2\pi)^{-3/2} \exp(i\mathbf{k}\mathbf{r}_T)$ and $\tilde{\varphi}$ the momentum representation of φ , and make use of the spectral representation (1.24) of the free Greens function (with $H_\lambda = T_e$). If a complete set of plane waves $|\mathbf{q}\rangle$ is introduced behind $G_0^{(+)}$ in (1.30) and use is made of the time-independence of V_f in the target frame, one finds

$$a_{fi}^{(2)} = -i \int d\mathbf{q} d\mathbf{k} \langle \mathbf{k} | V_f | \mathbf{q} \rangle e^{i\mathbf{k}\mathbf{b}} \tilde{\varphi}'^*(\mathbf{k} - \mathbf{v}) \frac{1}{\epsilon_f + \mathbf{k}\mathbf{v} - v^2/2 - q^2/2 + i\epsilon} \times \int_{-\infty}^{\infty} dt e^{i(\epsilon_f + \mathbf{k}\mathbf{v} - v^2/2)t} \langle \mathbf{q} | V_i(t) | \varphi_i(t) \rangle \tag{1.33}$$

where ϵ_f is the energy of the state φ'_f and a straight-line path has been taken for \mathbf{R} .

In a similar way, the third Born term (arising from the third term of (1.29) with G replaced by G_0) can be evaluated^{22,35,37}, and so on. Up to now, only the second Born term has been calculated numerically without approximations^{38,39}. If a full-peaking type approximation is applied to (1.33) which bases on the fact that the momentum function $\varphi'_f(\mathbf{k} - \mathbf{v})$ is strongly peaked at $\mathbf{k} = \mathbf{v}$, the high-energy behavior of the second^{35,40,41} and third^{35,37} Born approximation can be extracted. A v^{-12} dependence is found for the Brinkman-Kramers cross section for $K-K$ capture, while the second Born approximation contains an additional v^{-11} term, which is not altered by the third Born approximation. The dominance of the second Born theory over the first-order BK theory emerges, however, only at velocities which make a relativistic description necessary.

At nonrelativistic velocities, the BK theory overestimates the experimental capture cross sections up to a factor of three. Recent investigations have aimed at correcting for this deficiency not by the second Born, but by taking the Coulomb boundary conditions into account. If the Coulomb tails of V_i and V_f are eliminated by a phase transformation as discussed in Sec. 1.2.1, the initial and final states are changed into

$$\chi_i^{(+)\text{B}} = \varphi_i e^{-i(Z_P/v) \ln(vR - v^2t)} ; \quad \chi_f^{(-)\text{B}} = \varphi_f e^{i(Z_T/v) \ln(vR + v^2t)} . \tag{1.34}$$

This gives the following representation of the exact scattering function in place of (1.29):

$$\psi_f^{(-)}(t) = \chi_f^{(-)\text{B}}(t) + \int d\tau G^{(-)}(t, \tau) \left[V_T(\tau) + \frac{Z_T}{R(\tau)} \right] \chi_f^{(-)\text{B}}(\tau) , \tag{1.35}$$

which leads to the boundary-corrected Born series if $G^{(-)}$ is iterated in terms of $G_0^{(-)}$. The first term of this series, the boundary corrected (B) first-order theory⁴² (also called ‘‘true first Born’’⁴³) is given by

$$a_{fi}^{\text{B}1} = -i \int dt \langle \chi_f^{(-)\text{B}}(t) | V_i + \frac{Z_P}{R} | \chi_i^{(+)\text{B}}(t) \rangle . \tag{1.36}$$

This expression leads to a rather good agreement with the data as far as total cross sections are concerned (cf. Figs. 3 and 4). However, in the scattering-angle dependence a spurious

dip will occur, which arises from the mutual cancellation of the two transition operators in (1.36). This deficiency is well-known from the special case of $p + H$ collisions³⁸, where an erroneous inclusion of the nucleus-nucleus potential into the BK theory accidentally leads to an expression identical to (1.36). Another deficiency of the boundary-corrected first-order theory is of course its wrong asymptotic velocity dependence. In order to overcome these difficulties, the boundary-corrected second Born theory has to be evaluated³⁸. This theory agrees somewhat better with experimental data than the standard second Born approximation (1.30) at the lower collision velocities⁴⁴.

1.3.2. *Continuum Distorted Wave series (CDW)*

Another theory which is suited for symmetric collision systems has been developed by Cheshire⁴⁵. In contrast to the Born series, this theory is built upon distorted waves χ_i, χ_f which include the perturbation in the entrance and exit channel. A formulation with distorted waves aims at a good approximation for the transition amplitude already with the lowest-order expansion term of the series.

Let us write the potentials \hat{V}_i and \hat{V}_f of (1.6) in the following general form⁴⁶

$$\hat{V}_i = (H_e - i\partial_t)|\chi_i^{(+)}\langle\chi_i^{(+)}|, \quad \hat{V}_f = (H_e - i\partial_t)|\chi_f^{(-)}\langle\chi_f^{(-)}|. \quad (1.37)$$

The CDW theory emerges from the special choice of distorted waves which include both the projectile and the target field to all orders. This choice aims at a fast convergence of the series because the long-range Coulomb interactions are avoided in \hat{V}_i and \hat{V}_f .

The distorted waves are constructed as product of a bound-state function to one potential and a continuum function to the other field. If a frame centered at the midpoint between projectile and target nucleus is taken as the reference frame, a corresponding transformation \hat{U} is necessary (with $x_i = 0, x_f = R/2$ for $\chi_i^{(+)}$ and $x_i = R, x_f = R/2$ for $\chi_f^{(-)}$ in (1.2)). Explicitly, the distorted waves are^{45,47}

$$\begin{aligned} \chi_i^{(+)}(\mathbf{r}_P, \mathbf{r}_T) &= e^{-iv^2t/8 - iv\mathbf{r}'/2 - i\epsilon_f t} \varphi_i(\mathbf{r}_T) \hat{\psi}_{-v}^{(+)}(Z_P, \mathbf{r}_P), \\ \chi_f^{(-)}(\mathbf{r}_P, \mathbf{r}_T) &= e^{-iv^2t/8 + iv\mathbf{r}'/2 - i\epsilon_f t} \varphi_f(\mathbf{r}_P) \hat{\psi}_v^{(-)}(Z_T, \mathbf{r}_T), \end{aligned} \quad (1.38)$$

$$\hat{\psi}_v^{(\pm)}(Z, \mathbf{r}) = e^{\pi Z/2\nu} \Gamma(1 \mp iZ/\nu) {}_1F_1(\pm iZ/\nu, 1, \pm ivr - iv\mathbf{r}),$$

where \mathbf{r}' is the coordinate with respect to the midpoint and ${}_1F_1$ is a confluent hypergeometric function. The functions $\hat{\psi}_{-v}^{(+)}$ and $\hat{\psi}_v^{(-)}$ are proportional to incoming and outgoing Coulomb waves, respectively. However, the distorted waves (1.38) are not exact solutions to H_e because of the nonorthogonality of the coordinates \mathbf{r}_P and \mathbf{r}_T . Upon acting with the Schrödinger operator onto χ_i , gradient terms remain as residual interaction⁴⁷

$$(H_e - i\partial_t)\chi_i^{(+)}(\mathbf{r}_P, \mathbf{r}_T) = -[\nabla_{\mathbf{r}_T} \varphi_i(\mathbf{r}_T) \nabla_{\mathbf{r}_P} \hat{\psi}_{-v}^{(+)}(Z_P, \mathbf{r}_P)] e^{-iv^2t/8 - iv\mathbf{r}'/2 - i\epsilon_f t}. \quad (1.39)$$

A similar equation holds for χ_f . The gradient terms, i.e. the deviation from the exact solution, diminish with increasing velocity.

If the exact wavefunction $\psi_f^{(-)}(t)$ is expressed with the help of the Lippmann-Schwinger equation (1.27) inserting χ_f for χ_λ , the prior form (1.11) of the transition amplitude can be written in the following way

$$a_{fi} = a_{fi}^{D-} - i \int dt \langle \chi_f^{(-)}(t) | H_e - i\partial_t | \chi_i^{(+)}(t) \rangle - i \int dt d\tau \langle \chi_f^{(-)}(\tau) | (H_e - i\partial_\tau) G^{(+)}(\tau, t) (H_e - i\partial_t) | \chi_i^{(+)}(t) \rangle. \quad (1.40)$$

The CDW series is obtained by iterating G in terms of G_0 . The standard CDW theory is given by the first term of this series which upon insertion of (1.38) and (1.39) reads

$$a_{fi}^{CDW1} = i \int dt e^{i(\varepsilon_f - \varepsilon_i)t} \langle \varphi_f(\mathbf{r}_P) \hat{\psi}_v^{(-)}(Z_T, \mathbf{r}_T) | e^{-i\nu(\mathbf{r}_P + \mathbf{r}_T)/2} \times \nabla_{\mathbf{r}_T} \varphi_i(\mathbf{r}_T) \nabla_{\mathbf{r}_P} \hat{\psi}_v^{(+)}(Z_P, \mathbf{r}_P) \rangle. \quad (1.41)$$

The surface term a_{fi}^{D-} vanishes because $\chi_i^{(+)}$ contains the target state φ_i as a factor⁴⁸. At asymptotically high velocities the standard CDW theory for $K-K$ transfer has the same velocity dependence as the second Born approximation⁴⁵. However, the high-energy behavior is only correct for total capture cross sections, whereas the differential cross section exhibits a spurious dip (cf. Fig. 2). Like in the case of the boundary corrected Born series, one can cope with this deficiency by including the second term of the CDW series which is obtained from (1.40) if G is replaced by G_0 . Only then is the second-order Born approximation completely incorporated⁴⁶. Note that the Coulomb boundary conditions are from the outset satisfied in the CDW theory through the specific choice of the distorted waves: upon expanding the hypergeometric functions for large arguments, $\chi_i^{(+)}$ and $\chi_f^{(-)}$ from (1.38) are found to agree at asymptotically large distances R with $\chi_i^{(+)B}$ and $\chi_f^{(-)B}$ from (1.34), respectively, because then $\mathbf{r}_P \rightarrow -\mathbf{R}$ and $\mathbf{r}_T \rightarrow \mathbf{R}$, respectively. Hence, it seems that an inclusion of the Coulomb boundary conditions is only possible at the expense of an insufficiency of the first-order term of the corresponding series expansion.

1.3.3. Strong Potential Born Theory (SPB)

For strongly asymmetric collision systems (and we shall assume that $Z_P < Z_T$) the weak electron-projectile field V_P can serve as a natural expansion parameter for the transition operator; it is, however, crucial that the expansion is only carried so far that the boundary condition at $t \rightarrow \infty$ (where the electron is in a projectile eigenstate) is not violated^{30,49}. As starting point for the derivation of the SPB theory we take the transition amplitude in its prior form (1.11), and use the decomposition $H_e = H_{i0} + V_i = H_{f0} + V_f$ in the following form (including recoil)

$$H_{i0} = T_e + V_T, \quad V_i = V_P - (M_P/M)\ddot{\mathbf{R}}\mathbf{r}_T \\ H'_{f0} = T'_e + V'_P + (M_T/M)\ddot{\mathbf{R}}\mathbf{r}_P, \quad V_f = V_T \quad (1.42)$$

with $M = M_P + M_T$. We have given H_{f0} in the projectile reference frame to demonstrate that for $\dot{\mathbf{R}} \neq 0$, the recoil potential (1.22) is not small and has to be included in the definition of the final state φ_f . In contrast, in the target frame of reference, the recoil is approximately proportional to Z_P and therefore of the same order as V_P . This means that V_i can serve as expansion parameter.

The exact wavefunction is expanded in the following way

$$\psi_f^{(-)}(t) = \chi_f^{(-)\text{SPB}}(t) + \int dt' d\tau G_{i0}^{(-)}(t, \tau) V_i(\tau) G^{(-)}(\tau, t') V_f(t') \varphi_f(t'), \quad (1.43)$$

$$\chi_f^{(-)\text{SPB}}(t) = \varphi_f(t) + \int dt' G_{i0}^{(-)}(t, t') V_f(t') \varphi_f(t'),$$

where the function $\chi_f^{(-)\text{SPB}}$ is of zeroth order in the weak field V_P , and $G_{i0}^{(-)}$ is the Greens function relating to H_{i0} . The SPB approximation for the capture amplitude is obtained by insertion of $\chi_f^{(-)\text{SPB}}$ into (1.11):

$$a_{fi}^{\text{SPB}} = -i \int dt \langle \chi_f^{(-)\text{SPB}}(t) | V_i(t) | \varphi_i(t) \rangle. \quad (1.44)$$

From this formulation it is clear that the Brinkman-Kramers amplitude (which is obtained if $\chi_f^{(-)\text{SPB}}$ is replaced by $\varphi_f(t)$) is not the only term which is of first order in V_P , but there appears an additional scattering term. Hence, it is not surprising that asymptotically, the SPB theory does not reduce to the first-order, but to the second-order Born approximation.

The calculation of $\chi_f^{(-)\text{SPB}}$ can be achieved by using the spectral representation (1.24) of the Greens function $G_{i0}^{(-)}$ and by inserting (1.31) and (1.32) for the final state function $\varphi_f(t)$

$$\chi_f^{(-)\text{SPB}}(t) = \frac{1}{2\pi} \int d\mathbf{k} d\tau d\omega e^{-i\omega(t-\tau)} e^{-i\mathbf{k}\mathbf{R}} e^{(i/2) \int \dot{\mathbf{R}}^2 d\tau} \tilde{\varphi}'_f(\mathbf{k} - \dot{\mathbf{R}}, \tau) \psi_{\mathbf{k},\omega}^{(-)}. \quad (1.45)$$

The wave function $\psi_{\mathbf{k},\omega}^{(-)}$ is an off-shell function with energy ω . It is defined through the relation⁵⁰

$$(\omega - H_{i0} - i\varepsilon) \psi_{\mathbf{k},\omega}^{(-)} = (\omega - k^2/2 - i\varepsilon) |\mathbf{k}\rangle, \quad \varepsilon \rightarrow +0. \quad (1.46)$$

In the case of a non-linear nuclear trajectory, the reduction of the multiple integral (1.45) is no longer trivial because the recoil potential introduces a complicated time-dependence into $\tilde{\varphi}'_f(\mathbf{k} - \dot{\mathbf{R}}, \tau)$, and one has to resort to further approximations⁵¹. In the following we shall restrict ourselves to a recoil-free trajectory which is a good high-energy approximation for total cross sections, and also for differential cross sections at small scattering angles. In this case the time-dependence of $\tilde{\varphi}'_f$ is given exclusively by the

energy phase $\exp(-i\varepsilon_f\tau)$, and the τ -integral in (1.45) reduces to a δ -function, which makes the ω -integration trivial. The transition amplitude (1.44) thus becomes³⁰

$$a_{fi}^{\text{SPB}} = -i \int dt \int d\mathbf{k} e^{i\mathbf{k}\cdot\mathbf{b}} e^{i(E_f(\mathbf{k}) - \varepsilon_f)t} \tilde{\varphi}_f'^*(\mathbf{k} - \mathbf{v}) \langle \psi_{\mathbf{k}, E_f(\mathbf{k})}^{(-)}(\mathbf{r}_T) | V_i(t) | \varphi_i(\mathbf{r}_T) \rangle, \quad (1.47)$$

$$E_f(\mathbf{k}) = \mathbf{k}\mathbf{v} + \varepsilon_f - \frac{1}{2}v^2.$$

It is composed of two parts, the excitation of the target electron through the potential V_i into an intermediate continuum state in the target field, and the subsequent capture into a projectile state which is expressed through the folding with the projectile momentum function $\tilde{\varphi}_f'$.

Although the SPB theory goes beyond the second-order Born approximation as it includes the strong target field to all orders, and should thus have a larger region of applicability, it suffers—in contrast to the Born series—from a divergence in the elastic scattering contribution which originates from the long range of the Coulomb interaction⁵². In order to isolate this divergence a complete set of eigenstates φ_{n0} to H_{i0} is inserted into the SPB amplitude (1.44):

$$a_{fi}^{\text{SPB}} = -i \int dt \langle \varphi_f(t) | V_i(t) | \varphi_i(t) \rangle - i \sum_{n_0} \int dt d\tau \langle \varphi_f(\tau) | V_f(\tau) G_{i0}^{(+)}(\tau, t) | \varphi_{n0}(t) \rangle \langle \varphi_{n0}(t) | V_i(t) | \varphi_i(t) \rangle. \quad (1.48)$$

If the representation (1.25) of G_{i0} in terms of the time-development operator \hat{P}_{i0} is used, it becomes evident that the τ -integral contains the following term

$$\int_{-\infty}^{\tau} dt \langle \varphi_{n0}(t) | V_i(t) | \varphi_i(t) \rangle \quad (1.49)$$

which is the amplitude for the scattering into the states φ_{n0} . In the case of elastic scattering, $\varphi_{n0} = \varphi_i$, the integrand of (1.49) behaves like $1/R$ for $|t| \rightarrow \infty$, which means that (1.49) diverges logarithmically at the lower limit $t \rightarrow -\infty$.

Several methods to avoid such singularities have been suggested in the literature. The most obvious one is to use the boundary-corrected version⁵² of the strong potential Born theory (BSPB) which can be constructed in complete analogy to the case of the Born series, leading to the following transition amplitude

$$a_{fi}^{\text{BSPB}} = -i \int dt \langle \chi_f^{(-)\text{BSPB}}(t) | V_i(t) + Z_P/R | \chi_i^{(+)\text{B}}(t) \rangle \quad (1.50)$$

$$\chi_f^{(-)\text{BSPB}}(t) = \chi_f^{(-)\text{B}}(t) + \int d\tau G_{i0}^{(-)}(t, \tau) \left[V_f(\tau) + \frac{Z_T}{R} \right] \chi_f^{(-)\text{B}}(\tau)$$

It is easy to verify that in this case, the transition operator V_i in (1.49) is replaced by $V_i + Z_P/R$, and the integral converges. Also the BSPB theory is a consistent first-order theory in the projectile field. It has, however, the drawback that $G_{i0}^{(-)}(t, \tau)(V_T + Z_T/R)$ can no longer be accounted for by means of a single off-shell function; instead, one has to introduce a complete set of target eigenstates, which makes the calculation much more involved. A more promising method has been put forward by Macek²⁵ who suggests working with off-shell matrix elements (which are unphysical, but well defined for long-range potentials), and only eventually to perform the on-shell limit when calculating physical quantities such as the transition probability. In the on-shell limit $\omega \rightarrow k^2/2$, the wave function $\psi_{\mathbf{k},\omega}^{(-)}$ from (1.46) behaves like⁵³

$$\psi_{\mathbf{k},\omega}^{(-)}(\mathbf{r}_T) \rightarrow g(k, \omega)\varphi_{\mathbf{k}}(\mathbf{r}_T), \quad g(k, \omega) = \left[\frac{2\omega - i\varepsilon - k^2}{4(2\omega - i\varepsilon)} \right]^{i\eta_T} \Gamma(1 - i\eta_T)e^{-\pi\eta_T/2} \quad (1.51)$$

with $\eta_T = Z_T/k$ and $\varphi_{\mathbf{k}}$ a continuum eigenstate to $H_{i0} = T_e + V_T$. Like for two particles, an off-shell function may also be defined for the scattering of three particles, with its on-shell limit governed by a factor g in complete analogy to (1.51). Rather than calculating the transition probability from the on-shell expression (1.8), $\psi_i^{(+)}$ is replaced by the off-shell function multiplied with the corresponding renormalization factor g^{-1} (such that the on-shell limit exists). The main difference to the standard SPB theory lies in the fact that not only the wave function, but also the factor g^{-1} is expanded in terms of the weak field V_P . Thus, one obtains additional terms by which the divergence is cancelled. The advantage of this approach as compared to the boundary-corrected SPB lies in the fact that as for the standard SPB, the transition amplitude can be evaluated by means of a single intermediate off-shell state, and that the structure of the additional terms is very simple. However, while the standard SPB is a first-order theory in V_P as it is derived from the systematic expansion (1.43) of the scattering states in terms of the weak field, the off-shell corrected SPB (OSPB) contains contributions which are of second order in V_P , arising from the expansion of the renormalization factor:

$$a_{fi}^{\text{OSPB}} = -i \int dt \langle \chi_f^{(-)\text{SPB}}(t) | V_P(t) | \varphi_i(t) \rangle - i \int dt \langle \varphi_f(t) | V_P(t) | \varphi_i(t) \rangle \frac{Z_P}{v} \left[i\psi(1) + \frac{\pi}{2} - i \ln \left| \frac{E - E_T}{4(E - \varepsilon_i)} \right| \right] \quad (1.52)$$

with $E \rightarrow E_T = K^2/2 + \varepsilon_i$ where $K^2/2$ is the energy of the relative nuclear motion and $\psi(1)$ the digamma function of argument one. From this one may draw the conclusion that unphysical divergences originate from an insufficient inclusion of the coupling to the weak field. It should be stressed, however, that divergences do not occur in the near-shell limit of the SPB, where (1.51) is used in place of the exact intermediate off-shell state⁵⁴, or in the on-shell limit (to be discussed in the next subsection), and also not in more realistic cases with several target electrons, if inner and outer screening is properly taken

into account⁵⁵. Only if such nondivergent models differ considerably from experiment and from each other, higher-order contributions will indeed be important.

1.3.4. Impulse approximation and its peaking versions

Historically, the impulse approximation (IA) has been obtained from the intuitive assumption that in fast collisions with light projectiles, charge transfer is basically described as ejection of an electron with velocity close to the projectile velocity \mathbf{v} . The allowed velocity spread of the electron is determined from the momentum distribution of the bound final state. This consideration leads to the transition amplitude^{40,56,57}

$$a_{fi}^{IA} = -i \int dt \int d\mathbf{k} e^{i\mathbf{k}\cdot\mathbf{b}} e^{i(E_f(\mathbf{k}) - \epsilon_i)t} \tilde{\varphi}'_f^*(\mathbf{k} - \mathbf{v}) \langle \varphi_{\mathbf{k}}(\mathbf{r}_T) | V_i(t) | \varphi_i(\mathbf{r}_T) \rangle. \quad (1.53)$$

A comparison with (1.47) reveals that the impulse approximation is obtained from the SPB theory by merely replacing the off-shell state $\psi_{\mathbf{k}, E_f(\mathbf{k})}^{(-)}$ by an (on-shell) target Coulomb wave $\varphi_{\mathbf{k}}$, hence neglecting the energy difference $E_f(\mathbf{k}) - k^2/2$. The reasoning that this is legal for $Z_P \ll Z_T$ because the neglected contribution is of second order in V_P , should be taken with care for Coulomb potentials: from (1.51) it is obvious that the convergence of the off-shell state to the on-shell one is non-uniform, because $g(k, E_f(\mathbf{k}))$ is Z_T -dependent and does not tend to unity for $Z_P/Z_T \rightarrow 0$. The IA treats the boundary condition $\epsilon_f \neq 0$ incorrectly, and is thus not a consistent first-order theory in V_P . However, for high velocities the deviations between IA and SPB are generally rather small (cf. Fig. 2 and Sec. III).

Several peaking approximations have been introduced for the evaluation of (1.53) and related expressions. All are based on the fact that the momentum function $\tilde{\varphi}'_f(k - \mathbf{v})$ is strongly peaked at $\mathbf{k} = \mathbf{v}$ while the remaining integral shows a weak k -dependence in this region. This is more true the smaller Z_T/v and Z_P/Z_T are. These peaking approximations are successively more restrictive (and thus less valid at given Z_P, v): The transverse peaking approximation³⁰ retains in the function $\varphi_{\mathbf{k}}$ the momentum component k_z which is parallel to \mathbf{v} , while putting the transverse components to zero. The next version consists in retaining the plane-wave factor of $\varphi_{\mathbf{k}}$ unchanged, but putting $\mathbf{k} = \mathbf{v}$ elsewhere⁵⁸. Finally, in the full peaking approximation⁴⁰, \mathbf{k} is replaced by \mathbf{v} everywhere except in $\tilde{\varphi}'_f(\mathbf{k} - \mathbf{v})$. Then the capture cross section becomes proportional to the differential cross section $d\sigma^{\text{ion}}/d\mathbf{k}$ for electron ejection into a state with momentum equal to \mathbf{v}

$$\sigma_{(\text{full peaking})}^{IA} = (2\pi)^3 |\varphi'_f(\mathbf{r}_P = 0)|^2 \left(\frac{d\sigma^{\text{ion}}}{d\mathbf{k}} \right)_{\mathbf{k}=\mathbf{v}}. \quad (1.54)$$

This simple formula is, however, only valid for capture into s states because otherwise, the final state wave function vanishes at the origin. It preserves the correct asymptotic velocity dependence, but merges with the second Born approximation only in the limit $Z_P/Z_T \rightarrow 0$ ^{34,40}. In contrast, the transverse peaking approximation preserves the correct asymptotics without restrictions.

1.3.5. Distorted-wave Born approximation

The distorted-wave Born (DWB) theory³³ has been introduced as a symmetric version of the strong potential Born approximation in order to extend its validity to systems with $Z_P \approx Z_T \approx \nu$. Its formulation is very similar to that for the CDW theory, but with a different choice for the distorted waves $\chi_i^{(+)}$ and $\chi_f^{(-)}$. In order to derive the DWB theory from a CDW-type expansion, the Hamiltonian $H_e = H_i + \hat{V}_i = H_f + \hat{V}_f$ is split in the following way⁴⁸

$$\begin{aligned} H_i &= T_e + V_T + V_P - V_T G_0^{(+)} V_P, & \hat{V}_i &= V_T G_0^{(+)} V_P \\ H_f &= T_e + V_P + V_T - V_P G_0^{(-)} V_T, & \hat{V}_f &= V_P G_0^{(-)} V_T \end{aligned} \quad (1.55)$$

with the short-hand notation

$$V_1 G_0 V_2 |\psi(t)\rangle \equiv \int d\tau V_1(t) G_0(t, \tau) V_2(\tau) |\psi(\tau)\rangle. \quad (1.56)$$

In order to calculate the eigenfunction $\chi_f^{(-)}$ to H_f , the function $\chi_f^{(-)}$ is written in terms of φ_f , the eigenstates to $H_{f0} = T_e + V_P$ by means of the Lippmann-Schwinger equation (1.27), and the appearing Greens function $G_f^{(-)}$ is expressed in terms of $G_T^{(-)}$ via the relation (1.26). It then follows that $\chi_f^{(-)}$ is identical to the SPB approximation (1.43) of the exact scattering function; a similar consideration holds for $\chi_i^{(+)}$. Explicitly⁴⁸

$$\begin{aligned} \chi_f^{(-)} &\equiv \chi_f^{(-)\text{SPB}} = \varphi_f(t) + \int dt' G_T^{(-)}(t, t') V_T(t') \varphi_f(t'), \\ \chi_i^{(+)} &\equiv \chi_i^{(+)\text{SPB}} = \varphi_i(t) + \int dt' G_P^{(+)}(t, t') V_P(t') \varphi_i(t'), \end{aligned} \quad (1.57)$$

where G_P and G_T are the Greens functions for $T_e + V_P$ and $T_e + V_T$, respectively. The series expansion of the transition amplitude is obtained by inserting (1.57) into the general distorted-wave formula (1.40) with (1.37)

$$\begin{aligned} a_{fi} &= a_{fi}^{D-} - i \int dt \langle \chi_f^{(-)\text{SPB}}(t) | \hat{V}_i(t) | \chi_i^{(+)\text{SPB}}(t) \rangle \\ &\quad - i \int dt d\tau \langle \chi_f^{(-)\text{SPB}}(\tau) | \hat{V}_f^+(\tau) G^{(+)}(\tau, t) \hat{V}_i(t) | \chi_i^{(+)\text{SPB}}(t) \rangle \end{aligned} \quad (1.58)$$

upon iteration of G in terms of G_0 . The surface term a_{fi}^{D-} does not vanish, but reduces to the Brinkman-Kramers amplitude⁴⁸. The distorted-wave Born approximation is the lowest-order expansion term, i.e. it consists of the first two terms of (1.58):

$$\begin{aligned}
 a_{fi}^{\text{DWB}} = & -i \int dt \langle \varphi_f(t) | V_T(t) | \varphi_i(t) \rangle \\
 & - i \int dt d\tau \langle \chi_f^{(-)\text{SPB}}(t) | V_T(t) G_0^{(+)}(t, \tau) V_P(\tau) | \chi_i^{(+)\text{SPB}}(\tau) \rangle . \quad (1.59)
 \end{aligned}$$

Interestingly, the identical form of the transition amplitude can be obtained if the Faddeev-Watson series²¹ is used and is cut off after the second term. This series which can be derived from an iteration of the Faddeev equations¹⁸ has mainly been used for the description of direct reactions, and has only recently been applied for transfer reactions⁵⁹.

It is easy to see that in the limits $Z_P/Z_T \ll 1$ and $Z_T/Z_P \ll 1$, the DWB theory reduces to the prior and post form of the SPB approximation, respectively. Upon collecting all first-order terms in V_P , $\chi_i^{(+)\text{SPB}}$ has to be replaced by φ_i , while to first order in V_T , $\chi_f^{(-)\text{SPB}}$ must be replaced by φ_f . Thus

$$\begin{aligned}
 a_{fi}^{\text{DWB}} \rightarrow a_{fi}^{\text{SPB}}(\text{prior}) &= -i \int dt \langle \chi_f^{(-)\text{SPB}}(t) | V_P(t) | \varphi_i(t) \rangle , \quad Z_P \ll Z_T \\
 a_{fi}^{\text{DWB}} \rightarrow a_{fi}^{\text{SPB}}(\text{post}) &= -i \int dt \langle \varphi_f(t) | V_T(t) | \chi_i^{(+)\text{SPB}}(t) \rangle , \quad Z_T \ll Z_P . \quad (1.60)
 \end{aligned}$$

Also the CDW theory can be obtained from an approximation to the DWB theory: if the on-shell limit of, e.g. $\chi_f^{(-)\text{SPB}}$ is taken, and in its momentum representation (cf. (1.47)) a peaking approximation⁵⁸ is applied, the resulting wave function coincides with the CDW function $\chi_f^{(-)}$ from (1.38) transformed into the target frame³⁰. Note, however, that the boundary conditions are changed by this procedure (the CDW satisfies Coulomb boundary conditions while the DWB does not).

An exact evaluation of the DWB approximation seems rather involved due to the large numbers of couplings to the two nuclear fields. Equation (1.59) has only been evaluated with the help of peaking approximations⁵⁹⁻⁶¹ (see Fig. 5); it then remains, however, unclear which fraction of the deviations between DWB and SPB must be ascribed to inaccuracies from the peaking approximations.

1.3.6 Eikonal Approximation

The Glauber theory or eikonal approximation has originally been developed for problems of potential scattering^{62,63}. In this theory the electron-nucleus interaction is accounted for by means of a path integral which modifies the energy phase. This treatment is only possible if the collision time is short compared to typical electronic transition times, i.e. it is a high-energy approximation. For rearrangement collisions, the Glauber theory was first formulated by Dewangan⁶⁴.

The eikonal theory (E) in its symmetric form can be obtained from a distorted-wave series, similar to the CDW or DWB approaches. The eikonal distorted wave can be derived from the SPB approximation to the exact scattering function $\psi_f^{(-)}$, which is defined through (cf. (1.43) with (1.26))

$$\chi_f^{(-)\text{SPB}}(t) = \varphi_f(t) + \int d\tau G_0^{(-)}(t, \tau) V_f(\tau) \chi_f^{(-)\text{SPB}}(\tau) . \quad (1.61)$$

If $\chi_f^{(-)SPB}(t)$ is written as the product of $\varphi_f(t)$ times an unknown function $\phi_E^{(-)}(t)$ and use is made of the relation (1.25) between G_0 and the time development operator \hat{P}_0 , an equation for $\phi_E^{(-)}(t)$ is obtained from (1.61):

$$\varphi_f(t)\phi_E^{(-)}(t) = \varphi_f(t) + i \int d\tau \Theta(\tau - t) \hat{P}_0(t, \tau) V_f(\tau) \varphi_f(\tau) \phi_E^{(-)}(\tau) . \quad (1.62)$$

For the eikonal approximation it is assumed that $V_f(\tau)$ and $\phi_E^{(-)}(\tau)$ are slowly varying functions in space as compared to $\varphi_f(\tau)$ which, if one works in the center of mass frame, contains the phase factor $\exp(iM_T/(M_P + M_T)\dot{\mathbf{R}}\mathbf{r}')$. For sufficiently large velocities $\dot{\mathbf{R}}$ one can therefore neglect the action of \hat{P}_0 on V_f and $\phi_E^{(-)}$ and also consider φ_f as a quasi-free electron state, i.e. take $\hat{P}_0(t, \tau)\varphi_f(\tau) \approx \varphi_f(t)$. With these approximations, $\varphi_f(t)$ drops out of (1.62). Upon differentiation, one obtains the differential equation for $\phi_E^{(-)}$

$$\frac{d\phi_E^{(-)}(t)}{dt} = -iV_f(t)\phi_E^{(-)}(t) \quad (1.63)$$

which is easily integrated. In a similar way, the eikonal approximation to the scattering state $\psi_i^{(+)}$ can be derived. For a straight-line internuclear trajectory, the eikonal distorted waves are thus given by

$$\chi_f^{(-)E} = \varphi_f(t) e^{i \int_t^\infty V_f(\tau) d\tau} = \varphi_f(t) e^{i(Z_T/v) \ln(vr_T + \mathbf{v}\mathbf{r}_T)} , \quad (1.64)$$

$$\chi_i^{(+)E} = \varphi_i(t) e^{-i \int_{-\infty}^t V_i(\tau) d\tau} = \varphi_i(t) e^{-i(Z_P/v) \ln(vr_P + \mathbf{v}\mathbf{r}_P)} .$$

The eikonal series is obtained upon inserting (1.64) into the series expansion (1.40) of the transition amplitude. The symmetric eikonal approximation consists of the first term of this series⁶⁵

$$a_{fi}^{SE} = -i \int dt \langle \chi_f^{(-)E}(t) | H_e - i\partial_t | \chi_i^{(+)E}(t) \rangle . \quad (1.65)$$

Like the CDW theory, the eikonal approximation neglects gradient terms. Moreover, by comparing (1.64) with the CDW distorted waves (1.38), it becomes clear that the symmetric eikonal theory is identical to the asymptotic form of the CDW theory⁶⁵, and that the Coulomb boundary conditions (1.34) are included.

If one of the distorted waves χ^E in (1.65) is replaced by the asymptotic state φ , the asymmetric eikonal theory⁶⁶ in its prior and post form is recovered

$$a_{fi}^{E}(\text{prior}) = -i \int dt \langle \chi_f^{(-)E}(t) | V_i(t) | \varphi_i(t) \rangle , \quad (1.66)$$

$$a_{fi}^{E}(\text{post}) = -i \int dt \langle \varphi_f(t) | V_f(t) | \chi_i^{(+)E}(t) \rangle .$$

From the above derivation it follows that the symmetric eikonal theory is an approximation to the DWB or CDW, while the asymmetric eikonal theory is an approximation to the SPB (albeit satisfying Coulomb boundary conditions). However, the coupling to either of the electron-nucleus potentials inherent in the path integral only describes an infinite number of ‘‘soft’’ collisions, and not ‘‘hard’’ collisions as in the case of the SPB which includes the same potential exactly. Consequently, the eikonal approximation contains the Brinkman-Kramers term, but not the second-order Born term⁶⁷. This leads to an incorrect asymptotic high-energy behavior, although the experimental data are well reproduced in a large region of the high-energy regime (cf. Fig. 4).

2. Coupled Channel Calculations in a Finite Basis

The models described in the preceding section are not appropriate for the lower collision velocities because the lowest-order terms of the series expansions are no longer sufficient. The strong coupling to the projectile and the target field in slow collisions makes it necessary to include both interactions in the electronic wave function if a fast convergence is to be achieved. This can be done in several ways. One method consists in writing the wave function as a superposition of target- and projectile-centered atomic states, which is expected to give good results for systems with $v \geq v_e$ and $Z_P \approx Z_T$, or for systems with $v \leq v_e$ and $Z_P \ll Z_T$, even if only a few states are included. On the other hand, if $Z_P \approx Z_T$ and $v \leq v_e$ or $Z_P \ll Z_T$ and $v \ll v_e$, an expansion in terms of two-center (molecular) functions should be preferred. Alternatively, a combination of atomic and molecular basis states may be of advantage. In any case, the basis functions should be carefully selected for each problem of interest in order to get a good description of the transfer process with as few basis states as possible. For the formulation of these methods, which is given below, we shall use the semiclassical picture and restrict ourselves to one-electron systems, deferring the extension to multi-electron systems to a later section.

2.1. Atomic basis

It is usually of advantage to include the initial and the final electronic state in the basis set. For rearrangement collisions this implies that the basis states are centered at different origins and thus are no longer mutually orthogonal. In the general case, the exact solution to the Hamiltonian H_e can be approximated as superposition of projectile states (φ_n^P) and target states (φ_m^T)^{68,69}

$$\psi(\mathbf{r}, t) = \sum_{n=1}^N a_n(t) \varphi_n^P(\mathbf{r}_P, t) + \sum_{m=1}^M b_m(t) \varphi_m^T(\mathbf{r}_T, t), \quad (2.1)$$

$$\varphi_n^P(\mathbf{r}_P, t) = \varphi_n^P(\mathbf{r}_P) e^{i\mathbf{v}\mathbf{r} \cdot \boldsymbol{\alpha}_0} e^{-i\varepsilon_n^P t - (i/2)v^2 \boldsymbol{\alpha}_0^2 t},$$

$$\varphi_m^T(\mathbf{r}_T, t) = \varphi_m^T(\mathbf{r}_T) e^{-i\mathbf{v}\mathbf{r} \cdot \boldsymbol{\beta}_0} e^{-i\varepsilon_m^T t - (i/2)v^2 \boldsymbol{\beta}_0^2 t},$$

where N and M is the number of projectile and target states, respectively, which are included in the expansion of ψ , and we assume these numbers to be rather small. In (2.1), the reference frame of $\psi(\mathbf{r}, t)$ has its origin on the line connecting the projectile and the

target nucleus but is otherwise arbitrary. In order to guarantee the independence of the capture probability from the chosen reference frame it is important to include the translational factors, i.e. the phases resulting from the transformation \hat{U} (eq. (1.2)) in the basis functions (2.1). $\alpha_0 R$ ($\beta_0 R$) is the distance between the origin and the projectile (target), and ε_n^P and ε_m^T are the energies of the states φ_n^P and φ_m^T , respectively. The initial state is denoted by $m = i$ and the final state by $n = f$.

When (2.1) is inserted into the Schrödinger equation, $i\partial_t\psi = H_e\psi$, a system of differential equations for the amplitudes a_n and b_m is obtained

$$\begin{aligned} & i \sum_n \dot{a}_n \langle \varphi_k(t) | \varphi_n^P(t) \rangle + i \sum_m \dot{b}_m \langle \varphi_k(t) | \varphi_m^T(t) \rangle \\ &= \sum_n a_n \langle \varphi_k(t) | V_T + V_R | \varphi_n^P(t) \rangle + \sum_m b_m \langle \varphi_k(t) | V_P + V_R | \varphi_m^T(t) \rangle \\ & \varphi_k(t) \in \{ \varphi_n^P(t), \varphi_m^T(t) \} . \end{aligned} \quad (2.2)$$

We have used $H_e = T_e + V_P + V_T + V_R$ with V_R the recoil field. Equations (2.2) take into consideration that for finite times the overlap between a target state and a projectile state is non-vanishing. Due to the use of atomic basis states there is a purely potential coupling between the states. The potentials are time-dependent through the internuclear coordinate \mathbf{R} which is described by a classical path with impact parameter b . The system (2.2) has to be solved subject to the initial condition that the electron is in the bound target state φ_i^T at time $t \rightarrow -\infty$:

$$\begin{aligned} a_n(-\infty) &= 0, & n &= 1 \dots N \\ b_m(-\infty) &= 0, & m &\neq i; & b_i(-\infty) &= 1 . \end{aligned} \quad (2.3)$$

The probability P_{fi} of the electron ending up in the projectile state φ_f^P , is then obtained from

$$P_{fi}(b) = |a_f(+\infty)|^2 . \quad (2.4)$$

Often, the expansion (2.1) is just restricted to the two states φ_i^T and φ_f^P ^{68,70}. However, this approximation breaks down as soon as the coupling to other states becomes important. In particular, this restricted basis does not allow for an equivalent to the second-order Born approximation, i.e. it gives incorrect results at high collision velocities.

In the unitarised distorted-wave approximation (UDWA)^{71,72}, other projectile states are included in the basis besides initial and final states. However, an approximation to the scattering matrix is chosen which conserves unitarity, but neglects the time-ordering operator which occurs in the expansion of the scattering matrix in terms of a time-dependent interaction. Like in the case of a two-state expansion, the region of validity of the UDWA is restricted to velocities around the maximum of the capture cross section⁷³ ($v \sim v_e$).

Recent calculations^{74,75} which include up to 34 basis states exactly, show even at lower collision energies a satisfactory agreement with experiment.

2.2. Molecular Basis

At low impact velocities the electronic transitions take place mostly at rather small internuclear distances, such that it is of advantage to expand the wave function ψ in terms of molecular orbitals⁶⁹ (MO)

$$\psi(\mathbf{r}, t) = \sum_{n=1}^N a_n(t) \varphi_n(\mathbf{r}, \mathbf{R}, t) \quad (2.5)$$

with $\varphi_n(\mathbf{r}, \mathbf{R}, t) = \varphi_n(\mathbf{r}, \mathbf{R}) \exp(-i \int dt \varepsilon_n(R))$ where $\varepsilon_n(R)$ is the molecular energy. The states $\varphi_n(\mathbf{r}, \mathbf{R})$ are stationary eigenstates of the full Hamiltonian H_e . One possibility is to work in the (space-fixed) center of mass system. Then, φ_n is the solution to

$$[T_e + V_P(\mathbf{r} - \alpha \mathbf{R}) + V_T(\mathbf{r} + \beta \mathbf{R})] \varphi_n(\mathbf{r}, \mathbf{R}) = \varepsilon_n(R) \varphi_n(\mathbf{r}, \mathbf{R}) \quad (2.6)$$

with $\alpha = M_T/(M_P + M_T)$ and $\beta = 1 - \alpha$. These basis states depend parametrically on the internuclear coordinate $\mathbf{R}(t)$ and hence implicitly on time. Upon inserting (2.5) into the Schrödinger equation and considering the orthogonality of the basis states, one obtains

$$i\dot{a}_m(t) = a_m(t)\varepsilon_m - i \sum_n a_n(t) \langle \varphi_m(\mathbf{r}, \mathbf{R}, t) | \partial_t | \varphi_n(\mathbf{r}, \mathbf{R}, t) \rangle, \quad m = 1 \dots N \quad (2.7)$$

For molecular basis states, the coupling is based on the time change of the two-center potential. As for $R \rightarrow \infty$, the molecular functions reduce to projectile or target states, (2.7) has to be solved with the initial conditions

$$a_m(-\infty) = 0, \quad m \neq i; \quad a_i(-\infty) = 1 \quad (2.8)$$

where i denotes that MO-state which asymptotically is identical to the initial target state.

Instead of working in the space-fixed frame, it is, however, often of advantage to use a rotating reference frame in which the quantization axis points into the direction of $\mathbf{R}(t)$. As \mathbf{R} is the natural quantization axis of the stationary molecular orbitals, the MO's then only depend on the absolute value R . The functions in the space-fixed frame ($\psi(\mathbf{r}, t)$) and in the rotating frame ($\psi'(\mathbf{r}', t)$) are connected by a rotation^{4,5}

$$\psi'(\mathbf{r}', t) = e^{-i\Theta \hat{L}_y} \psi(\mathbf{r}, t) \quad (2.9)$$

Here, \hat{L}_y is the angular momentum operator with respect to the y-axis (perpendicular to the scattering plane), and \mathbf{R} is parametrized as $\mathbf{R} = (R \sin \Theta, 0, R \cos \Theta)$ with the z-axis pointing to the opposite direction of \mathbf{v} . The Schrödinger equation can likewise be transformed into the rotating frame

$$e^{-i\Theta \hat{L}_y} (i\partial_t - H_e) e^{i\Theta \hat{L}_y} \psi'(\mathbf{r}', t) = (i\partial_t - \Theta \hat{L}_y - H'_e) \psi'(\mathbf{r}', t) = 0 \quad (2.10)$$

where use has been made of the time-independence of \hat{L}_y . If the function $\psi'(\mathbf{r}', t)$ is expanded in terms of rotating basis functions $\varphi'_n(\mathbf{r}', R, t)$ which are solutions to H'_e , one arrives at the system of coupled equations for the expansion coefficients a'_n

$$i\dot{a}'_m(t) = a'_m(t)\varepsilon_m + \sum_n a'_n(t)\langle\varphi'_m(\mathbf{r}', R, t)|\hat{\Theta}\hat{L}_y - i\dot{R}\partial/\partial R|\varphi'_n(\mathbf{r}', R, t)\rangle,$$

$$m = 1 \dots N. \quad (2.11)$$

Equations (2.11) are seen to have the same form as the equations of the space-fixed frame if one makes the following identification of the coupling operator

$$\partial_t = \dot{R} \frac{\partial}{\partial R} + \hat{\Theta} \frac{\partial}{\partial \Theta} \quad (2.12)$$

with $\hat{\Theta} = b\dot{\nu}/R^2$, as $\hat{L}_y = -i\partial/\partial\Theta$. For $t \rightarrow -\infty$ the angle Θ is zero, which means that the rotating and the space-fixed functions are identical. Hence, the initial conditions are the same as given in (2.8).

It should be noted that some authors define Θ as the angle between the direction of \mathbf{v} and the direction of \mathbf{R} , which are chosen as quantization axes in the space-fixed and rotating frame, respectively. This implies that $\Theta = 0$ at $t \rightarrow +\infty$ and that the derivative $\hat{\Theta}$ is negative. Hence, for this definition the space-fixed and the rotating functions coincide at $t \rightarrow +\infty$.

If the energies $\varepsilon_n(R)$ are calculated as a function of R for the different states φ'_n , one obtains a so-called correlation diagram. From such a diagram it is easy to determine which states will be important for the transfer into a given final state, as long as the collision velocity is not too high: There exist avoided crossings of the energy levels of adjacent molecular states, where the transition from one state to the next is very likely to occur⁷⁶. Correlation diagrams offer thus the possibility of following the "path" of the electron as a function of impact parameter and time.

The inclusion of only two MO basis states in the expansion of $\psi'(\mathbf{r}', t)$ may already be sufficient. This is, for example, the case for the capture of an electron from the K-shell of the lighter collision partner into the L-shell of the heavier partner, where one can restrict oneself to the $2p\sigma$ and the $2p\pi$ states⁷⁷. (However, a relativistic description of the same process requires six MO-states⁷⁸).

An expansion of the type (2.5) with a low number N holds, however, only in cases where all electronic transitions are restricted to small internuclear distances. If the relevant avoided crossings are situated at an R which is of the order of the electronic shell radius (n/Z) or even larger, the results are rather poor. The reason lies in the fact that the MO states have the wrong asymptotic behavior at $R \rightarrow \infty$ because they do not contain any translational factors^{5,6,69}. In order to cope with this deficiency, Schneiderman and Russek⁷⁹ have suggested the following ansatz in place of (2.5)

$$\psi(\mathbf{r}, t) = \sum_{n=1}^N a_n(t)\varphi_n(\mathbf{r}, \mathbf{R}, t)e^{i\mathbf{f}(\mathbf{r}, \mathbf{R})\cdot\mathbf{v}\mathbf{r}} \quad (2.13)$$

where the switching function $f(\mathbf{r}, \mathbf{R})$ has to be chosen in such a way that for $R \rightarrow \infty$, the correct translational factors are obtained, while for $R \rightarrow 0$ it shall describe an electron at rest in the center of mass frame. Thus, according to (2.1), $f(\mathbf{r}, \mathbf{R})$ is subject to the conditions

$$f(\mathbf{r}, \mathbf{R}) \rightarrow \begin{cases} \alpha_0, & r_P \ll r_T, R \rightarrow \infty \\ -\beta_0, & r_T \ll r_P, R \rightarrow \infty \\ 0, & R \rightarrow 0 \end{cases} \quad (2.14)$$

An exact determination of $f(\mathbf{r}, \mathbf{R})$ from a fundamental theory is not possible. Corresponding, there is a large body of publications on various forms of the switching function. Some of the switching functions, as used in the literature, are compiled in the work of Crothers and Todd⁸⁰. The simplest idea⁸¹ would be to split R into an interior region $R < R_0$ and an exterior region $R > R_0$ with the choice of $f = 0$ for $R < R_0$. However, this method does not provide reliable transition probabilities⁸² due to their dependence on the parameter R_0 . It is, for example, more reasonable to correlate the translational factor with a reference frame which slides on the line connecting the projectile and target nucleus, subject to the R -dependent attractive forces which the two nuclei exert on the electron⁵. A variational calculation is well suited for the determination of such a translational factor; the accuracy depends, however, strongly on the choice of the variational subspace (see also Sec. 3).

The inclusion of the phase factor in the expansion (2.13) of $\psi(\mathbf{r}, t)$ results in a modification of the system of coupled equations. In place of (2.7) one now has⁵

$$\begin{aligned} i\dot{a}_m(t) = & a_m(t)\varepsilon_m - i \sum_n a_n(t) \langle \varphi_m | \partial_t + f\mathbf{v}\nabla_{\mathbf{r}} | \varphi_n \rangle \\ & - i \sum_n a_n \langle \varphi_m | (\mathbf{v}\mathbf{r})(\nabla_{\mathbf{r}}f)\nabla_{\mathbf{r}} + (\mathbf{v}\mathbf{r})\left(\frac{1}{2}\nabla_{\mathbf{r}}^2f\right) + \mathbf{v}(\nabla_{\mathbf{r}}f) \\ & + i \frac{\partial}{\partial t}(f\mathbf{v}\mathbf{r}) + \frac{i}{2}(\nabla_{\mathbf{r}}(f\mathbf{v}\mathbf{r}))^2 | \varphi_n \rangle \end{aligned} \quad (2.15)$$

As f is a slowly varying function at low velocity v , mainly the terms of the first line in (2.15) are important, and it is just the operator $f\mathbf{v}\nabla_{\mathbf{r}}$ which causes a modification of (2.7). This operator is seen to cause a translation of the electronic reference frame from the center of mass system to a system moving with an effective velocity $f\mathbf{v}$.

In the expansion (2.13) it is assumed that the translational factor is common to all orbitals. One may relax this condition and define a separate function f_n for every orbital n . This idea has been put forth to account for the fact that the effective translational velocity depends not only on the motion of the nuclei, but also on the interaction with other electronic states via non-adiabatic couplings⁸³. f_n will in general be a complicated function, especially if it is determined from a variational calculation⁸⁰. Moreover, the

orthogonality between the basis states is lost, as is the interpretation that the translational factor is a property of the electron configuration space only.

2.3. Combined basis

In order to cover an extended range of collision velocities with as few basis states as possible, different sets of basis functions have been introduced besides the purely atomic and the purely molecular ones. As long as the electronic initial and final state is asymptotically included in the basis, the transfer probability is obtained in a similar way as described above.

An attempt has been made⁸⁴ to attach molecular switching functions to the atomic basis states. Calculations based on a two-center expansion show, however, no improvement over the results with purely atomic states (having constant translational factors) at low collision energies, while at high energies the molecular switching functions even fail to give the correct fall-off of the transfer probability with energy.

In order to avoid the problems which arise from an MO basis without translational factors, the so-called AO–MO matching procedure has been invented⁸⁵. In this approximation, an atomic basis is used in the outer region ($R > R_0$) and a molecular basis for $R < R_0$. The results depend only weakly on the choice of R_0 where the two expansions are matched, and lie, in the case of a 5-state basis⁸⁵, well within the spread of transition probabilities which are calculated within a pure MO basis with different choices of the translational factors.

A two-center expansion with the use of atomic and united-atom (UA) wave functions at each center (the so-called AO+ basis) has been considered by Fritsch and Lin⁸⁶. The UA wave functions are functions of atomic structure to the combined charge $Z_P + Z_T$, i.e. they are the $R \rightarrow 0$ limit of the molecular orbitals. Every state of the AO+ basis contains a constant (asymptotic) translational factor. An inclusion of up to 24 basis states yields very good agreement with experiment in the low and intermediate velocity region.

Also a three-center expansion has been applied successfully^{87,88}. In this model, united-atom orbitals without translational factors centered at the center of mass are added to the projectile- and target-centered atomic orbitals. The three-center expansion is applicable in a very large velocity region because the UA orbitals give not only a good description of the low-energy regime, but they also simulate the intermediate states which are important for the transfer at the higher energies.

3. Variational Methods

In general, not only the atomic three-body models, but also coupled-channel calculations within the bases discussed above are only meaningful in a restricted velocity region because otherwise the numerical effort will increase drastically. Variational methods may be considered as a way out of this dilemma, since in principle, they can cover the whole energy region within a small basis space.

A necessary condition for a variational method to be applicable is the fact that the exact transition amplitude emerges from the variation of an appropriate functional. A pair of functionals which obey this condition, are the so-called post and prior bilinear forms of the Schwinger functional for the transition amplitude^{17,21}

$$\begin{aligned}
a_{fi}(\text{post}) &= -i \int dt \{ \langle \psi_f^{(-)} | V_f [1 + G_{f0}^{(+)}(V_i - V_f)] | \varphi_i \rangle + \langle \varphi_f | V_f | \psi_i^{(+)} \rangle \\
&\quad - \langle \psi_f^{(-)} | V_f - V_f G_{f0}^{(+)} V_f | \psi_i^{(+)} \rangle \} \\
a_{fi}(\text{prior}) &= -i \int dt \{ \langle \varphi_f | [1 + (V_f - V_i) G_{i0}^{(+)}] V_i | \psi_i^{(+)} \rangle + \langle \psi_f^{(-)} | V_i | \varphi_i \rangle \\
&\quad - \langle \psi_f^{(-)} | V_i - V_i G_{i0}^{(+)} V_i | \psi_i^{(+)} \rangle \}
\end{aligned} \tag{3.1}$$

where the splitting of H_e from (1.1) and the short-hand notation (1.56) has been used. The functions G_{i0} , φ_i and G_{f0} , φ_f relate to H_{i0} and H_{f0} , respectively. The two functionals (3.1) prove to be stationary with respect to a variation of the trial functions $\psi_i^{(+)}$ and $\psi_f^{(-)}$ about their correct values (exact scattering states to H_e). They reduce to the post and prior form of the transition amplitude, Eqs. (1.8) and (1.11), respectively, if the exact scattering functions are inserted. Moreover, the use of specific trial functions allows one to reproduce the starting formulas of the various atomic perturbative models^{89,90}.

While the Schwinger functional is suited to derive the formal theories, other functionals are more appropriate for the practical purpose of constructing variational wave functions. Cheshire⁹¹ considers the functional

$$I = \int_{-\infty}^{\infty} dt \langle \psi | H_e - i \partial_t | \psi \rangle \tag{3.2}$$

which also satisfies the conditions mentioned above. This can be proved by expanding the test function ψ within a complete set of basis functions $\psi(t) = \sum_n a_n(t) \varphi_n(t)$, and by varying I with respect to the expansion coefficient a_n^* :

$$0 = \frac{\delta I}{\delta a_n^*(t)} = \sum_n [a_n(t) \langle \varphi_m(t) | H_e - i \partial_t | \varphi_n(t) \rangle - i \langle \varphi_m(t) | \varphi_n(t) \rangle \partial_t a_n(t)] . \tag{3.3}$$

This is the identical system of equations as obtained by inserting the expansion of ψ directly into the Schrödinger equation (see Sec. 2), and its solution is therefore exact as long as n extends to infinity.

Variational methods can be used to reduce the number of necessary basis states in the expansion of the exact scattering function. To this aim one introduces, for example, a parameter $Z_n(t)$ into the basis functions, which may be interpreted as an effective nuclear charge:

$$\psi(\mathbf{r}, t) = \sum_{n=1}^N a_n(t) \varphi_n(Z_n(t), \mathbf{r}, t) . \tag{3.4}$$

The parameters $Z_n(t)$ are determined by requiring that after inserting (3.4) into I , this functional be stationary for variations with respect to $a_n^*(t)$ and $Z_n(t)$. As shown above,

the variation with respect to $a_n^*(t)$ leads to the system (3.3) of coupled equations with dimension N , but with matrix elements depending on the parameters $Z_n(t)$. If I is varied with respect to Z_n , the Euler-Lagrange equations emerge

$$\frac{\partial}{\partial Z_n} \langle \psi | H_e - i\partial_t | \psi \rangle - \frac{\partial}{\partial t} \frac{\partial}{\partial \dot{Z}_n} \langle \psi | H_e - i\partial_t | \psi \rangle = 0. \tag{3.5}$$

Since $\partial_t \psi$ depends explicitly on \dot{Z}_n , the second term of (3.5) may be rewritten and one obtains

$$\frac{\partial}{\partial Z_n} \langle \psi | H_e - i\partial_t | \psi \rangle + i\partial_t \left\langle \psi \left| \frac{\partial \psi}{\partial Z_n} \right. \right\rangle = 0, \quad n = 1, 2 \dots N. \tag{3.6}$$

These equations have to be solved simultaneously with the N equations (3.3), subject to the boundary conditions $Z_n(t \rightarrow \infty) = Z_{n,\infty}$. The numbers $Z_{n,\infty}$ are the charges entering into those atomic basis functions to which φ_n reduce in the limit $t \rightarrow \infty$.

The method described above can easily be extended to wave functions containing several parameters $Z_{1n}(t), Z_{2n}(t), \dots$. However, even for a single parameter and a small number of basis states, the simultaneous solution of (3.3) and (3.6) requires a considerable numerical effort. There is, however, a simple way to find an approximate solution for $Z_n(t)$. To this aim, let us restrict ourselves to a single term ($N = 1$) in the expansion (3.4). Then the system (3.3) reduces to one equation only,

$$i\langle \varphi | \dot{\varphi} \rangle \dot{a} = \langle \varphi | H_e - i\partial_t | \varphi \rangle a. \tag{3.7}$$

The state φ shall describe a bound state, such that it can be normalized, i.e. $|a|^2 \langle \varphi | \varphi \rangle = 1$. With the use of (3.7), the equation for Z reads

$$\frac{\partial}{\partial Z} \frac{\langle \varphi | H_e - i\partial_t | \varphi \rangle}{\langle \varphi | \varphi \rangle} = -i \frac{\partial}{\partial t} \frac{\langle \varphi | \partial \varphi / \partial Z \rangle}{\langle \varphi | \varphi \rangle}. \tag{3.8}$$

For every basis state φ_n , one can obtain Z_n from the solution of (3.8) and subsequently use these values in the coupled equations (3.3). A still simpler procedure is, of course, to determine Z_n only for the lowest state from (3.8), while inserting the constant asymptotic charges into the remaining basis states. Even then, the numerical results for charge transfer in the intermediate velocity region are considerably improved as compared to the use of a molecular or an atomic basis of equal dimension⁹¹. This method has been successfully applied by several authors^{92,93} for systems with $Z_p = Z_T$ up to 10, where a coupling of only two states is often sufficient.

Instead of (3.8), even a static prescription may be used for the determination of an effective charge $Z(R)$, the time-dependence of which is implicitly contained in $R(t)$. With $\partial/\partial t = 0$ in (3.8) one finds

$$\frac{\partial E}{\partial Z} = 0; \quad E = \langle \varphi(Z) | H_e | \varphi(Z) \rangle \tag{3.9}$$

where φ is assumed to be normalized to unity. The solution of (3.9) is very easy to obtain and can subsequently be used in the coupled equations⁹⁴. Both prescriptions, (3.9) as well as (3.8), lead to an effective charge which is symmetric in time. This is a necessary condition for its use in a basis expansion. Other prescriptions for $Z(t)$ which depend explicitly on the time-derivative $\dot{Z}(t)$ are in general complex and include inelastic collision effects through the coupling to other states⁹⁵. Such a $Z(t)$ should not be used for the construction of a basis.

An alternative functional which takes special account of the initial and the final state has been suggested by Demkov²⁰. It is given by the expression (1.4) for the transition amplitude and has already been used as a starting point for the atomic three-body models. It is stationary upon variation with respect to the wave functions $\psi_i^{(+)}$ or $\psi_f^{(-)}$. Therefore, variational parameters contained in the wave functions can be determined from extremizing the transition amplitude or, alternatively, the transition probability or the cross section.

The Demkov functional is especially suited if variational parameters are introduced into the Hamilton operator itself. In order to bridge the transition region between the adiabatic regime where molecular wave functions are appropriate, and the high-energy regime where atomic wave functions can be used, the following splitting of the Hamiltonian into an unperturbed part H_i and a perturbation \hat{V}_i has been suggested⁹⁶

$$H_e = H_i(\lambda, x_i) + \hat{V}_i(\lambda, x_i), \quad H_i = T_e + V_T(\mathbf{r} - \mathbf{x}_i) + \lambda V_P(\mathbf{r} - \mathbf{R} - \mathbf{x}_i) \quad (3.10)$$

$$\hat{V}_i = (1 - \lambda)V_P(\mathbf{r} - \mathbf{R} - \mathbf{x}_i) .$$

This so-called sliding center model contains two variational parameters: λ , with $0 \leq \lambda \leq 1$, is a measure of the degree of atomic or molecular character of the eigenfunctions φ_i to $H_i(\lambda, x_i)$. Correspondingly, the coupling in (1.4) is predominantly given by the potential or by the time derivative $\partial/\partial t$. The other parameter x_i (with \mathbf{x}_i antiparallel to \mathbf{R}) characterizes the origin of the electronic reference frame (cf. Fig. 1). For a nonlinear motion $\mathbf{R}(t)$, an additional recoil field has to be included in (3.10).

Within the spirit of a variational approach, also the eigenfunctions to H_i are determined variationally. They are approximated by atomic functions with an effective nuclear charge $Z_i(R)$ as parameter. Both x_i and Z_i follow from the minimization of the total electronic energy

$$\frac{\partial E}{\partial Z_i} = 0, \quad \frac{\partial E}{\partial x_i} = 0; \quad E = \langle \varphi_i(Z_i, \lambda, x_i) | H_i(\lambda, x_i) | \varphi_i(Z_i, \lambda, x_i) \rangle . \quad (3.11)$$

Asymptotically, one has $Z_i(R = \infty) = Z_T$, $x_i(R = \infty) = 0$, as well as $Z_i(0) = \lambda Z_P + Z_T$ and $x_i(0) = \lambda Z_P / (\lambda Z_P + Z_T)$.

In the case of direct reactions it is advantageous to adopt for the final state the same values of Z_i and x_i as calculated for the initial state, in order to preserve orthogonality. The parameter λ is finally obtained from minimizing the coupling strength

$$\frac{d}{d\lambda} \left| \int_0^\infty dt \langle \varphi_f(\mathbf{r}, \lambda) | \hat{V}_i - i\partial_t | \varphi_i(\mathbf{r}, \lambda) \rangle \right|^2 = 0, \quad (3.12)$$

and describes correctly the transition from molecular to atomic functions with increasing velocity.

For transfer reactions, a different splitting of H_e has to be used for the final channel⁹⁷

$$H_e = H_f(\lambda, x_f) + \hat{V}_f(\lambda, x_f), \quad H_f = T_e + V_P(\mathbf{r}' - \mathbf{x}_f) + \lambda V_T(\mathbf{r}' + \mathbf{R} - \mathbf{x}_f) \quad (3.13)$$

$$\hat{V}_f = (1 - \lambda)V_T(\mathbf{r}' + \mathbf{R} - \mathbf{x}_f)$$

and the eigenfunctions $\varphi_f(Z_f, \lambda, x_f)$ to H_f have to be constructed in a similar way as for H_i . As x_i and x_f can be calculated for any given $R(t)$, the switching function is known as well, following immediately from the structure of the transformation operator \hat{U} , Eq. (1.2).

The variationally determined projectile-correlated and target-correlated wave functions can eventually be used as basis states for a coupled-channel calculation of low dimension; however, no calculations have been performed yet.

As the parameter λ is time-independent, it can only describe the global non-adiabaticity of the collision process. In order to get more detailed information, one has to introduce a time-dependent parameter. One may, for example, think of replacing the internuclear distance $R(t)$ by a variational parameter $\xi(t)$. The scattering state is expanded in terms of molecular eigenstates to $H_\xi \equiv H_e(R = \xi)$ ⁹⁸:

$$\psi(\mathbf{r}, t) = \sum_n a_n(t) \varphi_n(\mathbf{r}, \xi(t)) e^{-i\phi_n(t)}; \quad H_\xi \varphi_n(\mathbf{r}, \xi) = \varepsilon_n(\xi) \varphi_n(\mathbf{r}, \xi). \quad (3.14)$$

The energy phase ϕ_n is included in (3.14) in order to eliminate the diagonal coupling matrix elements. The parameter ξ in this model is also obtained from minimizing the coupling strength. For a specific expansion coefficient a_m the condition for ξ reads

$$\frac{\delta}{\delta \xi(t)} \int_{-\infty}^{\infty} dt \sum_{n \neq m} \left\{ \left| \left\langle \varphi_m \left| \frac{\partial H_\xi}{\partial \xi} \right| \varphi_n \right\rangle \frac{\dot{\xi}}{\varepsilon_n - \varepsilon_m} \right|^2 + |\langle \varphi_m | H_e - H_\xi | \varphi_n \rangle|^2 \right\} = 0. \quad (3.15)$$

This equation has been solved for small deviations $|\xi - R|/R \ll 1$ within the monopole approximation of the two-center potential. As a result, the measure $|\xi - R|$ for the non-adiabaticity increases with decreasing R at fixed collision velocity, and is the larger, the higher the state m is excited⁹⁸.

4. Numerical Solutions of the Schrödinger Equation

If one wants to obtain very accurate results especially in the intermediate velocity region, the only possibility is to solve the Schrödinger equation without further approximations. This requires usually an extremely large numerical effort; however, the

results can often serve as a substitute for experimental information which in its turn is indispensable for testing the approximative methods.

There are basically three different approaches for obtaining the solution of the Schrödinger equation, which shall be discussed in this section. One way is to use, as has been outlined in Sec. 2, an expansion of the scattering function in terms of easily tractable basis states; however, a very large dimension of the basis will now be required. The second method consists in a direct integration of the Schrödinger equation without resorting to equivalent representations. Finally, there are the statistical methods. They imply an integration of the equations of motion resulting from the classical Hamilton function or alternatively, of hydrodynamic equations which are an approximation to the Schrödinger equation, subject to statistically distributed initial conditions.

4.1. Representation in a very large basis

In contrast to the special basis functions discussed in Sec. 2, which often have to be selected anew for every collision system or even for every initial and final state in order to minimize the dimension of the resulting system of coupled equations, in the case of large bases one rather resorts to functions which are universal and easy to handle mathematically. Usually, these functions are neither eigenfunctions to the stationary Hamiltonian, nor to the target or projectile nucleus. Preferentially, a rotating reference frame is chosen. If the solution $\psi'(\mathbf{r}', t)$ of (2.10) is expanded in terms of the rotating basis functions φ'_n

$$\psi'(\mathbf{r}', t) = \sum_n c_n(t) \varphi'_n(\mathbf{r}', \mathbf{R}(t), t), \quad (4.1)$$

the following generalized system of differential equations is obtained

$$i \sum_n \dot{c}_n \langle \varphi'_m(t) | \varphi'_n(t) \rangle = \sum_n c_n \langle \varphi'_m(t) | H'_e + \hat{\Theta} \hat{L}_y - i \partial_t | \varphi'_n(t) \rangle. \quad (4.2)$$

The advantage of choosing nearly complete bases of pseudostates consists in the possibility that exclusively, normalized (i.e. bound) functions can be used. Nevertheless, the intermediate continuum states which are important for capture at high velocities can be represented with sufficient accuracy. There is no need for translational factors because both initial and final state can be described well enough within the very large bases, and hence the problem of finding appropriate switching functions does not arise. However, as none of the basis states yields asymptotically the correct initial state, the bound target state has first to be transformed into the rotating reference frame and then expanded in terms of the basis functions φ'_n

$$\begin{aligned} \varphi_i^{T'}(\mathbf{r}', t_0) &= e^{-i\Theta(t_0)\hat{L}_y} \varphi_i^T(\mathbf{r} + \beta_0 \mathbf{R}_0) e^{-i\mathbf{v}\mathbf{r} \cdot \beta_0 \mathbf{e}} e^{-i\mathbf{v}^2 t_0 \beta_0^2 / 2 - i\epsilon_i^T t_0} \\ &= \sum_n c_{ni}(t_0) \varphi'_n(\mathbf{r}', \mathbf{R}_0, t_0), \end{aligned} \quad (4.3)$$

with β_0 defined below Eq. (2.1). The rotation is necessary because numerically, one has to work with finite initial times t_0 and distances $R_0 = R(t_0)$. The system (4.2) has to be solved subject to the initial values $c_{ni}(t_0)$ which are obtained from (4.3).

The transition probability can be determined from the solution of (4.2) in two different ways. One may either insert the scattering function (4.1) with the calculated $c_n(t)$ into the post form (1.8) of the exact transition amplitude⁹⁹

$$a_{fi} = -i \int_{t_0}^{t_1} dt \langle \varphi_f^P(t) | V_T | e^{i\Theta \hat{L}_y} \psi'(\mathbf{r}', t) \rangle \quad (4.4)$$

where φ_f^P is the bound projectile state with its translational factor, and the time t_1 is chosen to be sufficiently large so as to obtain a good convergence of the transition amplitude.

The other possibility consists in calculating the transition amplitude from the projection of the scattering function $\psi'(\mathbf{r}', t_1)$ onto the final state. For this aim one has to expand the solution of (4.2) in terms of rotated asymptotic projectile and target states¹⁰⁰

$$\begin{aligned} \psi'(\mathbf{r}', t_1) &= \sum_n c_n(t_1) \varphi_n'(\mathbf{r}', \mathbf{R}(t_1), t_1) \\ &= e^{-i\Theta(t_1)\hat{L}_y} \left(\sum_n a_n(t_1) \varphi_n^P(\mathbf{r}_P, t_1) + \sum_m b_m(t_1) \varphi_m^T(\mathbf{r}_T, t_1) \right) \end{aligned} \quad (4.5)$$

with φ_n^P and φ_m^T from (2.1). The transfer probability into a projectile state with quantum numbers $\{n\}$ then follows from

$$P_n(b) = |a_n(t_1)|^2, \quad t_1 \rightarrow \infty. \quad (4.6)$$

This method has the advantage of providing simultaneously the capture into arbitrary final states.

As concerns the choice of the basis functions, it has proven convenient to work with two-center orbitals of the Hylleraas type¹⁰¹ which allow for an analytical evaluation of the matrix elements which occur in the coupled equations. Such functions are reasonable for collision systems with arbitrary nuclear charges. An inclusion of 64–144 functions is sufficient to avoid spurious dynamical couplings which would occur in bases of small dimension without consideration of translational factors, and to guarantee the existence of an asymptotic limit of the transition amplitude¹⁰².

In case of asymmetric ($Z_P \ll Z_T$) medium- to high-energy collisions where a single intermediate continuum state plays the dominant role, it is of advantage to construct pseudostates from a modification of the completeness relation for target eigenstates⁹⁹. Such pseudostates have the property that with growing dimension of the basis, the pseudofunctions which correspond to bound states develop eventually into the exact eigenfunctions. Also the exact continuum states can be more and more accurately approximated as long as the electronic coordinate is not too large. However, in many practical cases a comparably small basis is used, such that in the high-energy region, for example, the agreement with experiment is much improved as compared to the restricted bases discussed in Sec. 2, but not as good as with the best atomic models¹⁰³ (cf. Fig. 3).

Alternatively, the Sturmian functions are employed as basis states. They are solutions of the Schrödinger equation to a fixed negative energy. The strength of the potential is used as a free parameter which takes over the role of an eigenvalue. In this way a complete set of states can be obtained¹⁰⁴. Even with a restricted basis of Sturmian functions the experimental transfer cross sections can in most cases be satisfactorily reproduced¹⁰⁵.

The drawback of the bases consisting of pseudostates is the loss of the physical information about the specific intermediate states which are important during the reaction. Nevertheless, the collective dynamics of the transfer process, like density oscillations between the centers of charge¹⁰⁰, can be inferred from the time-dependence of the electronic density $|\psi(\mathbf{r}, t)|^2$.

4.2. Numerical integration of the time-dependent Schrödinger equation

If one wants to obtain the scattering function directly from the Schrödinger equation without its further transformation, one has to solve a partial differential equation in three-dimensional coordinate space. The numerical solution of this equation requires a discretization of the space and time coordinates.

For the discretization of the time coordinate it is convenient to work in the rotating reference frame and to split the corresponding Hamiltonian (2.10) into four parts according to¹⁰⁶

$$H'_e + \hat{\Theta}\hat{L}_y = \sum_{k=1}^4 H_k$$

$$H_1 = T_e + \frac{\partial^2}{\partial z^2} + \frac{1}{2}W; \quad H_2 = -\frac{\partial^2}{\partial z^2} + \frac{1}{2}W \quad (4.7)$$

$$H_3 = -\frac{i}{2}\hat{\Theta}\hat{L}_+; \quad H_4 = -\frac{i}{2}\hat{\Theta}\hat{L}_-$$

where $W = V_p + V_T$, and the representation of \hat{L}_y in terms of ascending (\hat{L}_+) and descending operators (\hat{L}_-) has been used. z is the coordinate in the direction of the quantization axis \mathbf{R} . For small time intervals Δt , the time-development of the wave function is approximated by the following relation

$$\psi(\mathbf{r}, t + \Delta t) = \frac{1}{\prod_{k=1}^4 \left(1 + \frac{i}{2}\Delta t H_k\left(t + \frac{\Delta t}{2}\right)\right)} \prod_{k=1}^4 \left(1 - \frac{i}{2}\Delta t H_k\left(t + \frac{\Delta t}{2}\right)\right) \psi(\mathbf{r}, t) \quad (4.8)$$

which agrees up to the order of $(\Delta t)^2$ with the relation obtained from the exact time-development operator at infinitesimal Δt , $\exp(-i\Delta t \sum_k H_k(t + \Delta t/2))$. Notice that formula (4.8) implies a separate inversion of each term $1 + i\Delta t H_k/2$, which is easier to achieve than an inversion of the total Hamiltonian.

For the evaluation of the spatial derivatives contained in the kinetic energy T_e , the coordinate space is discretized in a similar way. The derivatives are approximated by

high-order difference formulas which connect the wave function at neighboring space points. These lattice points have to be chosen in such a way that the Coulomb singularities are avoided. With the help of this space-time discretization, the Schrödinger equation can be cast into a matrix equation.

If the collision system is cylindrically symmetric, which is the case for zero impact parameter in the space-fixed reference frame¹⁰⁷, or when the Coriolis coupling is neglected in the rotating frame¹⁰⁸, the problem reduces to a two-dimensional one. For the higher collision velocities such an approximation is, however, no longer a good one. In order to avoid a three-dimensional spatial discretization one may use an expansion in terms of basis functions in the φ -coordinate

$$\psi(\rho, z, \varphi, t) = \sum_m F_m(\rho, z, t)e^{im\varphi} \quad (4.9)$$

which, in general, can be truncated after a few terms¹⁰⁶ ($m \lesssim 3$). With (4.9), the problem of discretization is again confined to two spatial dimensions. The initial values F_m in $t = t_0$ are found by expanding the initial target eigenstate in terms of $\exp(im\varphi)$.

The transfer probability is eventually obtained from a projection of the calculated wave function at large t_1 onto the final state in question. However, it is numerically more convenient to determine the transfer probability by means of integrating over that part of the electron density distribution which after the collision is localized in the vicinity of the projectile¹⁰⁶⁻¹⁰⁸. In this way a rather good agreement with experimental capture probabilities and cross sections is obtained.

4.3. Classical approach and statistical theories

Stimulated by the fact that in the case of a Coulomb potential the classical theory leads to the same scattering cross sections as the quantum mechanical theory, classical trajectory Monte Carlo methods have been applied to the calculation of transfer probabilities. In general, a classical description is less involved and numerically faster than the accurate solution of the Schrödinger equation and gives, especially in the intermediate energy region, results which are close to the quantum mechanical ones¹⁰⁹. The description of the collision dynamics is achieved by means of classical equations of motion or with a transport equation. With the help of large statistics one can try to simulate the uncertainty which is inherent in any quantum mechanical description. The standard approach is based on the Hamilton equations of motion for the coordinates q_i and the conjugate momenta p_i of all particles involved

$$\dot{q}_i = \frac{\partial H}{\partial p_i}; \quad \dot{p}_i = -\frac{\partial H}{\partial q_i}, \quad i = 1, 2, \dots, 9. \quad (4.10)$$

H is the full Hamilton function of the three-body problem. After the separation of the center-of-mass motion one is left with six degrees of freedom in the coordinate and momentum space, respectively.

For the solution of (4.10), initial conditions have to be specified. They are easily determined for the motion of the projectile nucleus relative to the target center of mass: In

coordinate space, one has to specify the internuclear distance $R(t = r_0)$ and the impact parameter b , while the initial momentum follows from energy conservation. Such a classical nuclear trajectory is also used in all semiclassical theories.

The difficulty of the classical methods lies, however, in the choice of the initial conditions for the electronic motion. The only information can be extracted from the quantum mechanical momentum and spatial distribution of the bound target state, which means that some sort of statistics has to be used for the initial conditions. The various versions of the standard approach differ just in the prescription for these initial conditions in terms of a distribution function $\rho(\mathbf{r}, \mathbf{p})$ which should give an optimal representation of the quantum mechanical spatial and momentum distribution. The simplest way consists in the choice of the microcanonical distribution¹¹⁰

$$\rho_M(\mathbf{r}, \mathbf{p}) = N_M \delta(E - H_0), \quad H_0 = p^2/2 + V(r) \quad (4.11)$$

where N_M is a normalization constant. For a Coulomb potential $V = -Z/r$, an integration of ρ_M over \mathbf{r} reproduces the exact quantum mechanical momentum distribution summed over the quantum numbers l and m , $\rho_m(\mathbf{p}) = \sum_{l,m} |\tilde{\varphi}_{nlm}(\mathbf{p})|^2$, if E is chosen to be the energy of the n th shell, $E = -Z^2/2n^2$. Although the spatial distribution calculated from (4.11) does not agree well with the quantum mechanical distribution, one expects good results for transfer reactions because it is basically the momentum transfer which is decisive¹¹¹. The energy conservation implemented in (4.11) reduces the free parameters of $\rho_M(\mathbf{r}, \mathbf{p})$ to five, which can be used to describe the shape and orientation of the Kepler orbit for the bound target electron¹². These parameters are taken to be equally distributed within their available parameter space¹¹⁰.

Apart from the microcanonical distribution, the Wigner distribution has obtained special consideration because it can reproduce the quantum mechanical distributions in both momentum and coordinate space exactly. However, in contrast to ρ_M , the Wigner distribution is not positive definite and thus cannot be interpreted as a probability density. There exists, though, the possibility of working with a modified Wigner distribution¹¹² which is cut off for energies smaller than E_{\min} and larger than E_{\max}

$$\rho_W(\mathbf{r}, \mathbf{p}) = \frac{N_W}{(2\pi)^3} \int d\mathbf{x} e^{i\mathbf{p}\cdot\mathbf{x}} \psi^* \left(\mathbf{r} - \frac{\mathbf{x}}{2} \right) \psi \left(\mathbf{r} + \frac{\mathbf{x}}{2} \right) \Theta(E_{\max} - H_0) \Theta(H_0 - E_{\min}) \quad (4.12)$$

where ψ is the exact quantum mechanical eigenstate to H_0 , and N_W a normalization constant. Θ is the Heaviside step function. This distribution obeys $\rho_W \geq 0$. The parameter E_{\min} is determined such that the expectation value of H_0 coincides with the quantum mechanical energy, while E_{\max} is a free parameter which can be adjusted to give a good description of the experimental results.

The initial conditions for \mathbf{r} and \mathbf{p} in this model are distributed statistically according to the distribution (4.12). This method yields a somewhat better agreement with experiment than the use of the parameters from the microcanonical distribution¹¹².

The solution of the equations of motion (4.10) is repeated N times with random numbers selected as initial conditions with the help of the Monte Carlo method, subject to

the abovementioned restrictions. N is chosen sufficiently large to allow for good statistics. Let us denote with N_1 the number of cases where at large times t_1 , the electron can be found in the vicinity of the projectile. The transfer probability is then determined by this fraction of the total number of runs

$$P(b) = N_1/n . \quad (4.13)$$

A different approach which is quantum statistical in nature is not based on the classical Hamilton equations, but on the classical limit of the quantum mechanical Liouville equation, the so-called Vlasov equation¹¹³

$$\frac{\partial}{\partial t} \rho(\mathbf{r}, \mathbf{p}, t) + (\nabla_{\mathbf{p}} H_e) \nabla_{\mathbf{r}} \rho(\mathbf{r}, \mathbf{p}, t) - (\nabla_{\mathbf{r}} H_e) \nabla_{\mathbf{p}} \rho(\mathbf{r}, \mathbf{p}, t) = 0 . \quad (4.14)$$

The distribution function $\rho(\mathbf{r}, \mathbf{p}, t)$ is the Wigner-Weyl representation of the single-particle density operator, and H_e is the Hamilton function for the electron. The solution of the Vlasov equation proceeds in a similar way as outlined for the Hamilton equations: Specifying a classical path for the nuclear trajectory $\mathbf{R}(t)$, Eq. (4.14) is solved for N ‘‘super-particles’’, each super-particle representing a fraction of the quantum fluid. The initial conditions are chosen randomly according to the initial distribution $\rho(\mathbf{r}, \mathbf{p}, t_0)$ which is taken as a reasonable representation of the electron in its bound target state. The capture probability is given by (4.13) where N_1 is now the number of super-particles which are attached to the projectile after the collision.

Another category of statistical methods aims at a partial consideration of quantum mechanics by means of a hydrodynamical equation for the motion of the electron¹¹⁴

$$m \frac{d\mathbf{v}}{dt} = -\nabla W_{\text{eff}}; \quad W_{\text{eff}} = W - \frac{1}{2\sqrt{\rho}} \Delta \sqrt{\rho} \quad (4.15)$$

which can formally be derived by inserting the ansatz $\psi = A \exp(iS)$ into the Schrödinger equation for the electron, such that one identifies $\rho = A^2$ and $\mathbf{v} = \nabla S/m$. For the numerical integration of (4.15) ‘‘probability particles’’ are introduced by dividing the three-dimensional space into N small volumes ΔV_i . For each volume, a coordinate \mathbf{r}_i is introduced accordingly

$$\mathbf{r}_i(t) = N \int_{\Delta V_i} \mathbf{r} \rho(\mathbf{r}, t) d\mathbf{r} , \quad (4.16)$$

and instead of (4.15), the resulting discretized problem is solved

$$m \frac{d^2 \mathbf{r}_i}{dt^2} = -\nabla_{\mathbf{r}_i} W_{\text{eff}}(\mathbf{r}_i, t), \quad i = 1, \dots, N , \quad (4.17)$$

with the help of a predetermined classical internuclear trajectory. The initial conditions for the integration of (4.17) are obtained by means of distributing the N probability particles

in space according to the quantum mechanical probability $|\varphi_i|^2$ and taking an initial velocity of zero. The difficulties of this method arise from the dependence of the effective potential W_{eff} on the density $\rho(\mathbf{r}, t)$ which is a functional of the coordinates \mathbf{r}_i of the particles that are at time t in the vicinity of \mathbf{r} . Due to the coarse-grained structure for finite N the statistical density fluctuations tend to be enhanced in the potential, and one has to introduce smoothing procedures to avoid this effect.

The probability-particle method differs from the standard approach as it requires the solution of a coupled system of $6N$ differential equations of first order, while the methods which are based on the Hamilton equations imply the solution of only six coupled equations, though N times. Correspondingly, it is very time-consuming to improve the statistics, such that the agreement with the experimental capture data¹¹⁴ is not so good.

5. Many-Electron Models

The cases where the collision system consists of only three particles are very rare and are either confined to collisions of fully stripped projectiles with hydrogen atoms, or to merged-beam experiments with hydrogen-like target ions. In all other cases one has to deal with the presence of several electrons. In this section, the full multi-electron problem is addressed.

The starting point for describing the transfer of one or more electrons in a collision where N electrons are present, is the N -particle Schrödinger equation

$$i\partial_t\psi(\mathbf{r}_1, \dots, \mathbf{r}_N, \mathbf{R}(t), t) = H_{el}\psi(\mathbf{r}_1, \dots, \mathbf{r}_N, \mathbf{R}(t), t),$$

$$H_{el} = -\frac{1}{2} \sum_{k=1}^N \nabla_{\mathbf{r}_k}^2 - \sum_{k=1}^N \left(\frac{Z_P}{r_{kP}} + \frac{Z_T}{r_{kT}} \right) + \sum_{j < k}^N \frac{1}{|\mathbf{r}_j - \mathbf{r}_k|},$$

where $\mathbf{r}_1, \dots, \mathbf{r}_N$ are the coordinates of the N electrons, while in the semiclassical picture, the internuclear motion is described by the trajectory $\mathbf{R}(t)$. \mathbf{r}_{kP} and \mathbf{r}_{kT} is the distance of the k th electron from the projectile and target nucleus, respectively. The coupling between the electrons is induced by the last term in H_e , the electron-electron repulsion.

As discussed below, it is in some cases possible to stick to one-electron models with modified wave functions and potentials, especially if the electron-electron interaction can be neglected. Even if it cannot be neglected, the construction of effective one-particle states is still feasible with the help of the Hartree-Fock method. However, as soon as the electron-electron correlations play a significant role in the collision dynamics, one has to cope with the full multi-electron problem. Some approaches to the full problem are discussed at the end of this chapter.

5.1. Reduction to a Modified Three-Body Problem

There are situations where the electron-electron coupling plays only a minor role and can be neglected. An example is the charge exchange between the innermost shells of projectile and target which are separated sufficiently well from higher shells so that they can be considered as isolated, as long as the collisions are very slow or very fast. As the

separation between the energy levels increases strongly with projectile charge, this approximation is especially suited for inner-shell excitation of superheavy systems¹¹⁵. The quas-one-electron systems are also candidates for the omission of the electron-electron interaction. These are systems with a single electron occupying the outermost shell, while the core electrons can be considered as passive spectators.

In all these cases one assumes that the electrons are independent of each other (independent electron model) and that their dynamics are described by one-particle potentials V_p and V_T which are modified in order to account for the presence of the passive electrons¹¹⁶. In the simplest case, they are Coulomb fields to an effective charge.

After the potentials are determined, any suitable one-electron model from Secs. 1–4 can be chosen to calculate the transfer probability P_i of an electron which is initially in a given state φ_i . Since the electrons are considered as independent, the probability of transferring m electrons from the subshell i (in which n electrons shall be present) is obtained from the formula^{117,118}

$$W_m = \binom{n}{m} P_i^m (1 - P_i)^{n-m}. \quad (5.2)$$

The factor $(1 - P_i)^{n-m}$ accounts for the fact that $n - m$ electrons shall remain in the subshell i ; it is, however, negligible when P_i is very small. If the number of available final states is smaller than the occupation number n in the initial subshell, the electronic spin has to be considered explicitly in the derivation of the transfer probability. This will modify (5.2), resulting in a non-binomial distribution of W_m . In order to describe the simultaneous transfer of electrons which originate from different subshells of the target, one has to calculate the probabilities separately for each subshell and multiply them afterwards. One then also has to sum over the possible initial distributions of the transferred electrons¹¹⁷.

The many-body classical trajectory Monte Carlo scheme¹¹⁹ provides a method to go beyond the independent electron model by describing the simultaneous motion of all target electrons with the help of classical trajectories, while the electron-electron interaction is still approximated by means of an effective Coulomb potential. In this way, the angular distributions and energies of all particles involved, the projectile ion, the target (recoil) ion and the ejected electrons can be determined.

5.2. Inclusion of the static electron-electron coupling

While in the modified three-body problems the electron-electron interaction enters at most implicitly through the choice of an effective potential, and antisymmetrization is completely neglected, the next step is to include the two effects in a static description while keeping the advantage of treating the collision dynamics in the framework of a one-electron model. To this aim the Hamiltonian is approximated by means of a sum of one-particle operators

$$H_i \approx \sum_{k=1}^N h_{\text{eff}}(\mathbf{r}_k, \mathbf{R}(t)), \quad h_{\text{eff}}(\mathbf{r}_k, \mathbf{R}) = -\frac{1}{2} \Delta_{\mathbf{r}_k} + V_{\text{eff}}(\mathbf{r}_k, \mathbf{R}). \quad (5.3)$$

$V_{\text{eff}}(\mathbf{r}, \mathbf{R})$ is an effective potential in which every single electron is moving. In the adiabatic approximation this potential is constructed anew for every fixed internuclear distance $R(t)$.

The most advanced solution to the stationary many-body problem is the Hartree-Fock method¹²⁰. The N -particle wave function is written in the form of a Slater determinant composed of one-particle wave functions, in order to include antisymmetrization. The one-particle functions are the self-consistent solutions to the Hartree-Fock equations and thus account for the electron-electron coupling. In case of very heavy collision partners, the Schrödinger operator (5.3) has to be replaced by the Dirac operator. This implies solution of the Dirac-Hartree-Fock-Slater (DHFS) equations^{121–123} instead of the Hartree-Fock equations. The equations are either solved by numerical integration¹²² or by expanding the wave functions in terms of a linear combination of projectile- or target-centered orbitals (LCAO), and determining the expansion coefficients upon insertion into the Hartree-Fock¹²⁴ or DHFS equations¹²¹. In this way, the one-particle energies as a function of R , i.e. the correlation diagrams, can be calculated very accurately^{124,125}.

Instead of using the rather numerically involved Hartree-Fock method for the construction of an effective one-particle potential, one may alternatively apply the density functional approach¹²⁶. This approach consists in representing the total energy of the many-electron system in terms of a one-particle density with the help of a gradient expansion, the density being determined from a variational equation. By constructing the effective potential from lowest-order terms in the gradient expansion one avoids the intricacies of a self-consistent solution of the one-particle equations inherent in the Hartree-Fock method.

The simplest way to obtain the density is provided by the Thomas-Fermi method which neglects any gradient terms in the energy functional. The Thomas-Fermi potential is set up for each of the colliding atoms separately, which are then added to yield the two-center effective potential^{127,128}. In contrast to the Hartree-Fock method, the Thomas-Fermi prescription is easily extended to ionized quasi-molecular systems. In order to account for the dependence of the screening on the internuclear distance, the “variable screening model” has been constructed. In this model, the effective charge which enters into each of the potentials, is interpolated between the limiting cases of separated and united atoms, respectively¹²⁹.

The Thomas-Fermi method can be improved by including a gradient term in the kinetic energy functional and by considering the exchange term to zeroth order (Thomas-Fermi-Dirac-Weizsäcker model)¹³⁰. For the lowest orbitals in the correlation diagram, the agreement with Hartree-Fock calculations is very good¹³¹. A further improvement can, in principle, be achieved by retaining higher terms in the gradient expansion, or even by including the correlation energy. Also, an extension to relativistic collision systems is feasible through the consideration of inhomogeneity corrections¹²⁶.

The construction of an R -dependent effective potential reduces the solution of (5.1) to the solution of N time-dependent one-particle equations

$$i\partial_t\psi_k(\mathbf{r}, \mathbf{R}, t) = h_{\text{eff}}(\mathbf{r}, \mathbf{R})\psi_k(\mathbf{r}, \mathbf{R}, t), \quad k = 1, 2, \dots, N. \quad (5.4)$$

For small N , a numerical integration of the time-dependent Hartree-Fock equations (5.4) is feasible with the technique of finite differences¹³², however, in most cases an expansion of ψ_k into basis states is preferred. For the basis, one may use atomic states¹³³ which are especially suited for asymmetric collision systems¹³⁴. If the Hartree-Fock method has been applied for the construction of the effective two-center potential, it is advantageous to expand the wave function in terms of Hartree-Fock orbitals $\varphi_n(\mathbf{r}, \mathbf{R})$ which are the stationary solutions to $h_{\text{eff}}(\mathbf{r}, \mathbf{R})$,

$$\psi_k(\mathbf{r}, \mathbf{R}, t) = \sum_n c_{nk}(t) \varphi_n(\mathbf{r}, \mathbf{R}) e^{if_n \mathbf{v} \cdot \mathbf{r}} \quad (5.5)$$

where f_n is an appropriate translational factor¹³⁵. Correspondingly, for near-symmetric very heavy ion collisions, the wave function is preferably expanded in terms of the DHFS orbitals¹²³.

Hence, the solution of the N -particle Schrödinger equation is reduced to the solution of N independent systems of differential equations for the expansion coefficients c_{nk} , in complete analogy to the case of a single electron. The initial state is represented by a Slater determinant which consists of the N occupied atomic states which are solutions to $h_{\text{eff}}(\mathbf{r}, \mathbf{R} \rightarrow \infty)$ in the limit of infinite internuclear separation. As electron-electron correlations are neglected, the wave function at arbitrary time t is also a Slater determinant of the solutions of (5.4).

In order to specify the transition probability, the final state is again represented as a Slater determinant of the stationary solutions to $h_{\text{eff}}(\mathbf{r}, \mathbf{R} \rightarrow \infty)$. The transition amplitude is obtained from the projection of the determinant built of the solutions of (5.4) at large times onto this final state. In general, the states of only a few of the electrons of the collision system are experimentally resolved; hence, the square of the transition amplitude has to be integrated over all possible final states of the remaining electrons^{136,137}.

5.3. Approaches to the dynamical N -body problem

The time-dependent N -particle Schrödinger equation can in principle also be solved without the explicit construction of time-dependent single particle states. To this aim one first calculates the solutions ϕ_n of the stationary N -particle problem according to Sec. 5.2. The exact wave function ψ is then expanded in terms of these Slater determinants ϕ_n ,

$$\psi(\mathbf{r}_1, \dots, \mathbf{r}_N, \mathbf{R}, t) = \sum_n a_n(t) \phi_n(\mathbf{r}_1, \dots, \mathbf{r}_N, \mathbf{R}) e^{i \sum_k f_n(\mathbf{r}_k, \mathbf{R}) \mathbf{v} \cdot \mathbf{r}_k} \quad (5.6)$$

where the phase factor represents a state-dependent translational factor¹³⁸. By inserting (5.6) into the Schrödinger equation (5.1) and projecting onto the function ϕ_m^* , the following system of coupled equations is obtained

$$\begin{aligned} i\dot{a}_m(t) &= a_m(t) \hat{\epsilon}_m - i \sum_n a_n(t) \langle \phi_m | \partial_t + \sum_k \{ \nabla_{\mathbf{r}_k}(\mathbf{r}_k f_n) \} (\mathbf{v} \nabla_{\mathbf{r}_k}) \\ &+ \frac{1}{2} \mathbf{v} \nabla_{\mathbf{r}_k}^2 (f_n \mathbf{r}_k) | \phi_n \rangle. \end{aligned} \quad (5.7)$$

Only the dominating coupling terms which are at most linear in the velocity \mathbf{v} have been retained in (5.7). Correspondingly, the terms proportional to $\dot{a}_n \mathbf{v}$ and $\hat{\epsilon}_n \mathbf{v}$ arising from the

non-orthogonality of the translated basis states, have also been dropped. The energy $\hat{\epsilon}_m$ is the sum of the energies of the single particle states contained in ϕ_m plus the translational energy induced by f_n . In this way one obtains directly for $t \rightarrow \infty$ the occupation numbers of the states ϕ_m and thus the transition probabilities into the atomic states into which ϕ_m develops asymptotically. As mentioned before, a summation over the final states of all unobserved electrons is required in order to compare the transition probability with experiment.

For heavy systems the solution of (5.1) with consideration of all existing electrons is very time-consuming. Therefore, a part of the electrons, for example the passive core electrons, is described by means of an effective atomic potential, and the complete time-dependent problem is only solved in the subspace of the remaining electrons. Numerical solutions have been obtained, e.g. in the special case of two active electrons¹³⁸.

Another possibility of approximating the time-dependent N -electron problem consists in omitting the electron-electron interaction when the stationary basis states ϕ_n are constructed. This means that ϕ_n is composed of hydrogenic or molecular Coulomb states. Then the electron-electron coupling appears as an additional transition operator in the dynamical equations; hence, a corresponding modification of the coupled equations (5.7) has to be solved. However, this is generally done within a rather limited space of basis states ϕ_n in the expansion (5.6)¹³⁹.

A quite different approach to the dynamical many-body problem is concerned with the introduction of a collective variable for the electronic motion, which is treated classically like the internuclear motion. For the collective variable, the charge asymmetry is used¹⁴⁰

$$\zeta = -\sum_{i=1}^N \frac{z_i}{R/2} + Z_P - Z_T \quad (5.8)$$

where z_i is the z -coordinate of the i th electron in a rotating frame, the origin of which is at the midpoint between projectile and target nucleus, with the z -axis along \mathbf{R} . The variable ζ characterizes the partition of the electrons between projectile and target. Its aim is an intuitive description of the transitions between the various ionic states of the collision system as a function of the internuclear distance. Like in the previously mentioned methods, at first the stationary problem has to be solved for fixed values of R and ζ by means of constrained Hartree-Fock equations

$$\left[h_{\text{eff}}(\mathbf{r}, \mathbf{R}) - \lambda \left(-\frac{z}{R/2} + \frac{Z_P - Z_T}{N} \right) \right] \varphi_k(\mathbf{r}, \mathbf{R}, \zeta) = \epsilon_k \varphi_k(\mathbf{r}, \mathbf{R}, \zeta) \quad (5.9)$$

where the Lagrange multiplier λ is determined through the condition that ζ has a given expectation value. From the solution of (5.9) one obtains generalized correlation diagrams $\epsilon_k(R, \zeta)$ which reveal the possible ways of how the exchange of electrons can take place.

The dynamics of the collision process can subsequently be obtained by expanding the exact N particle wave function in terms of the solutions to (5.9) and inserting it into the Schrödinger equation. For this purpose, the time-dependence of ζ has to be known. It can

be described with the help of Ehrenfest's theorem by a classical equation of motion, which is governed by a potential derived from the energy surface. An alternative way to handle the time-dependent problem¹⁴¹ proceeds similar to the Monte Carlo calculations: The equation of motion for ζ is solved repeatedly with initial conditions distributed around the equilibrium value of ζ at $R \rightarrow \infty$, and the fraction of trajectories leading to charge exchange determines the capture probability. However, due to the restriction to axial symmetry and the neglect of rotational coupling, the results are inferior to those of the other methods¹⁴¹.

6. Extension to Relativistic Velocities

A relativistic description of electron capture leads to a fundamentally different behavior as would be expected from an extrapolation of the nonrelativistic theories to the limit $v \rightarrow \infty$. The reason lies in the fact that the transformation from the projectile frame to the target frame, which is of increasing importance as v increases, is no longer mediated by \hat{U}^+ from (1.2). Instead, a spinor transformation \hat{S} has to be used¹⁴²,

$$\psi(\mathbf{r}, t) = \hat{S}\psi'(\mathbf{r}', t') \quad (6.1)$$

$$\hat{S} = \sqrt{\frac{1+\gamma}{2}} \left(1 + \frac{\gamma v/c}{1+\gamma} \alpha_z \right), \quad \alpha_z = \begin{pmatrix} 0 & \sigma_z \\ \sigma_z & 0 \end{pmatrix}, \quad \gamma = (1 - v^2/c^2)^{-1/2}$$

where σ_z is the Pauli spin matrix. This transformation does not only lead to a different velocity dependence, but it induces also an additional magnetic field when applied to the projectile potential V_P

$$\gamma_0 V_P(\mathbf{r}, t) = \hat{S} \gamma_0 V_P'(\mathbf{r}') \hat{S}^{-1} = \gamma_0 \gamma V_P'(\mathbf{r}') \left(1 - \alpha_z \frac{v}{c} \right) \quad (6.2)$$

where γ_0 is a Dirac matrix¹⁴², and the coordinates in the target frame (\mathbf{r}, t) are related to the ones in the projectile frame (\mathbf{r}', t') by means of a Lorentz transformation. In the following, atomic three-body models are investigated in order to extract the energy dependence of the capture cross section. A relativistic formulation of a coupled-channel approach as well as the numerical integration of the Dirac equation is also discussed.

6.1. Atomic theories

Generalizing the results from Sec. 1.1 to the relativistic case, the exact transition amplitude can be written in the following way¹⁴³

$$a_{fi} = -i \int dt \langle \bar{\psi}_f^{(-)}(\mathbf{r}', t') \hat{S}^{-1} | \hat{S} \gamma_0 V_i'(\mathbf{r}', t') \hat{S}^{-1} | \varphi_i(\mathbf{r}, t) \rangle \quad (6.3)$$

with $\bar{\psi} = \psi^\dagger \gamma_0$. In a similar manner, the post and prior distorted forms, (1.8) and (1.11), respectively, can be formulated relativistically and can serve as a starting point for a relativistic version of the high-energy atomic theories.

The relativistic first-order Born approximation¹⁴⁴⁻¹⁴⁶ which is obtained by replacing $\psi_f^{(-)}$ by φ_f' in (6.3) leads to an energy dependence of the capture cross section like E^{-1} where $E = \gamma M_p c^2$. An early attempt to calculate the double-collision term classically¹⁴⁵ resulted in an energy dependence like E^{-3} , in contradiction to the non-relativistic dominance of the second-order term. However, a quantal analysis of the relativistic second Born approximation shows the following high-energy behavior¹⁴³

$$\sigma^{(1+2)} = \text{const}(\ln E)^2/E, \quad E \rightarrow \infty \quad (6.4)$$

which supports the dominance of the second Born term. An approximation¹⁴⁷ to the second-order Born theory which considers only the leading terms in an expansion in powers of Z_p/c and Z_T/c does not reproduce (6.4), but leads to a decay of σ like E^{-1} . From an investigation of the third-order Born theory¹⁴⁸ within the same approximation it can be conjectured that the correction terms beyond second order show a much faster decay with E and thus play no role in the ultrarelativistic limit. This can also be seen from a relativistic formulation of the impulse approximation¹⁴⁹ where the same logarithmic energy dependence is found as given in (6.4).

Recently, further theories have been extended to relativistic collision velocities. The eikonal theory, both in its asymmetric¹⁵⁰ and symmetric form¹⁵¹ leads, as expected, to the identical energy dependence as the Brinkman-Kramers theory. Also the standard CDW theory¹⁵² behaves like $\sigma \sim E^{-1}$ and not like the second Born as in the nonrelativistic case. An inclusion of the second-order CDW term will therefore be necessary to give the correct asymptotic behavior.

Theories which contain intermediate off-shell states, like the SPB and the DWB, have not been investigated for relativistic velocities. For this purpose, an explicit representation of a relativistic off-shell function would be required, which has not yet been obtained.

6.2. Coupled channel calculations

For collisions with very heavy targets such as uranium, atomic theories are no longer able to reproduce experiments with sufficient accuracy for the heavier projectiles, because even for velocities approaching c , the ratio between v and the electronic velocity v_e is not considerably larger than one¹⁵³. Since the ratio Z_p/Z_T is not very small either, there does not exist a natural expansion parameter and one has to resort to non-perturbative approaches.

A possibility of treating charge transfer in very heavy ion collisions consists in the use of basis states which are Dirac eigenfunctions to the projectile ($\varphi_n^{P'}(\mathbf{r}', t')$) and to the target ($\varphi_m^T(\mathbf{r}, t)$), respectively. The exact wave function for the active electron is expanded according to¹⁵⁴

$$\psi(\mathbf{r}, t) = \sum_n a_n(t) \hat{S} \varphi_n^{P'}(\mathbf{r}', t') + \sum_m b_m(t) \varphi_m^T(\mathbf{r}, t). \quad (6.5)$$

Insertion into the two-center Dirac equation

$$i\partial_t \psi(\mathbf{r}, t) = \left[c\boldsymbol{\alpha}\mathbf{p} + \beta mc^2 + V_T(\mathbf{r}) + \gamma V_P(\mathbf{r}') \left(1 - \alpha_z \frac{v}{c} \right) \right] \psi(\mathbf{r}, t) \quad (6.6)$$

leads, like in the nonrelativistic case, to a system of coupled differential equations for the occupation numbers a_n and b_m . The main difference to the nonrelativistic description, the occurrence of long-range monopole and dipole couplings which originate from the induced magnetic interaction, only affects excitation, but not capture. Pilot calculations for 1 GeV $U + U$ collisions with twenty basis states show a considerable deviation of the K-shell capture cross section from results within the relativistic boundary-corrected first-order theory¹⁵⁴.

6.3. Numerical integration of the Dirac equation

For the sake of completeness we want to address a different approach to the relativistic one-electron problem which until now has only been applied to direct processes, but which may readily be extended to electron capture. It consists of a direct numerical integration of the two-center Dirac equation by means of discretization, either with the help of finite elements¹⁵⁵ or with the finite difference method¹⁵⁶. The latter method has recently been used not only for relativistic (i.e. very heavy) projectiles, but also for relativistic collision velocities¹⁵⁷. In the special case of zero impact parameter, the integration of (6.6) requires a discretization in the time coordinate and the two spatial coordinates ρ and z , which is done in a similar way to that described in Sec. II.4.2. The wave function obtained at large times is then projected onto the set of Dirac eigenstates of the target in order to obtain the probability for excitation or ionization. In the case studied, 1 GeV $U + U$, it is found that a considerable fraction of electrons is emitted into the direction of the projectile, but only a small part will be captured into bound states¹⁵⁷.

III. Applications

In atomic collision physics there exists a strong interdependence between theory and experiment. This is necessary in order to get insight into the fundamental processes which govern the reactions. Charge exchange provides a tool to investigate a large variety of problems. Only partly, are these problems specific to charge transfer; however, due to the fact that the rearrangement is basically a second-order process, there is in general a much stronger sensitivity to the properties of both the collision partners. A large field of application is the spectroscopy of quasi-molecular orbitals in slow collisions⁴. As the electronic transitions occur predominantly at avoided crossings of the energy levels, impact parameter measurements make it possible to locate these crossings if the collision energy is chosen appropriately. Such experiments also help to decide which reaction path is favored if there is more than one way to populate a given final state. Impact-parameter measurements are sensitive to interferences which reflect the possibility that capture can take place on the incoming or on the outgoing part of the internuclear trajectory. Such interferences can lead to an oscillatory structure of the capture probability from which the mean energy distance of the participating levels may be inferred^{158,159}. In case of a resonant nuclear reaction one even gets information about the lifetime of the corresponding compound nucleus^{160,161}. The decrease of the capture probability with impact parameter is strongly related to the energy transfer to the active electron. A study of the impact-parameter dependence of the vacancy production probability therefore allows in principle a distinction between electron capture and ionization. This is helpful

because ionization may contribute significantly even in the case of a small v or large Z_P/Z_T , where capture has some chance to dominate¹⁶².

If one compares electron transfer in different collision systems, there are similarities which may tentatively be expressed by means of scaling relations^{30,77,163}. The validity of such a scaling can, however, only be tested in comparison with experiment¹⁶⁴.

The description of electron transfer through a sequence of binary collisions implies the occurrence of critical angles where the differential scattering cross section has distinct maxima^{10,11,32,165}. An experimental verification of this classical picture has been accomplished in the case of the Thomas peak^{166,167} and recently also for the double-scattering peak at 60 degrees¹⁶⁸.

The knowledge of capture cross sections is of great importance for the determination of the charge state of the projectile inside a solid target. For sufficiently thick targets, the charge state follows from the balance between electron capture and loss, while for arbitrary target thickness rate equations have to be solved¹⁶⁹. The influence of the environment on the projectile charge state is crucial to the behavior of particles in thermonuclear fusion plasmas, but it governs also the losses in storage rings.

In the comparison between theoretical models and experimental capture data given below, we restrict ourselves to the presence of a single active electron because in such a case, experimental conditions are most precisely defined, and the basic assumptions of the theoretical descriptions become most transparent. This means that the large field of simultaneous multi-electron transfer, but also the transfer-excitation is not considered here. By selecting collision systems with high impact velocity or with large asymmetry between the nuclear charges Z_P and Z_T , one hopes that the multi-electron processes contribute only a negligible fraction to the non-coincident capture cross sections. Examples of electron transfer in low-energy collisions can be found in the review articles mentioned at the beginning^{2,4} or in the references of Secs. II.2 to II.5. Specific cases of Coulomb capture and radiative capture into both bound and continuum projectile states will be considered. Also, examples of capture during resonant nuclear scattering will be given, in relation to other experiments which are sensitive to nuclear reactions.

1. Charge Transfer in the Absence of Nuclear Reactions

In this section, collision systems are selected which allow for a classical description of the internuclear motion by means of a Rutherford trajectory (or some approximation to it). This implies that the projectile and target nuclei scatter elastically from each other and do not change their properties during the collision. This is the case for the great majority of capture reactions except the few where a compound nucleus is formed, or where the electron is captured into the nucleus.

Capture reactions can be mediated by two different transition operators, the Coulomb interaction between electron and projectile/target, as well as the photon field. The former case, also termed Coulomb capture, has been discussed extensively in the previous sections. However, theories for the second kind of reactions, the radiative electron transfer, can easily be obtained from the models for Coulomb capture by replacing one of the Coulomb transition operators by the radiation operator. The visibility of radiative

electron capture into bound projectile states (REC) in total capture cross sections or in the photon spectrum requires high projectile charges ($Z_P > Z_T$) as well as high impact energies. Therefore, the projectile correlated frame is usually taken as a reference frame for the electron, and the radiation operator transformed into this frame by means of the transformation \hat{U} from (1.2) reads

$$H'_R = \hat{U}H_R\hat{U}^+ = \frac{i}{c} e^{i\omega t} \mathbf{A}_\mu \left[\nabla_{\mathbf{r}'} - i \left(\dot{\mathbf{x}}_f - \frac{M_T}{M} \dot{\mathbf{R}} \right) \right] \quad (\text{III.1})$$

$$\mathbf{A}_\mu = \frac{c}{2\pi\sqrt{\omega}} \mathbf{u}_\mu$$

where the dipole approximation has been used. The unit vector \mathbf{u}_μ denotes the polarization direction of the photon, and ω its frequency. $M = M_P + M_T$ is the sum of the projectile and target mass. Since the coupling to the photon field is weak, a first-order theory in H_R is sufficient. In order to demonstrate how the REC theory is obtained from the theory for Coulomb capture, the strong potential Born approximation is selected as a specific example. Restricting ourselves to the case $Z_P \gg Z_T$, the post form of the transition amplitude has to be used, and by analogy to (1.47) we find (primed quantities are defined in the projectile frame, taking $x_f = 0$)

$$a_{fi}^{\text{RSPB}} = -i \int dt \int d\mathbf{q} \left\langle \varphi'_f(\mathbf{r}_P) \left| \frac{i}{c} \mathbf{A}_\mu \nabla_{\mathbf{r}_P} e^{i\omega t} \right| \psi_{\mathbf{q},E}^{\prime R(+)}(\mathbf{r}_P) \right\rangle$$

$$\times \tilde{\varphi}_i(\mathbf{q} + \mathbf{v}) e^{i\mathbf{q}\mathbf{R}} \exp \left(i \left(\varepsilon_f - \varepsilon_i + \frac{v^2}{2} \right) t \right) \quad (\text{III.2})$$

$$E = \varepsilon_f + \omega$$

where the second term of H'_R from (III.1) has been neglected because it is smaller by a factor M_T/M_P . In contrast to the Coulomb capture, into (III.2) enters an off-shell state which is renormalized, $\psi_{\mathbf{q},E}^R$. This renormalization is necessary because in the limit of vanishing target charge, the REC cross section has to coincide with the cross section for radiative recombination¹⁷⁰, which means that in this limit, $\psi_{\mathbf{q},E}^R$ is a physically observable state. For Coulomb capture on the other hand, a renormalization is not required because the corresponding matrix element vanishes identically for $Z_T = 0$. The specific choice of the renormalization factor is still an open question; however, the simplest choice of using the ratio between a Coulomb wave and an off-shell state in the limit $Z_T \rightarrow 0$ reproduces the experiment very well¹⁷¹. The results without renormalization¹⁷² are in severe contradiction to the data.

Besides the strong potential Born theory in its nonrelativistic^{171,172} and relativistic¹⁷³ version, other current theories for radiative electron capture are the impulse approximation¹⁷⁴, a two-state approximation¹⁷⁵ which essentially is a peaking approximation to the IA, as well as a theory developed from the correspondence of REC to the inverse photoionization¹⁷⁶. The latter theory as well as the impulse approximation is also easily extended to radiative transfer into projectile continuum states (termed radiative ionization)^{177,178}.

1.1. Capture into bound states

The total cross section for the capture of a target electron from the subshell i with N_i occupied states into the subshell f of the projectile is calculated from

$$\sigma = 2\pi N_i \int_0^\infty b db |a_{fi}(b)|^2 \quad (\text{Coulomb capture}) \quad (\text{III.3})$$

$$\sigma^R = 2\pi N_i \frac{\omega^2}{c^3} \sum_{\mu=1,2} \int_0^\infty b db \int d\omega d\Omega_\gamma |a_{fi}^R(b)|^2 \quad (\text{REC})$$

where Ω_γ is the solid angle into which the photon is emitted.

Figure 3 shows the cross section for capture from the Ar K-shell as a function of the energy of the impinging proton. The experimental data^{179,180} include the capture into excited states which according to the n^{-3} scaling contributes about 20% of the capture into the K-shell. Comparison is made with the following models: the SPB with the exact off-shell function⁵⁵, the transverse peaked SPB in the near-shell approximation (1.51)¹⁸¹, the exact impulse approximation⁵⁵, the boundary corrected first-order Born theory⁴², a

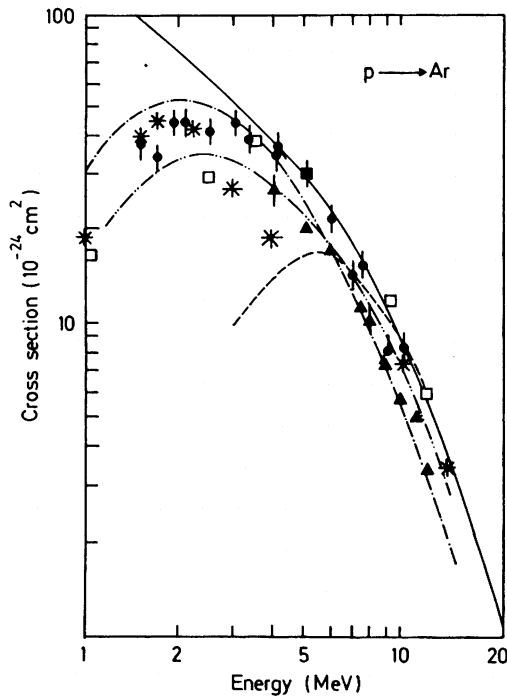


Fig. 3. Capture cross section from the Ar K-shell by protons as a function of collision energy. Experiments: \blacktriangle (McDonald *et al.*¹⁷⁹), \blacklozenge (Horsdal Pedersen *et al.*¹⁸⁰). Theory: $-\cdot-\cdot-$ IA (Jakubaša-Amundsen⁵⁵), * unpeaked SPB (Jakubaša-Amundsen⁵⁵), $-\cdot-\cdot-\cdot-$ transverse-peaked SPB (Jakubaša-Amundsen and Amundsen¹⁸¹), $-\cdot-\cdot-$ true first Born (Dewangan and Eichler⁴²), $-----$ two-state approximation (Lin and Tunnell⁷⁰), \square coupled-channel (Ford *et al.*¹⁸²).

two-state approximation⁷⁰ and a coupled-channel calculation¹⁸². All calculations consider only the capture into the projectile ground state except the Born theory which includes a factor 1.2 to account for capture into excited states. It follows from Fig. 3 that in case of high impact energies, all theories are able to explain the experimental data, while for energies below the capture maximum, the SPB gives the best results. (The rather low values of the unpeaked SPB slightly above the maximum are probably an artifact related to the handling of the divergence). Even at the lowest energies considered, a coupled-channel calculation is not yet required for such asymmetric systems.

Figure 4 shows the energy dependence of the capture cross section for the symmetric systems $p + H$, $p + H_2$, as well as for $p + He$. A supplementary figure for the lower collision energies ($E < 0.5$ MeV) can be found in Ref. 2. A comparison is made between the CDW theory⁸, the near-shell SPB which has been evaluated with the help of an asymptotic high-energy approximation¹⁸³, the impulse approximation¹⁸⁴, the eikonal approximation^{66,185} as well as the boundary corrected first Born approximation⁴³. With the exception of the SPB results, the calculations include capture into higher projectile states. All theories under consideration give an agreement with the experimental data^{186–192} within a factor of two in the whole energy region ($E > 0.5$ MeV). If, however, energies down to 25 keV are included, the (symmetric) CDW theory is best in explaining the data¹⁹³.

More detailed information about the capture process is provided by differential measurements. The comparison with the experimental impact-parameter dependence provides a much more sensitive test of the theories than is the case for total cross sections. For the same collision system as considered in Fig. 3 ($p + Ar$), the impact-parameter dependence at an energy of 6 MeV is depicted in Fig. 2 (shown in Sec. II.1.2). From this

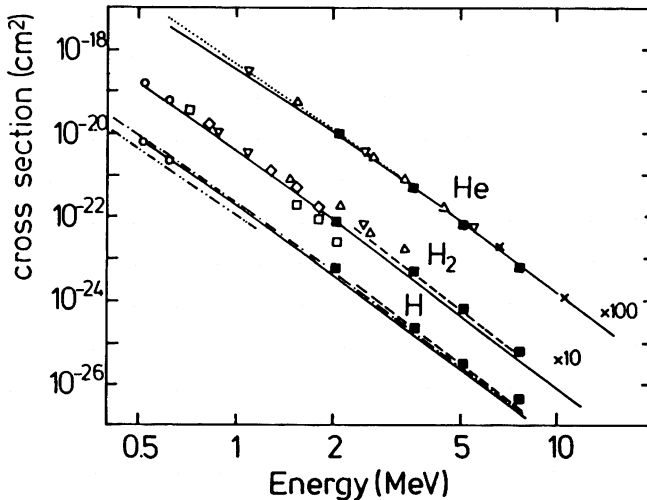


Fig. 4. Capture cross sections from H, H_2 and He by protons as a function of collision energy. Experiments: ■ (Schwab *et al.*¹⁸⁶), ○ (Hvelplund and Anderson¹⁸⁷), △ (Schryber¹⁸⁸), ▽ (Welsh *et al.*¹⁸⁹), □ (Williams¹⁹⁰), ◇ (Toburen *et al.*¹⁹¹), × (Berkner *et al.*¹⁹²). Theory: — CDW (Belkić *et al.*⁸), ---- SPB (McGuire *et al.*¹⁸³), true first Born (Belkić *et al.*⁴³), -·-·- eikonal approximation (Dewangan¹⁸⁵; Eichler and Chan⁶⁶), —·—·— IA (Coleman and Trelease¹⁸⁴).

figure it follows that atomic perturbation models like the transverse peaked SPB in near-shell approximation³¹ or the impulse approximation³⁰ reproduce not only the experimental total cross sections, but also the impact-parameter distribution. The b -dependence is also well described by the simple Brinkman-Kramers approximation^{27,29} although it is (as discussed previously) not an adequate theory, and often overestimates total capture cross sections at the higher energies¹⁶⁴. An exception is the (first-order) CDW theory²⁹ which cannot reproduce the data in the whole impact parameter region, and the discrepancy is increased when the collision velocity becomes higher. Although the deviations between CDW and experiment diminish at fixed velocity if the collision system gets more symmetric, the CDW2 approximation⁴⁶ is required to get a satisfactory agreement with the data.

At very high collision velocities a double peak structure becomes visible in the angular distribution. The additional peak corresponds to capture events where the projectile is deflected by the critical Thomas angle $\vartheta = (m/M_p) \sin 60^\circ$. For its explanation, a classical double-collision model for charge transfer can be used¹¹. In this model it is assumed that in a first encounter the projectile scatters from the target electron in such a way that the electron is deflected by 60° with respect to \mathbf{v} . This angle is required to accelerate an electron at rest to the velocity v . In a second encounter, this electron collides elastically with the target nucleus, and is again deflected by 60° . After the two collisions, the electron moves in the same direction as the projectile and hence is easily captured. As the projectile is unaffected in the second encounter, its deflection by the Thomas angle is an indication of an enhanced capture probability.

The first experimental observation of the double peak structure in the differential capture cross section has been achieved only recently¹⁶⁶ for the collision system $p + \text{He}$. Figure 5 shows $d\sigma/d\Omega$ at a proton energy of 7.4 MeV ($v \gg Z_p, Z_T$). For a theoretical description of the Thomas peak, capture theories are required which comprise the second-order Born approximation. The Brinkman-Kramers theory would only show a monotonous decrease with scattering angle over the whole ϑ -region¹⁹⁴. In the figure, calculations within the exact second-order Born theory¹⁹⁵, the near-shell SPB in its asymptotic high-energy approximation¹⁹⁵, as well as the DWB in two high-energy versions, an on-shell peaking-approximation⁵⁹ and an off-shell peaking approximation⁶⁰, are presented. The first-order CDW theory is inconsistent with experiment because it exhibits a sharp minimum near $\vartheta = 0.28$ mrad¹⁹⁶. However, the CDW2 (shown in Fig. 5) is, like the other models depicted in the figure, in good agreement with the experimental result. Note that all theories are folded with the experimental detector resolution which washes out the structure to some extent.

A second critical angle¹⁰ is predicted at a deflection of the projectile by 60° . An enhancement of the capture cross section at this angle is expected from a different classical double collision process: In a first encounter, the projectile scatters from the target electron, the latter being deflected by 60° (as in the Thomas scattering). In a second encounter, the projectile hits the target and is deflected by 60° . In this way, projectile and electron also emerge parallel to each other, which facilitates capture.

A clear experimental identification of this 60° peak has not yet been accomplished, however, there is some indication of a broad structure near 60° in energetic collisions of

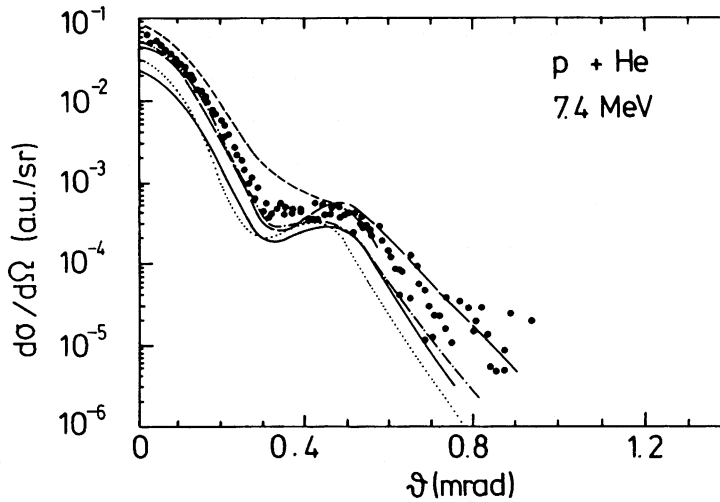


Fig. 5. Differential capture cross section in the collision of 7.4 MeV p + He as a function of scattering angle. Experiment: ● (Horsdal Pedersen *et al.*¹⁶⁶). Theory: ----- second Born (McGuire and Sil¹⁹⁵), — SPB (McGuire and Sil¹⁹⁵), ——— CDW2 (Rivarola, taken from Ref. 195), -·-·-·- off-shell DWB (Alston⁶⁰), on-shell DWB (Roberts⁵⁹).

protons with Ne^{168,197}. For a theoretical description, a straight-line internuclear trajectory as used for small-angle scattering or for total capture cross sections at high impact energy, is no longer appropriate. Instead, the Rutherford path may be approximated by its two asymptotes at time $t = -\infty$ and $t = +\infty$ for zero impact-parameter. Calculations within the peaked near-shell SPB (Ref. 51) as well as the peaked IA (Ref. 198) indeed show some structure at 60° ; however, the agreement with experiment is not too satisfactory.

Another point of interest is the dependence of the capture cross section on the specific parameters of the collision system. The dependence on the target charge is depicted in Fig. 6 for relativistic systems, where data for Xe⁵⁴⁺ impinging on Be, Mylar, Al, Ag and Au are compiled¹⁹⁹. A comparison with theoretical calculations for Coulomb capture in the relativistic eikonal approximation¹⁵⁰ and for radiative capture using a relativistic theory for the inverse photoeffect¹⁷⁶ reveals that for the heavier targets, Coulomb capture dominates at all energies. For light targets, however, the experimental data can be explained with REC alone.

The photon spectrum for the lightest of these collision systems, 197 MeV/amu Xe + Be, is shown in Fig. 7¹⁷⁸. The prominent peak around the energy $v^2/2 - \epsilon_f \approx 125$ keV originates from REC into the projectile K-shell (with binding energy $-\epsilon_f$). The calculations¹⁷⁸ reveal that for such a heavy projectile, a second well-separated peak emerges which is due to capture into the Xe L-shell. The background of the peak on its low-energy side is mainly due to radiative ionization¹⁷⁷, calculated with a high-energy approximation to the impulse approximation¹⁷⁸, while the photons beyond the peak arise from secondary electron bremsstrahlung.

For more symmetric collision systems, however, there remains an additional background, especially on the high-energy side of the REC peak²⁰⁰. This is an indication

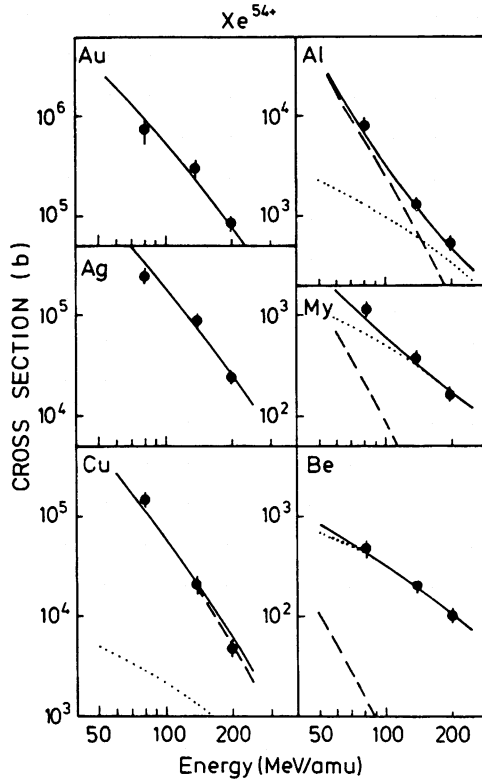


Fig. 6. Total capture cross section in the collision of Xe^{54+} with Be, Mylar, Al, Cu, Ag and Au as a function of projectile energy. Experiments: \blacklozenge (Meyerhof *et al.*¹⁹⁹). Theory: ----- Coulomb capture (Eichler), REC (Anholt), ——— sum of both theories (taken from Ref. 199). For Ag and Au, REC can be neglected.

that an atomic theory like the impulse approximation or the inverse photoeffect fails for photon energies far off the peak where high momentum transfers to the active electron are required. Indeed, the influence of molecular effects which are calculated from the variational sliding center model⁹⁷ lead, even for high velocities, to an increase of the cross section in the tails of the REC peak.

1.2. Capture to the Continuum

We now turn to the case where the target electron is in a continuum state after the collision. It will then not always be easy to determine whether the electron is at large times in a target continuum state, in a projectile continuum state, or in a free state. A classical consideration based on a comparison of the electron-target potential with the electron-projectile potential after the collision may shed some light on the situation²⁰¹, and in the following, some examples are discussed in which charge transfer plays a decisive role. Formally, the continuum solution to the three-body Schrödinger equation is most conveniently expressed in terms of the Faddeev equations¹⁸

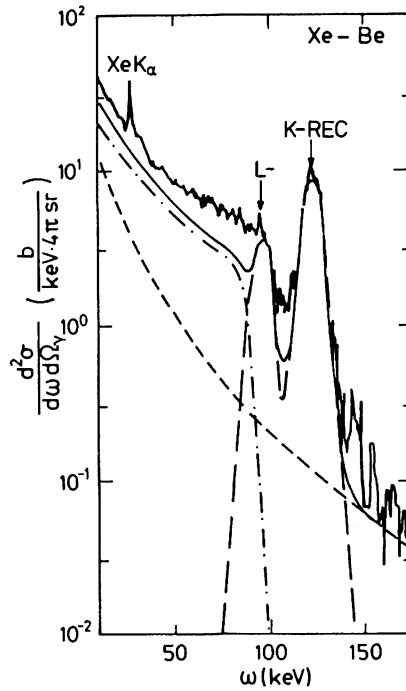


Fig. 7. Doubly differential cross section for photon emission under 90° in the collision of 197 MeV/amu Xe + Be as a function of photon frequency. Experiment: Histogram (Anholt *et al.*¹⁷⁸). Theory: ——— REC, - - - - - RI, ----- secondary electron bremsstrahlung, ——— sum of all theories (taken from Ref. 178).

$$\psi_f^{(-)}(t) = \varphi_{f0}(t) + \psi_1^{(-)}(t) + \psi_2^{(-)}(t)$$

$$\psi_1^{(-)}(t) = \int d\tau G_T^{(-)}(t, \tau) V_T(\tau) (\varphi_{f0}(\tau) + \psi_2^{(-)}(\tau)) \quad (\text{III.4})$$

$$\psi_2^{(-)}(t) = \int d\tau G_P^{(-)}(t, \tau) V_P(\tau) (\varphi_{f0}(\tau) + \psi_1^{(-)}(\tau))$$

where $\varphi_{f0}(t)$ is an electronic plane wave and we have restricted ourselves to recoil-free collisions. This representation of $\psi_f^{(-)}$ takes into consideration that both electronic fields V_P and V_T can influence the final state. If (III.4) is iterated, and in $\psi_1^{(-)}$ and $\psi_2^{(-)}$ only terms proportional to $G_T(t, \tau) V_T(\tau) \varphi_{f0}(\tau)$ are considered, the Born series for ionization into a target final state is obtained upon insertion into the transition amplitude (1.11). If the terms retained in the expansion of $\psi_f^{(-)}$ are symmetric with respect to V_P and V_T , the Faddeev approximation^{202,203} is recovered. This approximation includes a target final state as well as a projectile final state. If, on the other hand, only terms proportional to $G_P(t, \tau) V_P(\tau) \varphi_{f0}(t)$ are collected in $\psi_1^{(-)}$ and $\psi_2^{(-)}$, the final state is represented in terms of a projectile eigenstate. It is this last case which provides a description of Coulomb capture to the continuum (CTC) or to radiative ionisation (RI).

The pioneer experiment²⁰⁴ which led to the discovery of capture to the continuum, considered the angular and energy dependence of the doubly differential cross section for secondary electron production in collisions of protons with H₂ and He. As demonstrated in Fig. 8 for the case of 300 keV p + He, the experimental cross section rises at small emission angles Θ_f of the electron when Θ_f is decreased, as long as the electron energy is close to $v^2/2$. This is in contradiction to the first Born approximation for ionization. If, on the other hand, a projectile final state is included by means of the first-order Faddeev approximation²⁰² or by means of a three-state calculation²⁰⁵, qualitative agreement with experiment is found. The second-order Born theory for charge transfer, evaluated for the p + H system²⁰⁶, gives an even better explanation of the corresponding experimental data.

The necessity to represent the final state by means of a projectile Coulomb wave arises from the fact that electrons which are emitted with a velocity close to the collision velocity v into the beam direction ($\Theta_f = 0$) are strongly coupled to the projectile. A projectile Coulomb wave considers this coupling particularly in the normalization factor, which shows a square-root singularity when the electron momentum k_f becomes equal to v .

This cusp-like behavior near $k_f = v$ is readily observed in the spectra of secondary electrons at forward direction, independently of the projectile charge. This is demonstrated in the experimental spectra^{207,208} for Ne¹⁰⁺ + He and for p + Ne shown in Fig. 9. The finite peak height is solely due to the finite experimental resolution ($\Delta\Theta_f = 1.4^\circ$ for Ne¹⁰⁺ + He and 0.75° for p + Ne).

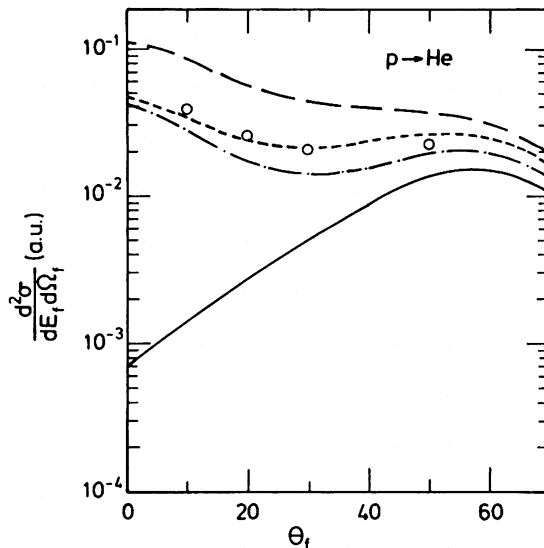


Fig. 8. Doubly differential cross section for the emission of secondary electrons of 100 eV in the collision of 300 keV p + He as a function of the electron emission angle Θ_f . Experiment: \circ (Rudd *et al.*²⁰⁴). Theory: — first Born (Band²⁰⁵), - · - · - 3 state calculation with effective charge Z_{eff} of the continuum state equal to the ground state, - - - - 3 state calculation with $Z_{\text{eff}} = 1$ (Band²⁰⁵) ——— first-order Faddeev theory (Macek²⁰²).

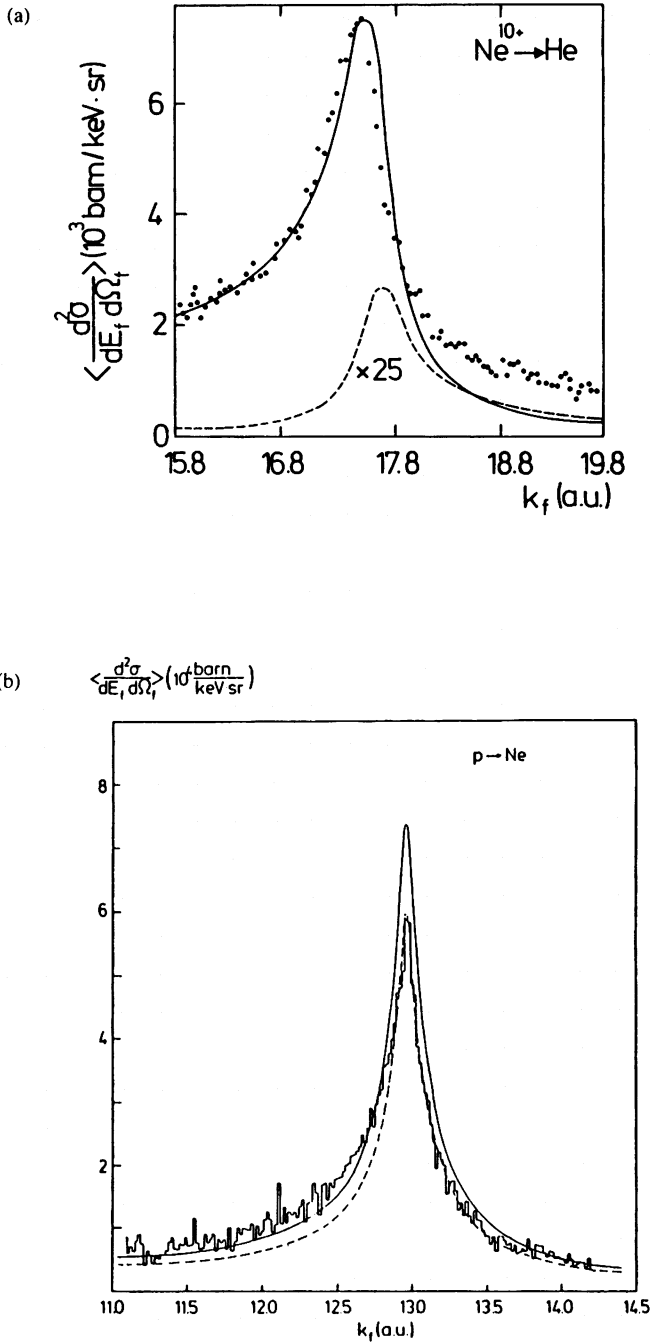


Fig. 9. Angle- and energy-averaged doubly differential cross section for electron emission under zero degree in (a) the collision of 155 MeV $\text{Ne}^{10+} + \text{He}$ and (b) 4.2 MeV $\text{p} + \text{Ne}$ as a function of electron momentum k_f . The experimental energy resolution is (a) $\Delta E_f/E_f = 1.4\%$, (b) 0.5%. Experiment: (a) \bullet (Berry *et al.*²⁰⁷), (b) histogram (Schramm *et al.*, taken from Ref. 214). Theory: (a) ——— post IA (Jakubaša-Amundsen²¹²), - - - - - RI (Jakubaša-Amundsen²¹³). (b) prior IA for - - - - - capture from K-shell, ——— capture from all shells (Jakubaša-Amundsen²¹⁴).

While for the light projectile ($Z_P \ll Z_T$), the forward peak is approximately symmetric, for the heavy projectile ($Z_P \gg Z_T$), there is a strongly enhanced intensity of secondary electrons on the low-energy side of the cusp. This peak asymmetry can neither be reproduced with the Brinkman-Kramers theory, nor with the first-order Faddeev approximation. However, it is inherent in any second- or higher-order capture theory like the second-order Born approximation²⁰⁹, the CDW theory²¹⁰, and the impulse approximation²⁰¹, but it emerges also in a direct numerical integration of the Schrödinger equation²¹¹. Mathematically, this peak asymmetry results from a discontinuity of the capture amplitude at $\mathbf{k}_f = \mathbf{v}$ in addition to the divergence, and provides a stringent test of the various higher-order theories. In contrast to the Thomas peak, the asymmetry of the cusp is easily accessible experimentally because it is the more pronounced the lower the collision velocity where high intensities can be achieved²¹².

In Fig. 9 the post impulse approximation in transverse peaking, both for Coulomb CTC (Ref. 212) and radiative ionization²¹³, is shown for $\text{Ne}^{10+} + \text{He}$. The collision velocity is far too low for RI to give an important contribution, but CTC reproduces the experimental cusp shape quite well (the cusp intensity is normalized to theory). For the system $p + \text{Ne}$, comparison is made with the full-peaked prior IA for Coulomb CTC. This theory even reproduces the absolute intensity within the experimental accuracy²¹⁴.

Electron capture to the continuum can also play a role in the secondary electron spectrum when the emission angle Θ_f differs from zero, provided the projectile is sufficiently heavy ($Z_P \gg Z_T$) and its velocity sufficiently high. Electron spectra²¹⁵ from 100 MeV $\text{Ne}^{10+} + \text{He}$ at angles between 20° and 150° are plotted in Fig. 10. Comparison is made with the first-order Born approximation for ionization, the first-order Faddeev theory (taking hydrogen-like wave functions with $Z_T = 1.7$), the transverse peaked impulse approximation²⁰², the continuum distorted wave theory²¹⁶ and a Monte Carlo calculation²¹⁵. At small emission angles and high electron energies where the relative velocity between electron and projectile is rather small, all theories except the IA underestimate the experimental doubly differential cross section. On the other hand, the IA overestimates the data drastically at the smaller energies where the electron occupies predominantly a target final state. In this region, the CDW theory gives rather good results. At energies below 0.1 keV, the Monte Carlo method provides too low cross sections at angles $\Theta_f \geq 90^\circ$, while the first Born approximation falls below the data for $\Theta_f \leq 90^\circ$; the Born theory can, however, be partially improved by the use of better wave functions²¹⁵. In the 60° data, in contrast to the smaller angles, the binary encounter peak is clearly seen, and the Born theory as well as the IA reproduce it fairly well. The first-order Faddeev theory does not work at all except for very high energies and large Θ_f , and an estimate of the second-order Faddeev approximation²⁰³ within the full peaking approximation shows no improvement either. In fact, the coherent superposition of terms relating to an electronic target final state and those relating to a projectile state, which is inherent in this theory, leads to strong oscillations in the cusp region as well as in the small-energy limit $E_f \rightarrow 0$ due to the different energy-dependent phase factors in the wave functions. Thus, a single theory for the description of the whole spectrum of secondary electrons does not seem to exist (at least not in the lowest orders of a perturbative approach) and the spectrum has to be divided up into regions where the target field

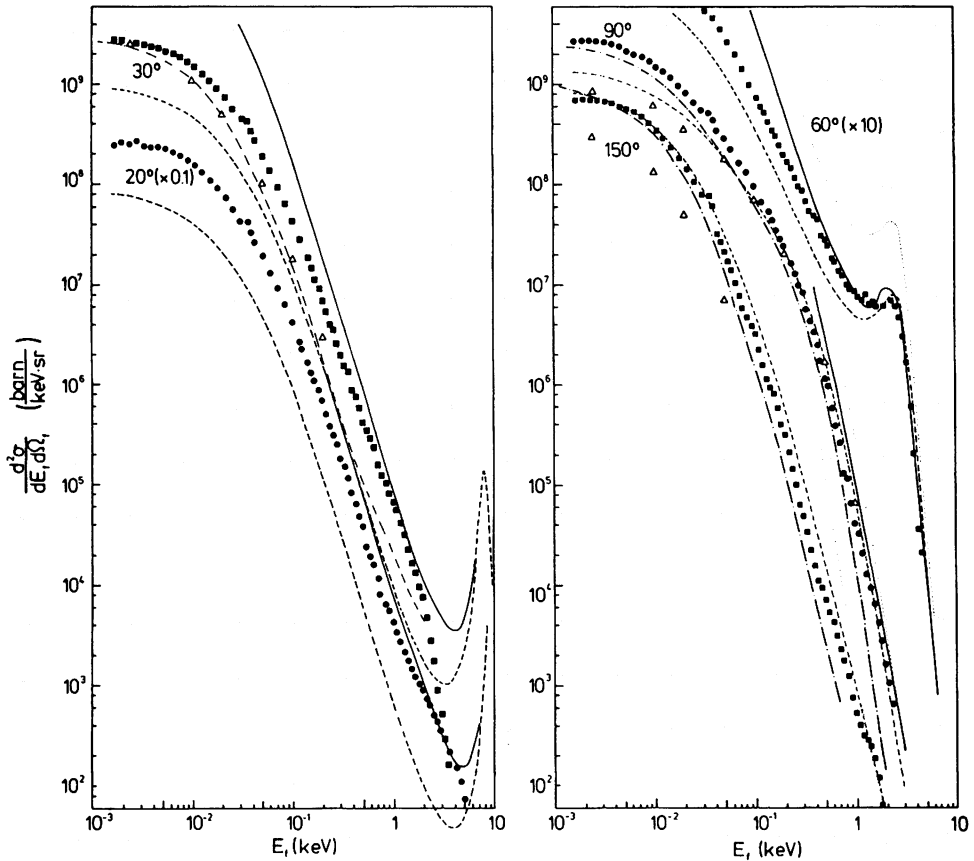


Fig. 10. Doubly differential cross section for secondary electron emission under the angles 20° – 150° in the collision of 100 MeV Ne^{10+} + He as a function of electron energy. Experiment: \bullet , \blacksquare (Schiwietz *et al.*²¹⁵). Theory: Δ Monte Carlo (Schiwietz²¹⁵), $-\cdot-\cdot-$ CDW (Fainstein *et al.*²¹⁶), $-\cdot-\cdot-$ first Born, $—$ transverse peaked IA, \dots first-order Faddeev theory (Jakubaša-Amundsen).

dominates and into other regions where the projectile field is more important. The best description of the whole body of experimental data is achieved with the CDW approximation, although it is with local deviations up to one order of magnitude.

The experimental identification of the radiative capture to continuum in electron spectra is very hard because RI dominates the Coulomb capture only at relativistic impact velocities. However, RI constitutes a contribution to the background in photon spectra²¹⁷, which terminates around $\omega = v^2/2$ as this is the maximum energy which can be radiatively emitted from target electrons moving with an average velocity v with respect to the projectile (compare Fig. 7).

From a theoretical point of view, radiative processes have the great advantage of providing simpler coupling matrix elements as compared to Coulomb capture. Therefore, they are well suited for a comparison between the theoretical models. In the Coulomb case, such a comparison is often falsified because in most cases additional approximations

have to be made. As an example, a comparison between the impulse approximation and the strong potential Born theory for REC and RI reveals²¹³ that for frequencies close to the K-REC peak, SPB and IA give nearly equal results for both bound-state capture and capture to the continuum up to an electron momentum around ν (in the projectile frame). A strong increase of the deviations between IA and SPB at momenta beyond ν can be related to the large momentum transfer which is necessary to speed up the electron such that it finally moves much faster than the projectile. A large momentum transfer is an indication that molecular effects will become important; in fact, due to the stronger coupling to the target field inherent in the (post) SPB as compared to the IA, large deviations between both theories may serve as an indication of the break-down of an atomic perturbative description.

2. Charge Transfer during Resonant Nucleus-Nucleus Scattering

Finally, we want to address a mutual interplay between atomic physics and nuclear physics. It concerns the influence of nuclear reactions on inelastic electronic processes. This influence reveals itself as a time-delay in the collision process, which may cause interferences in the atomic transition probability because the electronic transition can likewise occur before or after the nucleus-nucleus scattering. The interference effect has its maximum value if the energy transfer to the electron matches the width of an intermediately formed nuclear compound state. From a nuclear physics point of view this behavior makes it possible to determine the lifetime of resonant nuclear states, and to study the correlations between overlapping resonances. For deep inelastic reactions, on the other hand, the interaction time becomes accessible because the electronic excitation probability is strongly influenced by the specific time-dependence of the perturbing potential. As far as atomic physics is concerned, the interference phenomenon gives information on the relative phases of the electronic transition amplitude in the incoming and outgoing channel. In the case of a nuclear reaction where the Coulomb field is switched off in one channel (i.e. (p, γ) , but also α -decay) one is enabled to study the electronic transition on a half-trajectory in a head-on collision. It is obvious that such interference effects are particularly sensitive to the different theoretical models and provide therefore a crucial test of the theories when compared with experimental data of sufficiently good statistics.

The interrelation between nuclear physics and atomic physics has been studied extensively in the specific cases of ionization^{14,218}, positron production^{15,219} and bremsstrahlung^{220,221}. In this section, we concentrate on electron transfer in energetic collisions with light projectiles, where only elastic nuclear scattering will be considered. We also present a comparison with the time-delay effects from nuclear resonances or deep inelastic reactions, which appear in the probabilities for K -hole production, δ -electron emission and positron creation.

2.1. Capture during elastic scattering by light projectiles

The theory for electron transfer has to be reformulated if a nuclear reaction has to be accounted for. The occurrence of the nucleus-nucleus interaction V_N between projectile and target, which now comprises a short-range potential plus the Coulomb force, makes a

quantum mechanical formulation necessary. For a three-body problem the Hamiltonian under consideration is (in place of H_e)

$$H = T_N + V_N + T_e + V_T + V_P \quad (\text{III.5})$$

where T_N is the kinetic energy of the internuclear motion. The quantum mechanical formulation of electron capture within the distorted wave Born approximation can easily be generalized from the $V_N = 0$ case^{21,48} to nonzero internuclear potentials²²². From the DWB, successive approximations like the SPB (Refs. 13 and 223), the IA or the Brinkman-Kramers theory can likewise be derived.

As a specific example we consider the SPB theory. The inclusion of the internuclear potential leads to the following form of the capture amplitude (instead of 1.47))

$$\begin{aligned} A_{fi}^{\text{SPB}} = & \int d\mathbf{K} d\mathbf{k} \langle \psi_{fN} | e^{-i\beta_e \mathbf{K} r_T} \chi_{\mathbf{k}}^{(-)} \rangle \{ \langle \psi_{\mathbf{k},\varepsilon}^{(-)} e^{-i\beta_e \mathbf{K} r_T} \chi_{\mathbf{K}}^{(-)} | V_P | \psi_{iN} \rangle \\ & + \langle \psi_{\mathbf{k},\varepsilon}^{(-)} e^{-i\beta_e \mathbf{K} r_T} \chi_{\mathbf{k}}^{(-)} | V_N | \phi_i \rangle \} + \langle \psi_{fN} | V_P | \psi_{iN} - \phi_i \rangle. \end{aligned} \quad (\text{III.6})$$

Here, an integration over the intermediate momentum of both electron (\mathbf{k}) and nucleus (\mathbf{K}) is required. The electronic off-shell energy is $\varepsilon = E - K^2/2\mu_i$ where E is the total energy and μ_i the reduced mass. $|\mathbf{k}\chi_{\mathbf{K}}^{(-)}\rangle$ is the product of an electronic plane wave and an eigenfunction, ($\chi_{\mathbf{K}}^{(-)}$), of $T_N + V_N$, and $\beta_e = m/(M_T + m)$. Further, ψ_{iN} and ψ_{fN} are eigenstates of $T_N + V_N + T_e + V_T$ and $T_N + V_N + T_e + V_P$, respectively, and ϕ_i is eigenstate to $T_N + T_e + V_T$. Like in the semiclassical theory, the transfer is mediated by the projectile field V_P as well as by the recoil (the term proportional to $V_N|\phi_i\rangle$). In addition, a first-order correction term emerges in the case $V_N \neq 0$ (the last term in (III.6)).

As compared to the semiclassical case, the evaluation of A_{fi} is more involved because of the occurrence of the nuclear scattering functions $\chi_{\mathbf{K}}$. However, use can be made of the different length scales of nuclear and atomic processes to separate $\chi_{\mathbf{K}}$ into an interior part where the electronic matrix elements are approximately constant, and into an outer part where an asymptotic expansion of $\chi_{\mathbf{K}}$ can be used²²⁴. With this approximation, the transition amplitude can be expressed in terms of the nuclear scattering amplitude $f^{(+)}(K, \vartheta)$:

$$A_{fi}^{\text{SPB}} = a_{ii} f^{(+)}(K_f, \vartheta) + a_{if} f^{(+)}(K_f', \vartheta) + a_{ff} f^{(+)}(K_i, \vartheta) + A^S. \quad (\text{III.7})$$

The occurrence of *three* terms proportional to the scattering amplitude is a consequence of the fact that capture is described within a higher-order theory, namely as a two-step process consisting of excitation into a continuum state with subsequent capture (cf. III.6). The third term in (III.7) describes the electronic excitation plus capture *after* the nucleus-nucleus scattering, such that the relative momentum of the scattering nuclei is equal to the initial momentum \mathbf{K}_i . The first term in (III.7) denotes excitation plus capture *before* the nucleus-nucleus scattering which takes place with a relative momentum \mathbf{K}_f , which, as compared to \mathbf{K}_i , is reduced by the momentum transfer to the electron. Finally,

the second term relates to the case where excitation occurs before but capture after the nuclear collision. In the general case one has a sum (over K'_f) of such terms; however, in the full peaking approximation only the term with $K'_f \approx K_f$ survives. This last type of interaction terms is not present in a first-order theory. This is known from studies of ionization within the first Born approximation²²⁴; however, a close-coupling theory for ionization also leads to additional terms containing intermediate states^{219,225}.

The remaining term A^S accounts for the capture while the two nuclei stick together. This sticking term is proportional to the difference between two scattering amplitudes, and hence vanishes for non-resonant scattering. The transition probability as a function of scattering angle is obtained by means of

$$P(\vartheta) = N_i(2\pi)^4 \mu_i^2 |A_{fi}|^2 [f^{(+)}(K_i, \vartheta)]^{-2}. \quad (\text{III.8})$$

If the short-range part of V_N vanishes, i.e. if the scattering amplitude is a slowly varying function with energy such that $f^{(+)}(K_i, \vartheta) \approx f^{(+)}(K_f, \vartheta)$, (III.8) reduces to the semiclassical capture probability for large-angle scattering⁵¹.

If, on the other hand, an isolated nuclear resonance occurs at an energy E_0 with width Γ , oscillations in $P(\vartheta)$ can be observed under the condition that the width is approximately equal to the energy transfer ΔE to the electron

$$\Gamma \approx \Delta E \quad (\text{III.9})$$

with ΔE from (II.1). However, the scattering angle has to be taken sufficiently large such that the resonant part of the scattering amplitude is not too small as compared to the contribution from pure Coulomb scattering.

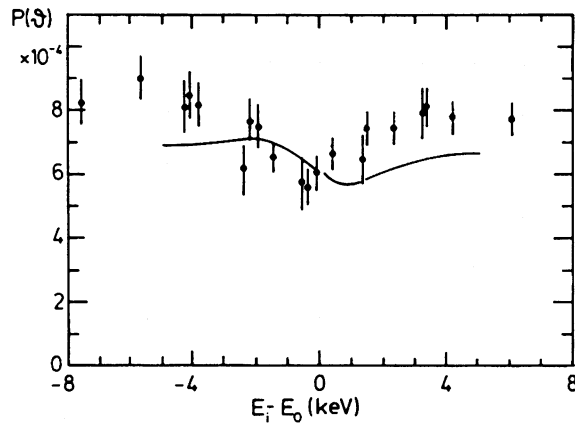


Fig. 11. Capture probability at $\vartheta = 30^\circ$ in the reaction $^{20}\text{Ne}(p, p')$ near the resonance at $E_0 = 1955$ keV as a function of projectile energy. Experiment: \blacklozenge (Horsdal *et al.*²²⁶). Theory: — full-peaked SPB (Jakubaša-Amundsen and Amundsen).

The first experiment with sufficient statistics²²⁶ has been performed with the collision system $p + {}^{20}\text{Ne}$ in the vicinity of the $l = 2$ nuclear resonance at $E_0 = 1955$ keV ($\Gamma = 4$ keV). The resulting capture probability is shown in Fig. 11 as a function of the collision energy E_i . As all target electrons contribute to the capture, the structure around $E_i = E_0$ is somewhat washed out, but as the criterion of (III.9) is violated by more than a factor of 2, the excursion of $P(\vartheta)$ is expected to be not too large anyhow. Comparison is made with the SPB theory in full peaking approximation²²³, and qualitative agreement is found. Theoretically, only capture into the projectile K-shell is considered, and also no fit of the parameters of $f^{(+)}(K, \vartheta)$ to the experimental elastic scattering cross section has been made, which might partly account for the deviations. It should also be noted that the first-order correction term in (III.6) has been neglected. For its evaluation, a better representation of the nuclear wave function in the outer region would be required in order to obtain the correct limit zero of this term at $\vartheta = 0$. The full peaking approximation should also be relaxed. Generally, the effect of that term will be a lowering of the capture amplitude at the larger scattering angles²²².

The sensitivity of the transition probability across a nuclear resonance to different theories is most readily demonstrated in the case of radiative capture where peaking approximations are not necessary. The quantum mechanical SPB expression for the REC amplitude consists of one term only, which corresponds to the first term of (III.6)²²⁷

$$A_{f_i}^{\text{RSPB}} = \int d\mathbf{K} d\mathbf{k} \langle \psi'_{f_N} | H'_R | \psi_{\mathbf{k},\epsilon}^{(+)} e^{i\alpha_e \mathbf{K} \cdot \mathbf{r}} p \chi_{\mathbf{K}}^{(+)} \rangle \langle e^{i\alpha_e \mathbf{k} \cdot \mathbf{r}} p \chi_{\mathbf{k}}^{(+)} | \psi_{iN} \rangle \quad (\text{III.10})$$

with $\alpha_e = m/(m + M_p)$ and the wave functions defined below (III.6). In Fig. 12, the capture probability per photon frequency and angle is shown for the collision system $\text{O}^{8+} + \text{He}$ in the vicinity of the $l = 1$ resonance at $E_0 = 20.01$ MeV (in the CM frame, the resonance energy is 4.002 MeV, and $\Gamma = 2.5$ keV). The selected frequency $\omega = 1.6$ keV is slightly above the REC maximum for capture into the K-shell which is considered here. As Γ matches the energy transfer, the excursion of $d^2P/d\omega d\Omega_\gamma$ is very pronounced at the larger angles. Comparison is made between the SPB, the impulse approximation ($\psi_{\mathbf{k},\epsilon}^{(+)}$ in (III.10) replaced by a projectile Coulomb wave), and the Brinkman-Kramers theory ($\psi_{\mathbf{k},\epsilon}^{(+)}$ replaced by a plane wave). As far as the position of the maxima and minima in $d^2P/d\omega d\Omega_\gamma$ is concerned the theories agree rather well, which confirms the expectation that the gross features of the interference structure is determined by the parameters of the resonance. However, there exist considerable deviations between the various models in the absolute values, and even the width is slightly model-dependent. Worthy of remark are the strong deviations between SPB and IA at the larger scattering angles where a large momentum transfer to the electron is required. This might point again to an insufficiency of an atomic perturbative approach in this angular region. A comparison with experiment would shed light on that problem, but no data are yet existing.

2.2. Comparison with other clocks for nuclear reaction times

Following the predictions^{228,229} that atomic transition probabilities should be influenced by nuclear reactions, interference effects caused by a nuclear resonance have at

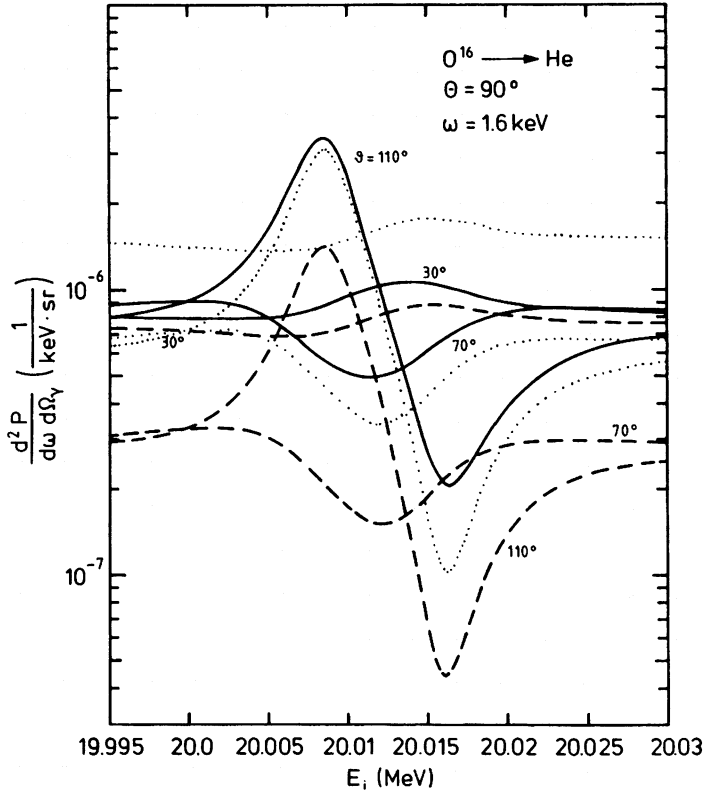


Fig. 12. Differential probability for photon emission at 90° in the collision of $\text{He}({}^{16}\text{O}, {}^{16}\text{O}')$ near the resonance at $E_0 = 20.01$ MeV as a function of projectile energy. The photon frequency is 1.6 keV, and the scattering angles range from 30° – 110° . Theory: — SPB, - - - IA (Jakubaša-Amundsen²²⁷), BK (Jakubaša-Amundsen).

first been experimentally observed in bremsstrahlung spectra²²⁰ as well as in the energy dependence of K-vacancy production²³⁰. Like for electron capture, the condition for the visibility of a distinct interference pattern in the ionization probability is the matching between the width of a nuclear resonance and the excitation energy of the electron, which now takes the form²²⁴

$$\Gamma \approx E_f - \varepsilon_i \quad (\text{III.11})$$

where the kinetic energy E_f of the ejected electron is typically up to one tenth of the binding energy $|\varepsilon_i|$ if energy-integrated ionisation probabilities are considered. Correspondingly, nuclear lifetimes τ with $\tau \approx |\varepsilon_i|^{-1}$ are accessible through such an experiment. Varying the target from, say, Li to U, these lifetimes are in the range of 10^{-17} s to 6×10^{-21} s for light projectiles, but down to 6×10^{-22} s for heavy projectiles. As an example where the condition (III.11) is met, the K-shell ionization probability for the system $p + {}^{138}\text{Ba}$ across the 10.00 MeV isobaric analog $f_{7/2}$ resonance is shown in Fig. 13a ($\Gamma/|\varepsilon_i| = 1.8$, $\tau = \Gamma^{-1} = 1.8 \times 10^{-20}$ s). The experimental data²³¹ are well

reproduced by a first-order ionization theory²³² including compound-elastic scattering which originates from the fine structure of the isobaric analog resonance²³³. Taking into consideration the rather large discrepancy between the data and a theory where compound-elastic scattering is neglected, such an experiment can be used to determine compound-elastic cross sections.

For comparison, Fig. 13b shows the capture probability in the collision $p + {}^{22}\text{Ne}$ across the isolated s -wave resonance at 1.51 MeV where the criterion (III.9) is also met ($\Gamma/\Delta E_K = 1.4$, $\Gamma/\Delta E_L = 2.9$; $\tau = 2.7 \times 10^{-19}$). The experimental data²³⁴ are compared with full-peaked SPB calculations for capture from all target shells into the projectile ground state²²³. The size of the measured effect in $P(\vartheta)$ amounts to a factor of 4 despite the damping from target L-shell contributions, while it is a factor of 3 for ionization. The greater sensitivity of charge transfer to a nuclear resonance is related to the fact that charge transfer is a two-step process which is more sensitive to phase changes than a first-order process like ionization. The difference in the excursion of $P(\vartheta)$ will be even more pronounced when electrons from different target shells cannot be experimentally separated. Then for ionization, the matching condition (III.11) will be severely violated, while in the case of capture, the presence of $v^2/2$ in the energy transfer (II.1) assures a similar energy transfer for all shells. If $v^2/2$ is of the order of the K-shell binding

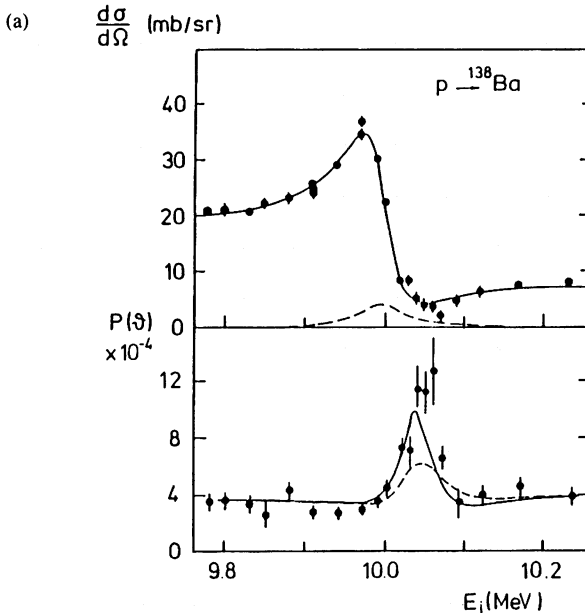
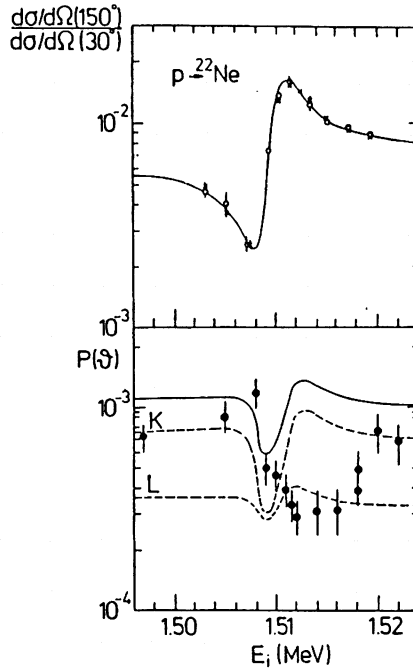


Fig. 13. (a) K-shell ionisation in the reaction ${}^{138}\text{Ba}(p, p')$ near the resonance at $E_0 = 9.965$ MeV as a function of projectile energy. Top: elastic scattering cross section at $\vartheta = 172^\circ$; Experiment: \bullet Spooner *et al.*²³¹; Theory: — Fit of the nuclear parameters to the data, --- upper limit to the compound-elastic scattering contribution (taken from Ref. 231). Bottom: K-shell ionisation probability at $\vartheta = 172^\circ$; Experiment: \blacklozenge Spooner *et al.*²³¹; Theory: First Born approximation — including the compound-elastic scattering contribution, ---- excluding this contribution (Amundsen and Aashamar).

(b)



(b) Electron capture in the reaction $^{22}\text{Ne}(p, p')$ near the resonance at $E_0 = 1.51$ MeV as a function of projectile energy. Top: ratio of the elastic scattering cross section at $\vartheta = 150^\circ$ to the cross section at 30° ; Experiment: \circ , \times Baker *et al.*²³⁴ (normalized to full curve) for a 75/25% mixture of $^{22}\text{Ne}/^{20}\text{Ne}$ in the target; Theory: — Fit of the nuclear parameters to the data (taken from Ref. 234). Bottom: capture probability at $\vartheta = 150^\circ$ for a pure ^{22}Ne target; Experiment: \blacklozenge Baker *et al.*²³⁴; Theory: Full-peaked SPB approximation for target --- K and L shells, respectively, and ——— K + L shells (Jakubaša-Amundsen and Amundsen).

energy, the range of accessible nuclear lifetimes will be shifted a factor of 2 downwards as compared to ionization. The large sensitivity of electron capture to nuclear reactions has been demonstrated by investigating a variety of resonances both experimentally¹⁶¹ and theoretically^{13,223} where a structure in $P(\vartheta)$ is seen even if (III.9) is violated up to a factor of 10.

It should be noted that the agreement between theory and experiment for ionization^{14,232} and δ -electron emission²³⁵ across a nuclear resonance is generally much better than for electron capture. In particular, the large discrepancy in the width of the $P(\vartheta)$ -structure between the data and the theory for $p + \text{Ne}$ (Figs. 11, 13b) is not understood. From a theoretical point of view, one would expect a width of approximately 2Γ as in the case of ionization, irrespective of the applied theory.

Time-delay effects have recently also been observed in deep-inelastic reactions. In such reactions, a considerable amount of the projectile energy is dissipated during nuclear contact^{218,236}, which means that the collision time is increased by the so-called delay time t_d which plays a similar role as the lifetime τ of a resonant state. From a first-order consideration one can show that the transition probability depends approximately on the energy ΔE transferred to the electron like²³⁶

$$dP/d\Delta E \sim e^{-(t_c+t_d)\Delta E} \quad (\text{III.12})$$

where $t_c \approx 2d_0/v$ (with d_0 as the distance of closest approach in a Coulomb head-on collision) is the collision time in a pure Coulomb field. Correspondingly, the delay time can be inferred from the slope of the spectra of electrons or positrons which are emitted during the collision^{236,237}. Alternatively, the influence of the delay time has been found to show up in the dependence of the K-shell ionization probability on the dissipated energy (the Q -value)^{14,238}, since the delay time is monotonically related to the Q -value.

Figure 14a shows δ -electron spectra which result from 8.6 MeV/amu Pb + Pb collisions in a small impact-parameter region²³⁷. For elastic nuclear scattering, the slope of the experimental spectra can be satisfactorily reproduced by a scaling model derived from the first Born approximation when a Rutherford trajectory is used for the internuclear motion. However, with increasing Q -value the deviation between this theory and the data becomes more and more apparent. In order to reproduce experiment, a nuclear trajectory has to be used which allows for friction. As can be seen from the figure, the friction model

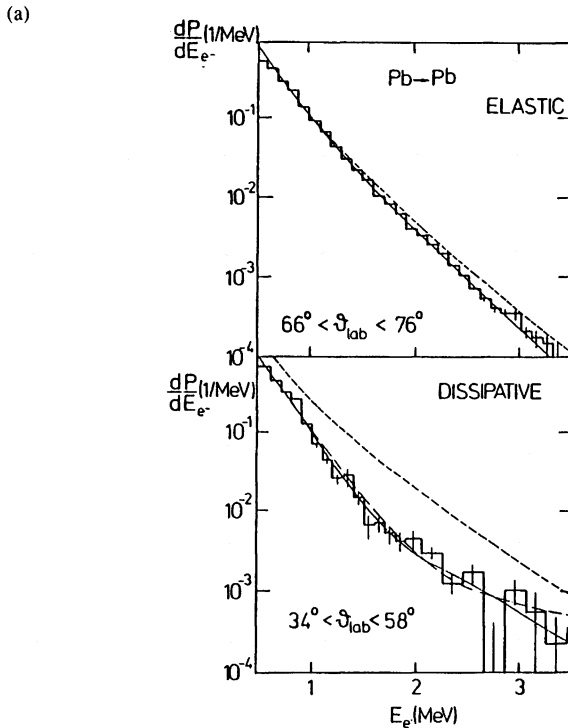
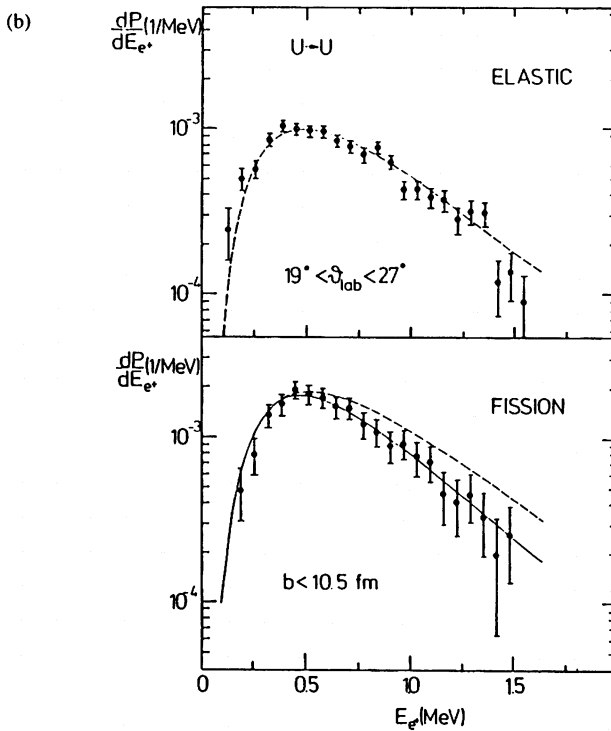


Fig. 14. (a) Probability for δ -electron emission in 8.6 MeV/amu Pb + Pb collisions as a function of electron energy. Top: elastic scattering ($Q = 0$) in the angular region $66^\circ < \vartheta_{\text{lab}} < 76^\circ$; Bottom: dissipative scattering ($-450 \text{ MeV} < Q < -250 \text{ MeV}$) corresponding to the angular region $34^\circ < \vartheta_{\text{lab}} < 58^\circ$. Experiment: (Histogram) Krämer *et al.*²³⁷; Theory: scaling model of first Born approximation using for the internuclear motion --- Coulomb trajectories, - - - reaction model of Schmidt *et al.*²³⁹, — fit of classical trajectories to the data (taken from Ref. 237).



(b) Probability for positron emission in 10 MeV/amu U + U collisions as a function of positron energy. Top: elastic scattering in the angular region $19^\circ < \vartheta_{\text{lab}} < 27^\circ$; theory is multiplied by a factor of 0.85. Bottom: dissipative scattering with fission in the angular region $\vartheta_{\text{lab}} > 27^\circ$ ($b < 10.5$ fm); theory is multiplied by a factor of 0.95. Experiment: \blacktriangle Krieg *et al.*²³⁶; Theory: coupled channel calculations of Müller *et al.*²¹⁸ using for the internuclear motion --- Coulomb trajectories, ——— reaction model of Schmidt *et al.*²³⁹ (taken from Ref. 236).

of Schmidt *et al.*²³⁹ is equally good in explaining the data, as a fit of the parametrized trajectory to experiment. An interesting feature of the electron spectrum at large Q -values is the occurrence of two different slopes which may be interpreted as a remnant of an oscillation pattern showing up in a semi-classical calculation for a well-defined nuclear sticking time²⁴⁰. Friction effects in δ -electron spectra have also been observed for I + Au collisions¹⁴ and U + U collisions²³⁶.

In Fig. 14b positron spectra from 10 MeV/amu U + U collisions are shown. Coupled channel calculations²¹⁸ can well reproduce the experimental slope if for the dissipative collisions (with subsequent fission of one or both uranium nuclei) the Rutherford trajectory is replaced by an appropriate friction trajectory. The corresponding interaction time amounts up to 2×10^{-21} s for the impact energy of 10 MeV/amu, depending on the impact parameter. As different reaction models lead to different slopes of the positron or δ -electron spectra, the experimental spectra provide a nice possibility of testing reaction models.

IV. Summary and Outlook

In this article, a survey has been given of recent developments in the theoretical description of electron transfer in ion-atom collisions. In studying the theories in comparison with experimental data, we have concentrated on the transfer of a single electron in collisions where either the impact velocity is large compared to atomic orbiting velocities, or where the ratio between the nuclear charges of projectile and target deviates strongly from unity. It has been demonstrated that for asymmetric collision systems, an atomic perturbation theory of first order in the weak field (the SPB) gives the best agreement with experimental data on electron capture into bound states over a large range of collision energies. The investigation of high-energy peaking approximations has led to the conclusion that electron transfer can conveniently be explained as proceeding through a single intermediate state which describes an unbound electron in the strong field, moving with the velocity of the projectile. In symmetric collision systems it has turned out that both the second Born approximation as well as SPB, give satisfactory results only in the case of very high impact velocities. Even at the lower velocities, capture experiments on symmetric systems are best described within the symmetric CDW theory which includes the projectile and the target field exactly at the expense of the kinetic energy. However, a second-order CDW theory is required to reproduce differential measurements.

For the emission of electrons into the continuum, a description in terms of capture is only appropriate for certain values of the electron momentum, because a strong correlation with the projectile is a necessary condition. This condition is fulfilled for electrons which are ejected into a small solid angle around the forward direction, and which have a velocity close to v . The higher the projectile charge as compared to Z_T , the more extended is this angular and velocity region where CTC is dominating. In fast collisions, electrons in the CTC region are best described within the IA; however, it does not seem possible to find a perturbative approach which reproduces the complete spectrum of secondary electrons to sufficient accuracy.

The transfer of a single electron in a system with $N - 1$ spectator electrons represents only a very small fraction of the multitude of inelastic reactions where transfer is involved. A reaction which requires at least two active electrons, the transfer excitation²⁴¹, has received much interest through a series of new experiments^{242,243}. For sufficiently high collision velocities, the multiparticle interaction may be split approximately into two-body interactions between the "quasifree" target electrons and the projectile ion as a whole on one hand, and between the target nucleus and the projectile electrons on the other hand. This is a simple way to describe the resonant as well as the nonresonant part of the reaction²⁴⁴.

Another interesting problem which occurs predominantly in astrophysics or plasma physics concerns the behavior of electron transfer in strong electric or magnetic fields. A strong laser field^{245,246}, for example, can provide a considerable enhancement of the capture cross section in low-energy symmetric collision systems, because it supplies additional energy. In contrast, a magnetic field leads in most cases to a reduction of the cross section^{247,248}.

Not only can electrons be transferred, it is even possible to capture whole atoms from a molecular complex into a bound or continuum molecular state of the projectile^{249,250}. Such a reaction is particularly suited to investigate the critical angles, because the extremely low excitation energy of molecular vibrations provides a very large ratio of collision velocity to internal velocity. In a recent scattering experiment of Ar⁺ on CH₄, a Thomas-peak like maximum has been discovered in the proton spectrum²⁵¹. These protons originate from the molecule ArH⁺ which is formed via hydrogen transfer to the continuum.

As far as the influence of nuclear reactions on electron transfer is concerned, the investigation of isolated resonances in elastic collisions is only the very first beginning in a large field. It would be interesting, for example, to study the influence of overlapping isobar analog resonances in the elastic channel, or to extend the theory to inelastic reactions where several reaction channels have to be taken into consideration²⁵². By means of comparing theory with the corresponding experiments, as has been attempted in the case of ionization or positron production in deep-inelastic reactions, one might gain precise information on the dependence of the transfer amplitude along half the trajectory on system parameters like charge, collision velocity or on the electronic initial and final state. On the other hand, nuclear physics could also profit from such kind of research as concerns the understanding of still unknown resonance parameters or reaction cross sections.

Acknowledgments

During the course of this research project, I have greatly benefitted from discussions with physicists of many experimental groups, in particular E. Horsdal Pedersen, W. Meyerhof, H.-D. Betz and K. O. Groeneveld. My special thanks are devoted to P. A. Amundsen who has contributed a great deal to the understanding of high-energy charge transfer. I would also like to thank P. Kienle, W. Greiner and R. Dreizler for their encouragement. Financial support from GSI Darmstadt is gratefully acknowledged.

References

1. J. C. Y. Chen and A. C. Chen, *Adv. At. Mol. Phys.* **8** (1972) 71.
2. K. Taulbjerg, "Fundamental processes in energetic atomic collisions", in *Proc. NATO A.S.I.*, eds. H. O. Lutz *et al.* (Plenum Press, New York, 1982) p. 349.
3. U. Fano and W. Lichten, *Phys. Rev. Lett.* **14** (1965) 627.
4. U. Wille and R. Hippler, *Phys. Rep.* **132** (1986) 129.
5. J. Vaaben and K. Taulbjerg, *J. Phys.* **B14** (1981) 181.
6. J. S. Briggs, *Rep. Prog. Phys.* **39** (1976) 217.
7. J. S. Briggs, J. Macek and K. Taulbjerg, *Comments At. Mol. Phys.* **12** (1982) 1.
8. Dž. Belkić, R. Gayet and A. Salin, *Phys. Rep.* **56C** (1979) 279.
9. L. Kocbach, J. M. Hansteen and R. Gundersen, *Nucl. Instrum. Methods* **169** (1980) 281.
10. K. Dettmann and G. Leibfried, *Z. Phys.* **218** (1969) 1.
11. L. H. Thomas, *Proc. R. Soc. London* **114** (1927) 561.
12. P. T. Greenland, *Phys. Rep.* **81** (1982) 131.
13. P. A. Amundsen and D. H. Jakubaša-Amundsen, *Phys. Rev. Lett.* **53** (1984) 222.
14. W. E. Meyerhof and J.-F. Chemin, *Adv. At. Mol. Phys.* **20** (1985) 173.

15. U. Heinz, B. Müller and W. Greiner, *Ann. Phys.* **151** (1983) 227.
16. N. F. Mott, *Proc. Cambridge Philos. Soc.* **27** (1931) 553.
17. B. A. Lippmann and J. Schwinger, *Phys. Rev.* **79** (1950) 469.
18. L. D. Faddeev, *Sov. Phys.-JETP* **12** (1961) 1014.
19. P. A. Amundsen, *J. Phys.* **B11** (1978) 3197.
20. Y. N. Demkov, *Sov. Phys.-JETP* **11** (1960) 1351.
21. J. Joachain, *Quantum Collision Theory* (North-Holland, Amsterdam, 1975) pp. 93, 355, 361, 368, 379, 411, 442, 528.
22. J. S. Briggs, *J. Phys.* **B8** (1975) L485.
23. K. Dettmann, *Springer Tracts in Modern Physics* (Springer Verlag, Berlin, 1971) Vol. 58, p. 119.
24. S. Alston, *Phys. Rev.* **A38** (1988) 636.
25. J. Macek, *Phys. Rev.* **A37** (1988) 2365.
26. R. McCarroll and A. Salin, *J. Phys.* **B1** (1968) 163.
27. P. T. Greenland, *J. Phys.* **B14** (1981) 3707.
28. C. L. Cocke, J. R. Macdonald, B. Curnutte, S. L. Varghese and R. Randall, *Phys. Rev. Lett.* **36** (1976) 782.
29. Dž. Belkić and A. Salin, *J. Phys.* **B11** (1978) 3905.
30. D. H. Jakubaša-Amundsen and P. A. Amundsen, *Z. Phys.* **A297** (1980) 203.
31. S. Alston, *Phys. Rev.* **A27** (1983) 2342.
32. R. Shakeshaft and L. Spruch, *Rev. Mod. Phys.* **51** (1979) 369.
33. K. Taulbjerg and J. Briggs, *J. Phys.* **B16** (1983) 3811.
34. L. J. Dubé, *J. Phys.* **B17** (1984) 641.
35. R. M. Drisko, Thesis (1955).
36. H. C. Brinkman and H. A. Kramers, *Proc. Acad. Sci. Amsterdam* **33** (1930) 973.
37. R. Shakeshaft, *Phys. Rev.* **A17** (1978) 1011.
38. P. J. Kramer, *Phys. Rev.* **A6** (1972) 2125.
39. J. H. McGuire, P. R. Simony, O. L. Weaver and J. Macek, *Phys. Rev.* **A26** (1982) 1109.
40. J. S. Briggs, *J. Phys.* **B10** (1977) 3075.
41. J. S. Briggs and L. Dubé, *J. Phys.* **B13** (1980) 771.
42. D. P. Dewangan and J. Eichler, *J. Phys.* **B19** (1986) 2939.
43. Dž. Belkić, R. Gayet, J. Hanssen and A. Salin, *J. Phys.* **B19** (1986) 2945.
44. Dž. Belkić, *Proc. 15th Int. Conf. on Physics of Electronic and Atomic Collisions*, Brighton eds. J. Geddes *et al.* (University Press, Belfast, 1987) p. 584.
45. I. M. Cheshire, *Proc. Phys. Soc. London* **84** (1964) 89.
46. D. S. F. Crothers and J. F. McCann, *J. Phys.* **B17** (1984) L177.
47. D. S. F. Crothers, *J. Phys.* **B15** (1982) 2061.
48. J. Burgdörfer and K. Taulbjerg, *Phys. Rev.* **A33** (1986) 2959.
49. J. H. Macek and R. Shakeshaft, *Phys. Rev.* **A22** (1980) 1441.
50. E. J. Kelsey and J. Macek, *J. Math. Phys.* **17** (1976) 1182.
51. P. A. Amundsen and D. H. Jakubaša-Amundsen, *J. Phys.* **B17** (1984) 2671.
52. D. P. Dewangan and J. Eichler, *J. Phys.* **B18** (1985) L65.
53. S. Okubo and D. Feldman, *Phys. Rev.* **117** (1960) 292.
54. J. Macek and S. Alston, *Phys. Rev.* **A26** (1982) 250.
55. D. H. Jakubaša-Amundsen, *Z. Phys.* **A316** (1984) 161.
56. M. R. C. McDowell, *Proc. R. Soc. London* **A264** (1961) 277.
57. M. R. C. McDowell and J. P. Coleman, *Introduction to the Theory of Ion-Atom Collisions* (North-Holland, Amsterdam, 1970) Chaps. 6–8.
58. B. H. Bransden and I. M. Cheshire, *Proc. Phys. Soc. London* **81** (1963) 820
59. M. J. Roberts, *J. Phys.* **B20** (1987) 551.
60. S. Alston, *Proc. 14th Int. Conf. on Physics of Electronic and Atomic Collisions*, Palo Alto eds. M. J. Coggiola *et al.* (North-Holland, Amsterdam, 1985) p. 516.

61. S. H. Hsin and M. Lieber, *Phys. Rev.* **A35** (1987) 4833.
62. R. J. Glauber, *Lectures in Theoretical Physics Vol. 1*, eds. W. E. Brittin *et al* (Interscience, New York, 1959) p. 315.
63. E. Gerjuoy and B. K. Thomas, *Rep. Prog. Phys.* **37** (1974) 1345.
64. D. P. Dewangan, *J. Phys.* **B8** (1975) L119.
65. J. M. Maidagan and R. D. Piacentini, *J. Phys.* **B17** (1984) 2477.
66. J. Eichler and F. T. Chan, *Phys. Rev.* **A20** (1979) 104.
67. J. Eichler and H. Narumi, *Z. Phys.* **A295** (1980) 209.
68. D. R. Bates, *Proc. R. Soc. London* **A247** (1958) 294.
69. D. R. Bates and R. McCarroll, *Proc. R. Soc. London* **A245** (1958) 175.
70. C. D. Lin and L. N. Tunnell, *J. Phys.* **B12** (1979) L485.
71. H. Ryufuku and T. Watanabe, *Phys. Rev.* **A18** (1978) 2005.
72. H. Ryufuku and T. Watanabe, *Phys. Rev.* **A20** (1979) 1828.
73. B. H. Bransden, C. W. Newby and C. J. Noble, *J. Phys.* **B13** (1980) 4245.
74. W. Fritsch, *Phys. Rev.* **A30** (1984) 1135.
75. R. Shingal, B. H. Bransden, A. M. Ermolaev, D. R. Flower, C. W. Newby and C. J. Noble, *J. Phys.* **B19** (1986) 309.
76. U. Fano and W. Lichten, *Phys. Rev. Lett.* **14** (1965) 627.
77. K. Taulbjerg, J. S. Briggs and J. Vaaben, *J. Phys.* **B9** (1976) 1351.
78. D. H. Jakubaša and K. Taulbjerg, *J. Phys.* **B13** (1980) 757.
79. S. B. Schneiderman and A. Russek, *Phys. Rev.* **181** (1969) 311.
80. D. S. F. Crothers and N. R. Todd, *J. Phys.* **B14** (1981) 2233.
81. A. S. Dickinson and R. McCarroll, *J. Phys.* **B16** (1983) 459.
82. A. Salin, *J. Phys.* **B16** (1983) L661.
83. J. Rankin and W. R. Thorson, *Phys. Rev.* **A18** (1978) 1990.
84. C. W. Newby, *J. Phys.* **B18** (1985) 1781.
85. M. Kimura and C. D. Lin, *Phys. Rev.* **A31** (1985) 590.
86. W. Fritsch and C. D. Lin, *J. Phys.* **B15** (1982) 1255; L281.
87. D. G. M. Anderson, M. J. Antal and M. B. McElroy, *J. Phys.* **B7** (1974) L118.
88. C. D. Lin, T. G. Winter and W. Fritsch, *Phys. Rev.* **A25** (1982) 2395.
89. J. E. Miraglia, *Phys. Rev.* **A26** (1982) 309.
90. L. J. Dubé, *J. Phys.* **B16** (1983) L47.
91. I. M. Cheshire, *J. Phys.* **B1** (1968) 428.
92. R. McCarroll, R. D. Piacentini and A. Salin, *J. Phys.* **B3** (1970) 137.
93. J. M. Maidagan and R. D. Piacentini, *Phys. Lett.* **88A** (1982) 128.
94. D. Campos, C. Ramirez and A. de Garcia, *J. Phys.* **B16** (1983) 853.
95. M. Kleber, *J. Phys.* **B11** (1978) 1069.
96. D. H. Jakubaša, *Z. Phys.* **A290** (1979) 13.
97. D. H. Jakubaša-Amundsen, *Phys. Rev.* **A32** (1985) 2166.
98. J. Theis, J. Reinhardt and B. Müller, *J. Phys.* **B12** (1979) L479.
99. J. F. Reading, A. L. Ford, G. L. Swafford and A. Fitchard, *Phys. Rev.* **A20** (1979) 130.
100. H. J. Lüdde and R. M. Dreizler, *J. Phys.* **B14** (1981) 2191.
101. E. A. Hylleraas, *Z. Phys.* **71** (1931) 739.
102. H. J. Lüdde and R. M. Dreizler, *J. Phys.* **B16** (1983) 1009.
103. A. L. Ford, J. F. Reading and R. L. Becker, *J. Phys.* **B12** (1979) 2905.
104. M. Rotenberg, *Ann. Phys.* **19** (1962) 262.
105. D. F. Gallaher and L. Wilets, *Phys. Rev.* **169** (1968) 139.
106. N. Grün, A. Mühlhans and W. Scheid, *J. Phys.* **B15** (1982) 4043.
107. V. Maruhn-Rezwani, N. Grün and W. Scheid, *Phys. Rev. Lett.* **43** (1979) 512.
108. C. Bottcher, *Phys. Rev. Lett.* **48** (1982) 85.
109. A. M. Ermolaev, R. N. Hewitt and M. R. C. McDowell, *J. Phys.* **B20** (1987) 3125.
110. R. Abrines and I. C. Percival, *Proc. Phys. Soc. London* **88** (1966) 861; 873.

111. R. E. Olson and A. Salop, *Phys. Rev.* **A16** (1977) 531.
112. D. Eichenauer, N. Grün and W. Scheid, *J. Phys.* **B14** (1981) 3929.
113. M. Horbatsch and R. M. Dreizler, *Phys. Lett.* **A113** (1985) 251.
114. G. Terlecki, N. Grün and W. Scheid, *J. Phys.* **B17** (1984) 3719.
115. J. Reinhardt, B. Müller, W. Greiner and G. Soff, *Phys. Rev. Lett.* **43** (1979) 1307.
116. J. N. Bardsley, *Case Studies in Atomic Collision Physics Vol. 4*, eds. M. R. C. McDowell and E. W. McDaniel (North-Holland, Amsterdam, 1974) p. 299.
117. J. M. Hansteen and O. P. Mosebekk, *Phys. Rev. Lett.* **29** (1972) 1361.
118. J. H. McGuire and L. Weaver, *Phys. Rev.* **A16** (1977) 41.
119. R. E. Olson, J. Ullrich and H. Schmidt-Böcking, *J. Phys.* **B20** (1987) L809.
120. C. C. J. Roothaan, *Rev. Mod. Phys.* **23** (1951) 69.
121. W.-D. Sepp, W. Sengler, D. Kolb, H. Hartung and B. Fricke, *Chem. Phys. Lett.* **109** (1984) 233.
122. D. Liberman, J. T. Waber and D. T. Cromer, *Phys. Rev.* **A137** (1965) 27.
123. T. H. J. de Reus, R. Reinhardt, B. Müller, W. Greiner, G. Soff and U. Müller, *J. Phys.* **B17** (1984) 615.
124. F. P. Larkins, *J. Phys.* **B5** (1972) 571.
125. B. Fricke, W.-D. Sepp and T. Morovic, *Z. Phys.* **A318** (1984) 369.
126. E. K. U. Gross and R. M. Dreizler, *Density Functional Methods in Physics (NATO A.S.I. Series B)* eds. R. M. Dreizler and J. da Providencia (Plenum Press, New York, 1985) Vol. 123, p. 81.
127. F. Hund, *Z. Phys.* **77** (1932) 12.
128. J. Eichler and U. Wille, *Phys. Rev. Lett.* **33** (1974) 56.
129. J. Eichler and U. Wille, *Phys. Rev.* **A11** (1975) 1973.
130. E. K. U. Gross and R. M. Dreizler, *Phys. Rev.* **A20** (1979) 1798.
131. A. Toepfer, E. K. U. Gross and R. M. Dreizler, *Phys. Rev.* **A20** (1979) 1808.
132. K. C. Kulander, K. R. Sandhya Devi and S. E. Koonin, *Phys. Rev.* **A25** (1982) 2968.
133. R. L. Becker, A. Ford and J. F. Reading, *J. Phys.* **B13** (1980) 4059.
134. G. Mehler, W. Greiner and G. Soff, *J. Phys.* **B20** (1987) 2787.
135. A. Toepfer, H. J. Lüdde, B. Jacob and R. M. Dreizler, *J. Phys.* **B18** (1985) 1969.
136. R. L. Becker, A. L. Ford and J. F. Reading, *Phys. Rev.* **A29** (1984) 3111.
137. H. J. Lüdde and R. M. Dreizler, *J. Phys.* **B18** (1985) 107.
138. M. Kimura, H. Sato and R. E. Olson, *Phys. Rev.* **A28** (1983) 2085.
139. C. Harel and A. Salin, *J. Phys.* **B13** (1980) 785.
140. J. Eichler, *Phys. Rev. Lett.* **46** (1981) 1619.
141. J. Eichler and T.-S. Ho, *J. Phys.* **B18** (1985) 451.
142. D. Bjorken and S. D. Drell, *Relativistische Quantenmechanik* (BI, Mannheim, 1964) p. 29, 299.
143. D. H. Jakubaša-Amundsen and P. A. Amundsen, *Phys. Rev.* **A32** (1985) 3106.
144. M. H. Mittleman, *Proc. Phys. Soc. London* **84** (1964) 453.
145. R. Shakeshaft, *Phys. Rev.* **A20** (1979) 779.
146. B. L. Moiseiwitsch and S. G. Stockman, *J. Phys.* **B13** (1980) 2975.
147. B. L. Moiseiwitsch, *J. Phys.* **B21** (1988) 603.
148. W. J. Humphries and B. L. Moiseiwitsch, *J. Phys.* **B18** (1985) 1209.
149. D. H. Jakubaša-Amundsen and P. A. Amundsen, *Z. Phys.* **A298** (1980) 13.
150. J. Eichler, *Phys. Rev.* **A32** (1985) 112.
151. B. L. Moiseiwitsch, *J. Phys.* **B19** (1986) 3733.
152. G. R. Deco and R. D. Rivarola, *J. Phys.* **B19** (1986) 1759.
153. R. Anholt and J. Eichler, *Phys. Rev.* **A31** (1985) 3505.
154. N. Toshima and J. Eichler, *Phys. Rev. Lett.* **60** (1988) 573.
155. C. Bottcher and M. R. Strayer, *Phys. Rev. Lett.* **54** (1985) 669.
156. U. Becker, N. Grün and W. Scheid, *J. Phys.* **B16** (1983) 1967.

157. U. Becker, N. Grün, W. Scheid and G. Soff, *Phys. Rev. Lett.* **56** (1986) 2016.
158. R. Schuch, G. Nolte, H. Schmidt-Böcking and W. Lichtenberg, *Phys. Rev. Lett.* **43** (1979) 1104.
159. R. Schuch, H. Ingwersen, E. Justiniano, H. Schmidt-Böcking, M. Schulz and F. Ziegler, *J. Phys.* **B17** (1984) 2319.
160. E. Horsdal Pedersen, P. Loftager and J. L. Rasmussen, *J. Phys.* **B15** (1982) 4423.
161. O. K. Baker, C. Stoller, W. E. Meyerhof and J. N. Scheurer, *Nucl. Instrum. Methods* **B24/25** (1987) 89.
162. G. Nolte, J. Volpp, R. Schuch, H. J. Specht, W. Lichtenberg and H. Schmidt-Böcking, *J. Phys.* **B13** (1980) 4599.
163. V. S. Nikolaev, *Sov. Phys.-JETP* **24** (1967) 847.
164. M. Rødbro, E. Horsdal Pedersen, C. L. Cocke and J. R. Macdonald, *Phys. Rev.* **A19** (1979) 1936.
165. J. S. Briggs, *J. Phys.* **B19** (1986) 2703.
166. E. Horsdal Pedersen, C. L. Cocke and M. Stockli, *Phys. Rev. Lett.* **50** (1983) 1910.
167. H. Vogt, R. Schuch, E. Justiniano, M. Schulz and W. Schwab, *Phys. Rev. Lett.* **57** (1986) 2256.
168. E. Horsdal Pedersen, *J. Phys.* **B20** (1987) 785.
169. H.-D. Betz, *Rev. Mod. Phys.* **44** (1972) 465.
170. H. A. Bethe and E. E. Salpeter, *Handbuch der Physik Vol. 35*, ed. S. Flügge (Springer Verlag, Berlin, 1957) p. 408.
171. D. H. Jakubaša-Amundsen, R. Höppler and H.-D. Betz, *J. Phys.* **B17** (1984) 3943.
172. M. Gorriz, J. S. Briggs and S. Alston, *J. Phys.* **B16** (1983) L665.
173. K. Hino and T. Watanabe, *Phys. Rev.* **A36** (1987) 581.
174. M. Kleber and D. H. Jakubaša, *Nucl. Phys.* **A252** (1975) 152.
175. J. S. Briggs and K. Dettmann, *Phys. Rev. Lett.* **33** (1974) 1123.
176. G. Raisbeck and F. Yiou, *Phys. Rev.* **A4** (1971) 1858.
177. D. H. Jakubaša and M. Kleber, *Z. Phys.* **A273** (1975) 29.
178. R. Anholt, Ch. Stoller, J. D. Molitoris, D. W. Spooner, E. Morenzoni, S. A. Andriamonje, W. E. Meyerhof, H. Bowman, J.-S. Xu, Z.-Z. Xu, J. O. Rasmussen and D. H. H. Hoffmann, *Phys. Rev.* **A33** (1986) 2270.
179. J. R. Macdonald, C. L. Cocke and W. W. Eidson, *Phys. Rev. Lett.* **32** (1974) 648.
180. E. Horsdal Pedersen, C. L. Cocke, J. L. Rasmussen, S. L. Varghese and W. Waggoner, *J. Phys.* **B16** (1983) 1799.
181. D. H. Jakubaša-Amundsen and P. A. Amundsen, *J. Phys.* **B14** (1981) L705.
182. A. L. Ford, R. L. Becker, G. L. Swafford and J. F. Reading, *J. Phys.* **B12** (1979) L491.
183. J. H. McGuire, R. E. Kletke and N. C. Sil, *Phys. Rev.* **A32** (1985) 815.
184. J. P. Coleman and S. Trelease, *J. Phys.* **B1** (1968) 172.
185. D. P. Dewangan, *J. Phys.* **B10** (1977) 1083.
186. W. Schwab, G. B. Baptista, E. Justiniano, R. Schuch, H. Vogt and E. W. Weber, *J. Phys.* **B20** (1987) 2825.
187. P. Hvelplund and A. Andersen, *Phys. Scr.* **26** (1982) 375.
188. U. Schryber, *Helv. Phys. Acta* **40** (1967) 1023.
189. L. M. Welsh, K. H. Berkner, S. N. Kaplan and R. V. Pyle, *Phys. Rev.* **158** (1967) 85.
190. J. F. Williams, *Phys. Rev.* **157** (1967) 97.
191. L. H. Toburen, M. Y. Nakai and R. A. Langley, *Phys. Rev.* **171** (1968) 114.
192. K. H. Berkner, S. N. Kaplan, G. A. Paulikas and R. V. Pyle, *Phys. Rev.* **A140** (1965) 729.
193. Dž. Belkić, *J. Phys.* **B10** (1977) 3491.
194. J. S. Briggs, P. T. Greenland and L. Kocbach, *J. Phys.* **B15** (1982) 3085.
195. J. H. McGuire and N. C. Sil, *Phys. Rev.* **A28** (1983) 3679.
196. R. D. Rivarola and A. Salin, *J. Phys.* **B17** (1984) 659.
197. E. Horsdal Pedersen, P. Loftager and J. L. Rasmussen, *J. Phys.* **B15** (1982) 2461.

198. L. Kocbach and J. S. Briggs, *J. Phys.* **B17** (1984) 3255.
199. W. E. Meyerhof, R. Anholt, J. Eichler, H. Gould, Ch. Munger, J. Alonso, P. Thieberger and H. E. Wegner, *Phys. Rev.* **A32** (1985) 3291.
200. E. Spindler, H.-D. Betz and F. Bell, *J. Phys.* **B10** (1977) L561.
201. D. H. Jakubaša-Amundsen, *J. Phys.* **B16** (1983) 1767.
202. J. Macek, *Phys. Rev.* **A1** (1970) 235.
203. D. H. Jakubaša-Amundsen, *J. Phys.* **B14** (1981) 3139.
204. M. E. Rudd, C. A. Sautter and C. L. Bailey, *Phys. Rev.* **151** (1966) 20.
205. Y. B. Band, *J. Phys.* **B7** (1974) 2557.
206. J. E. Miraglia and V. H. Ponce, *J. Phys.* **B13** (1980) 1195.
207. S. D. Berry, G. A. Glass, I. A. Sellin, K. O. Groeneveld, D. Hofmann, L. H. Andersen, M. Breinig, S. B. Elston, P. Engar, M. M. Schauer, N. Stolterfoht, H. Schmidt-Böcking, G. Nolte and G. Schiwietz, *Phys. Rev.* **A31** (1985) 1392.
208. R. Schramm, W. Oswald, H.-D. Betz, E. Szmola and R. Schuch, *Proc. 15th Int. Conf. on Physics of Electronic and Atomic Collisions*, Brighton eds. J. Geddes *et al.* (University Press, Belfast, 1987) p. 603.
209. R. Shakeshaft and L. Spruch, *Phys. Rev. Lett.* **41** (1978) 1037.
210. D. S. F. Crothers and J. F. McCann, *J. Phys.* **B20** (1987) L19.
211. C. Bottcher, *Phys. Rev. Lett.* **48** (1982) 85.
212. *Lecture Notes in Physics*, eds. K. O. Groeneveld *et al.* (Springer Verlag, Berlin 1984) Vol. 213.
213. D. H. Jakubaša-Amundsen, *J. Phys.* **B20** (1987) 325.
214. D. H. Jakubaša-Amundsen, *Phys. Rev.* **A38** (1988) 70.
215. G. Schiwietz, H. Platten, D. Schneider, T. Schneider, W. Zeitz, K. Musiol, R. Kowallik and N. Stolterfoht, HMI Berlin Report B447 (1987).
216. P. D. Fainstein, V. H. Ponce and R. D. Rivarola, *J. Phys.* **B21** (1988) 287.
217. P. Kienle, M. Kleber, B. Povh, R. M. Diamond, F. S. Stephens, E. Grosse, M. R. Maier and D. Proetel, *Phys. Rev. Lett.* **31** (1973) 1099.
218. U. Müller, G. Soff, J. Reinhardt, T. de Reus, B. Müller and W. Greiner, *Phys. Rev.* **C30** (1984) 1199.
219. U. Heinz, *Rep. Prog. Phys.* **50** (1987) 145.
220. A. Cristallini, C. Maroni, A. Massa and G. Vannini, *Phys. Lett.* **56B** (1975) 245.
221. R. Anholt, *Atomic Inner-Shell Physics*, ed. B. Craseman (Plenum Press, New York, 1984).
222. D. H. Jakubaša-Amundsen, *J. Phys.* **B20** (1987) L705.
223. D. H. Jakubaša-Amundsen and P. A. Amundsen, *J. Phys.* **B18** (1985) 757.
224. J. S. Blair and R. Anholt, *Phys. Rev.* **A25** (1982) 907.
225. T. Tomoda and H. A. Weidenmüller, *Phys. Rev.* **C28** (1983) 739.
226. E. Horsdal, B. Jensen and K. O. Nielsen, *Phys. Rev. Lett.* **57** (1986) 675.
227. D. H. Jakubaša-Amundsen, *Z. Phys.* **A322** (1985) 191.
228. R. M. Eisberg, D. R. Yennie and D. H. Wilkinson, *Nucl. Phys.* **18** (1960) 338.
229. P. C. Gugelot, *Direct Interactions and Nuclear Reaction Mechanisms*, eds. Clementel *et al.* (Gordon and Breach, New York, 1962) p. 382.
230. J. S. Blair, P. Dyer, K. A. Snover and T. A. Trainor, *Phys. Rev. Lett.* **41** (1978) 1712.
231. D. W. Spooner, Ch. Stoller, J.-F. Chemin, W. E. Meyerhof, J. N. Scheurer and X.-Y. Xu, *Phys. Rev. Lett.* **58** (1987) 341.
232. P. A. Amundsen and K. Aashamar, *J. Phys.* **B19** (1986) 1657.
233. R. Anholt, J. F. Chemin and P. A. Amundsen, *Phys. Lett.* **B118** (1982) 245.
234. O. K. Baker, W. E. Meyerhof, D. W. Spooner, Ch. Stoller and J. N. Scheurer, *Phys. Rev. Lett.* **60** (1988) 913.
235. P. Vincent, L. Goldman, T. Fink and P. A. Amundsen, *Phys. Rev. Lett.* **59** (1987) 2423.
236. R. Krieg, E. Božek, U. Gollerthan, E. Kankeleit, G. Klotz-Engmann, M. Krämer, U. Meyer, H. Oeschler and P. Senger, *Phys. Rev.* **C34** (1986) 562.

237. M. Krämer, B. Blank, E. Božek, E. Kankeleit, G. Klotz-Engmann, C. Müntz, H. Oeschler and M. Rhein, *Phys. Lett.* **B201** (1988) 215.
238. M. Nessi, Ch. Stoller, E. Morenzoni, W. Wölfli, W. E. Meyerhof, J. D. Molitoris, E. Grosse and Ch. Michel, *Phys. Rev.* **C36** (1987) 143.
239. R. Schmidt, V. Toneev and G. Wolschin, *Nucl. Phys.* **A311** (1978) 247.
240. G. Soff, J. Reinhardt, B. Müller and W. Greiner, *Phys. Rev. Lett.* **43** (1979) 1981.
241. D. Brandt, *Phys. Rev.* **A27** (1983) 1314.
242. A. Itoh, T. J. M. Zouros, D. Schneider, U. Stettner, W. Zeitz and N. Stolterfoht, *J. Phys.* **B18** (1985) 4581.
243. M. Schulz, E. Justiniano, R. Schuch, P. H. Mokler and S. Reusch, *Phys. Rev. Lett.* **58** (1987) 1734.
244. J. M. Feagin, J. S. Briggs and T. M. Reeves, *J. Phys.* **B17** (1984) 1057.
245. M. H. Mittleman, *Phys. Rev.* **A14** (1976) 586.
246. G. Ferrante, L. Lo Cascio and B. Spagnolo, *J. Phys.* **B14** (1981) 3961.
247. S. Bivona and M. R. C. McDowell, *J. Phys.* **B20** (1987) 1541.
248. U. Wille, *Phys. Lett.* **A125** (1987) 52.
249. D. R. Bates, C. J. Cook and F. J. Smith, *Proc. Phys. Soc. London* **83** (1964) 49.
250. R. Shakeshaft and L. Spruch, *Phys. Rev.* **A21** (1980) 1161.
251. M. Breinig, G. J. Dixon, P. Engar, S. B. Elston and I. A. Sellin, *Phys. Rev. Lett.* **51** (1983) 1251.
252. A. M. Lane and R. G. Thomas, *Rev. Mod. Phys.* **30** (1958) 257.